ASPIRATION NOISE DURING PHONATION: SYNTHESIS, ANALYSIS, AND PITCH-SCALE MODIFICATION

by

DARYUSH MEHTA

B.S., Electrical Engineering (2003)
University of Florida

SUBMITTED TO THE DEPARTMENT OF ELECTRICAL ENGINEERING AND COMPUTER SCIENCE
IN PARTIAL FULFILLMENT OF THE REQUIREMENTS FOR THE DEGREE OF

MASTER OF SCIENCE IN ELECTRICAL ENGINEERING AND COMPUTER SCIENCE

at the

MASSACHUSETTS INSTITUTE OF TECHNOLOGY

February 2006

Author ....
Department of Electrical Engineering and Computer Science
January 31, 2006

Certified by...
Thomas F. Quatieri
Senior Member of Technical Staff, MIT Lincoln Laboratory
Faculty of MIT Speech and Hearing Bioscience and Technology Program
Thesis Supervisor

Accepted by ....
Professor A. C. Smith
Chair, Department Committee on Graduate Students

This work was sponsored by the Department of Defense under Air Force Contract FA8721-05-C-0002. Opinions, interpretations, conclusions, and recommendations are those of the author and are not necessarily endorsed by the United States Government.

Aspiration Noise during Phonation: Synthesis, Analysis, and Pitch-Scale Modification

by

Daryush Mehta

Submitted to the Department of Electrical Engineering and Computer Science on January 31, 2006,
in partial fulfillment of the requirements for the degree of
Master of Science in Electrical Engineering and Computer Science

Abstract

The current study investigates the synthesis and analysis of aspiration noise in synthesized and spoken vowels. Based on the linear source-filter model of speech production, we implement a vowel synthesizer in which the aspiration noise source is temporally modulated by the periodic source waveform. Modulations in the noise source waveform and their synchrony with the periodic source are shown to be salient for natural-sounding vowel synthesis. After developing the synthesis framework, we research past approaches to separate the two additive components of the model. A challenge for analysis based on this model is the accurate estimation of the aspiration noise component that contains energy across the frequency spectrum and temporal characteristics due to modulations in the noise source. Spectral harmonic/noise component analysis of spoken vowels shows evidence of noise modulations with peaks in the estimated noise source component synchronous with both the open phase of the periodic source and with time instants of glottal closure.

Inspired by this observation of natural modulations in the aspiration noise source, we develop an alternate approach to the speech signal processing aim of accurate pitch-scale modification. The proposed strategy takes a dual processing approach, in which the periodic and noise components of the speech signal are separately analyzed, modified, and re-synthesized. The periodic component is modified using our implementation of time-domain pitch-synchronous overlap-add, and the noise component is handled by modifying characteristics of its source waveform. Since we have modeled an inherent coupling between the original periodic and aspiration noise sources, the modification algorithm is designed to preserve the synchrony between temporal modulations of the two sources. The reconstructed modified signal is perceived to be natural-sounding and generally reduces artifacts that are typically heard in current modification techniques.

Thesis Supervisor: Thomas F. Quatieri
Title: Senior Member of Technical Staff, MIT Lincoln Laboratory
Faculty of MIT Speech and Hearing Bioscience and Technology Program

Acknowledgements

My primary thanks is owed to my adviser, Tom, without whom this document and research ideas would not have come together. Thank you, Tom, for pushing me through my periods of pessimism and for helping me think like a scientist and innovate like an engineer.

To Nick, whose footsteps I have quietly followed because they have been laid out so well. Nick, thanks for those endless discussions that contributed to many insights in this thesis. And for those times that often started with an academic seed like Kalman filtering and somehow ended up with the physics of snowboarding.

To the Speech group at Lincoln Lab, my home away from home—thank you for creating an environment in which creative and organized thinking can occur and for constructively critiquing my research at each stage. Special thanks to Mike Brandstein for his always congenial attitude toward my incessant and sometimes inane software queries.

To the Voice Quality Study Group for starting the seeds of a great discussion forum for the exchange of ideas and insightful critiquing of papers.

To Andrea—thank you for the motivation and drive for me to do my best each day.

And thank you to Mom, Dad, Nazneen, and Parendi—without your love and unwavering support, I would not be here.

Contents

List of Figures

List of Tables

Chapter 1

Introduction

A common theme of research is to link observations from different domains and explain or even predict the data observed in one domain using results from a second domain. One such domain is the physiological world, consisting of complex chemical, biological, and electrical interactions within anatomical structures. Another, the acoustic domain, can provide indirect measurement of properties that have their root in physiological processes. Thus, for example, we can analyze a system such as the human speech production mechanism by making quantitative and qualitative observations of the speech acoustics. To link acoustic data to processes in the physiological domain, we turn to modeling. Modeling forms this link and thus affords the experimenter a tool with which predictions can be made across domains. In this study, inspiration from observations in the physiology and anatomy of voice production is used as a basis for developing a signal processing model for speech synthesis, analysis, and modification applications.

The current study investigates the synthesis and analysis of aspiration noise in synthesized and spoken vowels. The approach builds on the linear source-filter modeling of speech (see [73] for a review) and research that aims at decomposing the speech signal into periodic and noise components for speech modification purposes [7, 31, 43, 53, 75, 80]. In speech synthesis, the voicing source is often synthesized using an additive noise model that represents noise as modulated at the pitch rate and synchronized with the voiced component before vocal tract filtering [36]. A challenge for analysis based on this model is accurate separation to estimate both temporal and spectral characteristics of the noise component. Previous researchers have documented the perceptual importance of noise modulations (e.g., [20]) and have further applied this understanding to the development of speech modification techniques [75].

1.1 Motivation

It is important in many applications to understand the inherent characteristics of the aperiodic component during voiced and unvoiced speech. For example, text-to-speech synthesis applications desire the highest quality and most natural-sounding speech. This is one case in which synthesizing an accurate representation of the aperiodic part of speech can help. If there are temporal characteristics that occur at certain phase relationships within a glottal period, then these relationships should be kept intact during synthesis. Along the same line of thinking, current speech modification algorithms (see [43, 45, 54, 59, 65, 75]) would also benefit from estimating and modifying the aspiration noise components, according to a physiologically-based model.

The goal for a speaker identification application is to recognize distinct traits for different speakers. The noise characteristics of speech may be unique to different speakers, and if true, the pattern recognition approach to speaker identification may benefit from a supplementary source of feature vectors derived from the noise component. The analysis of the acoustic speech signal can also aid in vocal assessment in the clinical setting, where it is desired to effectively and efficiently assess, diagnose, and alleviate pathologies associated with the voice production mechanism. Though it has been shown that acoustic measures may not correlate well with disordered structures in the vocal fold region [19, 23, 25, 26, 42], an analysis of solely the aperiodic component of speech may offer critical insights not gained by simply analyzing the cumulative pressure signal.

1.2 Outline

The organization of the material is as follows. Chapter 2 begins with a background of the speech production system, specifically focusing on the physiological mechanisms that control the production of the aspiration noise source. A physiologically-based vowel synthesizer is implemented, and its parameters are described. Chapter 3 deals with the problem of estimating the aspiration noise from an aggregate speech signal. A brief description of previous noise estimation techniques is presented, and one technique is selected for subsequent analysis on synthesized and real vowels. This technique is then used as the first step in our proposed pitch-scale modification algorithm that is introduced in Chapter 4. Current pitch modification algorithms are presented with their limitations to motivate the development of our proposed modification algorithm. Each stage of the proposed algorithm is described, followed by example processing on synthesized and real vowels. Chapter 5 draws conclusions and provides a summary of current challenges that prove interesting for future work on the subject and summarize the major conclusions from this study.

Chapter 2

Synthesis of a Vowel with Aspiration Noise

This chapter addresses the synthesis of a vowel motivated by physiological mechanisms of the voicing source with aspiration noise. First, Section 2.1 presents the relevant physiological mechanisms of speech production, and Section 2.2 describes a vowel production model inspired by the observed physiology. Next, Section 2.3 explains our implementation of a vowel synthesizer and its parameters. As an aside, Section 2.4 mentions alternative models of the speech production mechanism that form a more complete picture but are not of focus in this study. Finally, Section 2.5 discusses the perceptual consequences of various aspiration noise characteristics in the context of synthesized vowels.

2.1 Physiology and Acoustics

The system is often simplified to two independent mechanisms—the source and the filter. The source mechanism arises from the vocal folds of the larynx that are set into periodic vibration by a combination of muscle tensions and aerodynamic forces that form the myo-elastic aerodynamic theory [73]. Vibration of the vocal folds provide for an excitation source of periodic puffs of air that subsequently are input into the supraglottal system, including the vocal tract and external environment. Due to the relatively high acoustic impedance at the glottis [73], these post-source stages effectively act as linear filters that shape the spectral characteristics of the periodic source mechanism. This study focuses on the dual nature of the voicing source that consists of both periodic and noise factors due to turbulent noise at the glottis.

Typically, speech researchers refer to the term ”breathiness” to refer to a voice quality that has been correlated with the presence of a noise percept due to airflow turbulences at the source of the voicing mechanism [11-13, 22, 23, 38, 40, 41]. The breathy voice quality implicates many acoustic correlates in the speech spectrum that will not be addressed here, including harmonic relationships, first formant bandwidth, speed quotient, and spectral tilt [16-19, 22, 41]. This thesis will focus on characterizing the aspiration noise component of speech that can occur during the production of breathy vowels, modal phonation, or dysphonic speech [19].

More generally, turbulence can be created at a number of locations in the speech production system downstream from the glottis. These turbulent sources occur during voiced and unvoiced fricative production, and although the output speech is not perceptually breathy, a noise component is introduced at the vocal tract output. The aspiration noise source is generated at the level of the glottis and acts as a stochastic excitation source simultaneously with the periodic excitation. High-velocity air passes through the glottal constriction and results in the generation of a jet stream that forms eddies of air that introduce noise sources into the speech production system [34]. Turbulent air flow generates several sources that are distributed over various structures near the glottis [72, 73], such as the false vocal folds, the pharyngeal walls, and, in pathological speakers, anomalous masses on the true vocal folds themselves. The following sections describe empirical observations made of the properties of this turbulent air flow.

2.1.1 Frequency-domain Observations

Stevens [72] relates the generation of aspiration noise in speech to the generation of turbulence at a spoiler impeding the airflow in a cylindrical tube. Alluding to empirical observations performed by Gordon [14, 15], who measured the spectral characteristics of the source and radiated pressure signal in context of the tube-spoiler setup, Stevens concludes that the spectral characteristics of the turbulent noise at the location of the spoiler are within 6 dB up to a certain cutoff frequency dictated by the length of the cylindrical tube.

Empirical observations have also been made regarding noise source spectra generated in another tube model and in real whispered vowels. The spectral characteristics of the turbulent noise source during whispered speech are assumed to closely mirror that of the modulated noise source occurring during phonation. Hillman et al. have simulated the effect of turbulent noise at the glottis by using an acoustic tube model, and have also compared their model with estimated noise spectra of the source of human-produced whispered vowels [24]. Results point to a broadband spectral quality of the aspiration noise source, varying within ±10 dB from 100 Hz to 10 kHz.

2.1.2 Time-domain Observations

The aspiration noise source can occur during modal phonation, breathy vowels, voiced fricatives, and utterances of speakers with certain types of dysphonia [23, 25, 26, 28, 40]. When the vocal folds vibrate during phonation, the concomitant generation of turbulence noise is thought to be maximum during the open phase of the glottal volume velocity waveform, with larger pressure sources resulting from higher-velocity turbulences [36-38, 73]. Contrarily, other analyses of vowels have observed that locations of maximum noise amplitude occur around the instant of glottal closure and not during the open phase [28, 66].

In addition, it has been observed that the vocal folds do not close completely along their length. While the *membranous* portion of the vocal folds vibrate during phonation, a posterior glottal opening is often present at the *cartilaginous* portion of the vocal folds where the arytenoid cartilages appear, allowing for a constant DC flow of air during phonation [16-19] (see Figure 2.1).

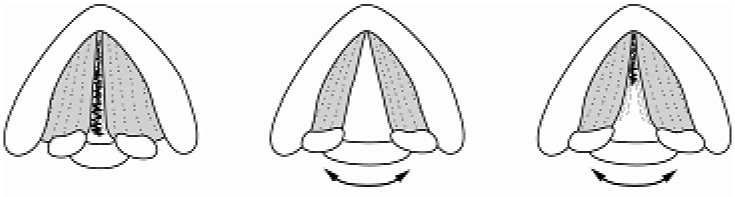

Figure 2.1 Vocal fold abduction and adduction during phonation. Axial view from above the vocal folds. The leftmost figure shows closure of the vocal folds along its length up to the two arytenoid cartilages. From [63].

Two effects of the DC flow offset are observed. First, the degree of the DC offset could be correlated with other aspects of the glottal waveform such as AC amplitude and opening and closing characteristics. The influence of the DC offset in this case is schematized in Figure 2.2a. Secondly, the DC term could simply act as a strict vertical offset so that the opening and closing characteristics of the waveform are not changed. Figure 2.2b schematizes this process.

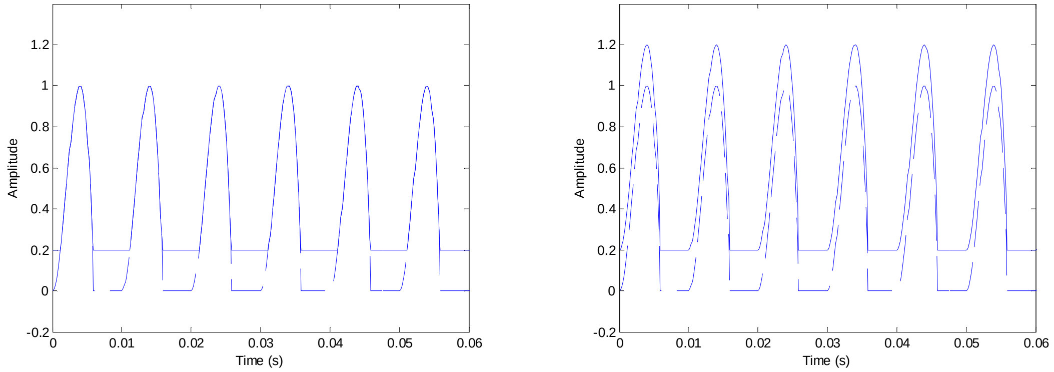

(a) (b)

Figure 2.2 Effect of the DC offset parameter on the glottal flow velocity waveform, DC = 0 (dashed line) and DC = 0.2 (solid line). (a) Increase in DC offset is accompanied by a decrease in the AC amplitude, and (b) increase in DC offset strictly vertically offsets the entire waveform. Pitch period is 0.01 s.

Empirical observations support both processes of Figure 2.2 in different cases. In one research study, Holmberg, Hillman, and Perkell derive inverse-filtered waveforms for the vowel /a/ from the oral airflow of male and female speakers at different loudness levels [27]. A DC offset was observed in the inverse-filtered waveform, especially when the vowel was phonated at a soft level. The effect of the DC offset mirrored what is schematized in Figure 2.2a. An increase in the DC flow was accompanied by a decrease in the AC amplitude of the airflow. In addition, the data point to a simultaneous increase in open quotient and rounding of the corners at the opening and closing portions of the waveform.

At a constant production level, however, the varying sizes of the glottal chink can be observed in the acoustics [27]. Empirical observations closely mirror the simulated glottal waveforms in Figure 2.2b. This process would lend itself to the notion that closure of the vocal folds maintains its abrupt nature even when a DC flow is observed. The two mechanisms—the AC waveform and the DC offset—are distinct and almost decoupled since each is due to a different portion of the vocal folds. Care must be taken to ascribe the AC waveform to the vibration of the membranous portion of the vocal folds, while the DC offset is due to the non-vibrating cartilaginous portion of the vocal folds. In the model and implementation that follow, the schematic in Figure 2.2b is selected as the effect of DC flow on the glottal volume velocity source.

Within a given speaker, the loudness level can significantly modify the glottal waveform, potentially affecting the AC amplitude of the noise source as well as open quotient and the abruptness of vocal fold opening and closure [27]. These secondary phenomena are not taken into account.

2.2 Vowel Production Model

Inspired by the above-mentioned physiological observations, we develop a model for the production of a vowel. The temporal characteristics of the noise source—modulations at the rate of the fundamental frequency and DC flow—and the observed broadband spectral characteristic will be taken into account. A block diagram summarizes the model in Figure 2.3. The output waveform consists of a linear sum of both a periodic and noise component. The periodic component is the output of the linear vocal tract filter with a periodic glottal flow velocity source, while the noise component is the output of the vocal tract filter with a modulated white noise input.

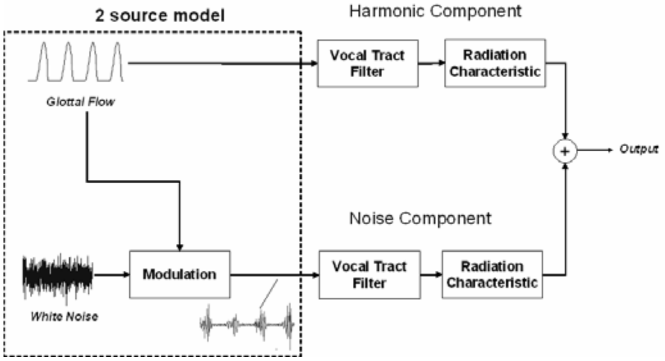

Figure 2.3 Vowel production model.

To put this flow diagram into formal equations, it helps to view the signals of interest in the time domain (from [63]). The periodic source, $u_g[n]$, arises from the periodic vibrations of the vocal folds and can be represented by one period of the glottal flow velocity waveform, $g[n]$, convolved with a train of impulses, $p[n]$, with its period equal to the inverse of the fundamental frequency:

$$u_g[n] = g[n] * p[n]. \tag{2.1}$$

This volume velocity source is input into a linear time-invariant filter representing the vocal tract, with impulse response $h[n]$, which effectively filters and shapes the spectrum of the glottal source. The output signal at the lips due to the periodic source, $x_p[n]$, is thus

$$x_p[n] = \left(g[n] * p[n]\right) * h[n]. \tag{2.2}$$

In the model of the noise component, air flows through the constrictions at the glottis and encounters obstructions that generate turbulence, which aggregates into a noise source denoted by $q[n]$. This noise source is effectively gated and modulated by the opening and closing of the vocal folds, where the modulation function is represented by $u_g[n]$ and is assumed multiplicative. The model assumes that the modulated noise source, $q[n]u_g[n]$, is then input into the same vocal tract filter that operates on the periodic glottal source. The output signal at the lips due to the noise source is $x_n[n]$:

$$x_n[n] = \left(q[n]u_g[n]\right) * h[n]. \tag{2.3}$$

Both $x_p[n]$ and $x_n[n]$ are volume velocity signals. The periodic portion is due to the periodic puffs of air generated at the glottis, and the noise portion is due to the acoustic realization of airflow turbulence at the glottis.

The overall signal that a standard condenser microphone measures manifests as acoustic pressure waves that propagate through the ambient air. Since the pressure signal is measured by the microphone at a certain distance from the lips, a transformation occurs from the volume velocity signals $x_p[n]$ and $x_n[n]$ to the pressure signals due to the radiation impedance in the atmosphere. Assumed to be a spherical acoustic source, the volume velocity signals at the lips are passed through a filter representing this radiation characteristic, which, in continuous time, is given by (a far-field approximation valid for frequencies up to 4000 Hz) [73]:

$$R(f) = j\frac{\rho}{2r}e^{-j\left(\frac{2\pi fr}{c}\right)}, \tag{2.4}$$

where ρ is the density of air, r is the distance from the velocity source to a far-field microphone, and c is the speed of sound. We are usually concerned with the magnitude of the radiation characteristic, $|R(f)|$, approximated by [73]

$$|R(f)| = \frac{\rho}{2r}f. \tag{2.5}$$

The magnitude of the radiation characteristic filter is effectively linearly proportional to frequency and thus emphasizes energy at higher frequencies. The discrete-time filter associated with $R(f)$ is denoted by $r[n]$.

The output pressure signal in the production model reflects the presence of the radiation characteristic. The total speech pressure signal at the microphone, $s[n]$, is modeled as the linear addition of the periodic and noise components:

$$\begin{aligned} s[n] &= \left(x_p[n]*r[n]\right)+\left(x_n[n]*r[n]\right) \\ &= \left(u_g[n]*h[n]*r[n]\right)+\left(q[n]u_g[n]*h[n]*r[n]\right) \\ &= \left(g[n]*p[n]*h[n]*r[n]\right)+\left(q[n]u_g[n]*h[n]*r[n]\right). \end{aligned} \tag{2.6}$$

2.3 Implementation of Vowel Synthesizer

In this section, we describe a MATLAB implementation of the production model in Figure 2.3 above to synthesize an aspirated vowel. The implementation is inspired by elements of the Klatt synthesizer and includes a periodic voicing source (Klatt's AV parameter) and a stochastic aspiration noise source (Klatt's AH parameter) [36, 37].

2.3.1 Periodic Source

The form chosen for the periodic source is a pulse shape by Rosenberg used in the Klatt synthesizer as the KLGLOTT88 source [36, 37]. Rosenberg has documented the effect of various glottal pulse shapes on listeners' perception of natural voice quality [67], and the main result is that listeners are not significantly receptive to differences in fine time structure of the source shape. A parametric polynomial fit to the shape of the periodic source, the classic Rosenberg pulse, was shown in that study to produce a natural quality when synthesizing vocalic speech sounds. The simplicity of this function and the lack of need to have detailed control over other glottal source parameters were factors in choosing the Rosenberg model (see [9, 17, 18] for more complex forms).

The equation for the Rosenberg model, $g(t)$, of the glottal pulse in continuous time is

$$g(t) = \begin{cases} t^2 - \dfrac{t^3}{OQ \cdot T_0}, & 0 \le t < \left(OQ \cdot T_0\right) \\ 0, & \left(OQ \cdot T_0\right) \le t < T_0 \end{cases}, \tag{2.7}$$

where OQ is the open quotient (fraction between 0 to 1) and T_0 is the fundamental period in Hz. The waveform is sampled at sampling rate f_s to yield the discretized waveform, $g[n]$, in Equation (2.1).

As mentioned above, the periodic source is implemented as the derivative of the glottal flow velocity, effectively taking into account the high-pass radiation characteristic. After this radiation characteristic is folded in, the derivative of Equation (2.7) yields the effective excitation to the acoustic filter of the vocal tract. The resulting glottal flow derivative, $g'(t)$, is simply

$$g'(t) = \begin{cases} 2t - \dfrac{3t^2}{OQ \cdot T_0}, & 0 \le t < \left(OQ \cdot T_0\right) \\ 0, & \left(OQ \cdot T_0\right) \le t < T_0 \end{cases}, \tag{2.8}$$

After sampling this waveform at f_s, the resulting signal is $u_g'[n] \approx u_g[n] * r[n]$, an approximation to the derivative of the glottal airflow waveform.

The rationale behind keeping the volume velocity waveform in the block diagram is due to an important assumption in the model that, before vocal tract filtering, the noise source is modulated by the glottal airflow waveform. This implementation differs from the approach of the Klatt synthesizer, in which the aspiration noise is simply modulated by a square wave with duty cycle equal to the open phase duration [36]. To emphasize our assumed coupling between the periodic and aspiration noise source, the periodic excitation is left undifferentiated in the production model of Figure 2.3. A sample glottal airflow waveform and corresponding derivative are shown in Figure 2.4. Arrows indicate open and closed phase portions of the waveform.

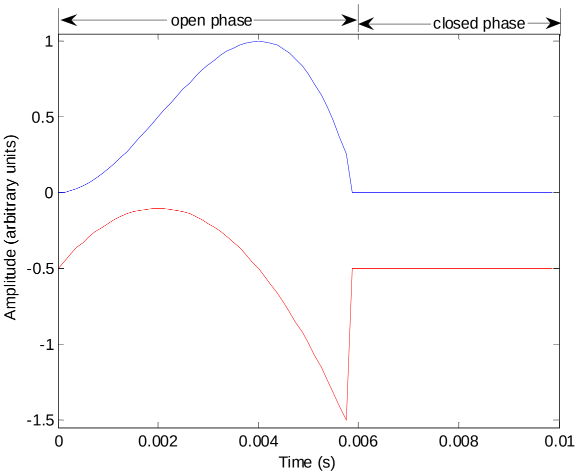

Figure 2.4 Glottal airflow velocity waveform. Rosenberg model (top) and its corresponding derivative waveform (bottom) representing the effective periodic input as a pressure source. T_0 = 0.01 s, OQ = 0.6, f_s = 8000 Hz. The waveforms are vertically offset for clarity.

2.3.2 Aspiration Noise Source

The aspiration noise source consists of AC and DC characteristics. The following sections clarify the implementation of these two components.

AC Component

Synthesis assumes that the aspiration noise amplitude is modulated by the area of the glottal opening, which is assumed to be related to the glottal airflow velocity function, $u_g[n]$ (Figure 2.4, top). Thus, concomitant with the volume velocity source due to the periodic vocal fold vibrations is the volume velocity source due to turbulent airflow at the glottis. Using the notation of Equation (2.3), the aspiration noise source is $u_g[n]$, where $q[n]$ represents the aggregate contribution from all glottal noise sources. We assume that $q[n]$ is from a zero-mean white Gaussian distribution and represents noise sources that occur at several locations around the glottis. Delays between sources are not currently modeled. Figure 2.5 displays a synthesized example of the AC component of the aspiration noise source. The glottal waveform, $u_g[n]$, modulates the white Gaussian noise source, $q[n]$. The result is the AC component of the aspiration noise source, $q[n]u_g[n]$.

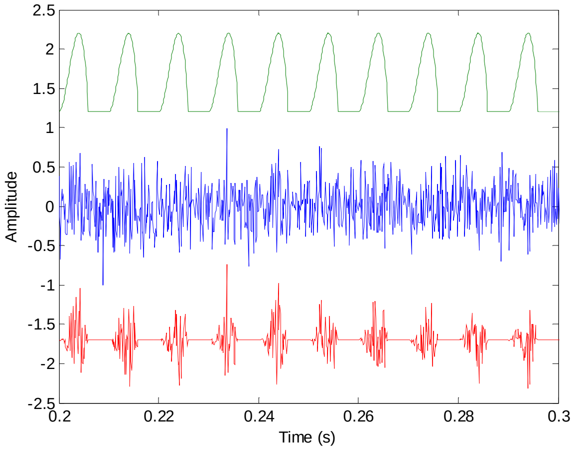

Figure 2.5 The AC component of the aspiration noise source. Glottal waveform (top), white Gaussian noise signal (middle), and noise signal modulated by the glottal waveform (bottom). T_0 = 0.01 s, OQ = 0.6, f_s = 8000 Hz. The waveforms are vertically offset for clarity.

DC Flow

In the discussion on vocal fold mechanics in Section 2.1, it was concluded that, for constant sound level production, the DC flow simply acts as a vertical offset to the AC waveform with zero offset (recall the bottom signal in Figure 2.5). This is the source signal model implemented in the MATLAB code and illustrated in Figure 2.6. Depending on the choice for the DC synthesis parameter, the glottal waveform is generated and acts as the noise modulation function. Figure 2.7 contrasts an unmodulated noise source with modulated sources with two different DC offsets.

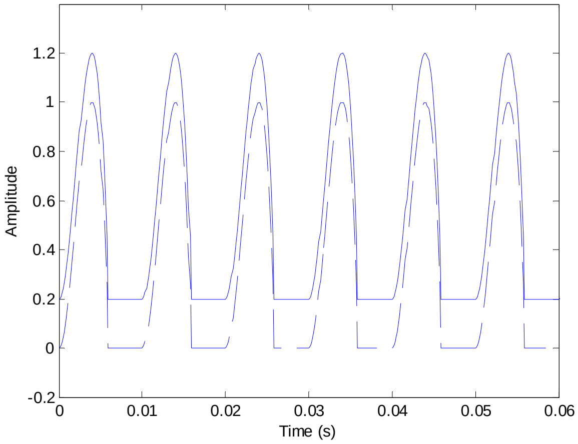

Figure 2.6 The DC component of the aspiration noise source. The glottal flow velocity waveform with no DC flow (dashed line) and DC flow of 0.2 (solid line). T_0 = 0.01 s, OQ = 0.6, f_s = 8000 Hz.

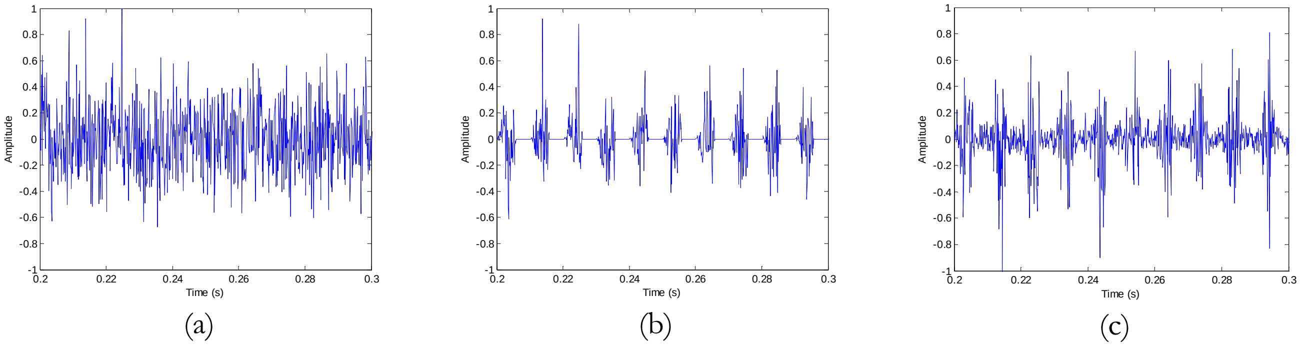

Figure 2.7 Generating the modulated aspiration noise source. (a) Unmodulated white Gaussian noise, (b) noise signal modulated by glottal waveform with no DC flow, and (c) noise signal modulated by glottal waveform with a DC flow of 0.2. T_0 = 0.01 s, OQ = 0.6, f_s = 8000 Hz.

2.3.3 Vocal Tract and Radiation Filters

The vocal tract is modeled as a cascade of three second-order filters or, as Klatt refers to them as, "digital formant resonators" [36, 37]. Each of the three digital resonators is in the form (z-domain):

$$\frac{Y(z)}{X(z)} = \frac{A}{1 - Bz^{-1} - Cz^{-2}}, \tag{2.9}$$

where

$$A = 1 - B - C,$$
$$B = 2e^{-\pi\frac{BW}{f_s}} \cos\left(2\pi\frac{F}{f_s}\right),$$
$$C = -e^{-2\pi\frac{BW}{f_s}},$$

and BW is the bandwidth of the formant, F is the formant frequency, and f_s is the sampling rate, all in Hz. Multiplication of three of these transfer functions results in the overall transfer function of the desired three-formant vocal tract configuration, with impulse response, $h[n]$. Formant frequencies and bandwidths used in this study are tabulated in Table 2.1. Although higher formants could have been included, it was decided to only draw from the Peterson and Barney data [62] and reduce complexity for the current analysis.

Phonetic Symbol	Synthesizer Symbol	Male			Female		
		F1	F2	F3	F1	F2	F3
/i/	i	270	2290	3010	310	2790	3310
/e/	e	460	1890	2670	560	2320	2950
/æ/	ae	660	1720	2410	860	2050	2850
/a/	a	730	1090	2440	850	1220	2810
/o/	o	450	1050	2610	600	1200	2540
/u/	u	300	870	2240	370	950	2670

Table 2.1 Vowel formant frequencies, in Hz. Data from [62] and [73].

Eliminating the need to explicitly indicate the density of air or a distance in Equation (2.5), the digital filter representing the radiation characteristic, $R(z)$, is often implemented as a first-difference filter, approximating its high-pass characteristic and is (in the z-domain)

$$R(z) = 1 - z^{-1}. \tag{2.10}$$

2.3.4 Parameters

Synthesis equations have been developed above for the glottal airflow waveform $u_g[n]$, the derivative of the glottal waveform $u_g'[n]$, and the aspiration noise source $q[n]$ prior to modulation due to the gating effect of vocal fold oscillations. Formulae were also derived for the effect of modulations and DC offsets on the aspiration noise source, as well as for the acoustic filter properties of the vocal tract. Variables for the synthesizer are set by nine synthesis parameters (see Appendix A for list with default values). It is noted that the addition of perturbations such as frequency jitter and amplitude shimmer would form a more complete synthesis system [21, 36, 37, 55, 56], especially when modeling disordered speech [10, 40, 51]. The analysis and modification sections in the following chapters do not include jitter and shimmer parameters; however, their anticipated effects are investigated for future improvements (Section 5.1).

For flexibility, the aspiration noise can either be modulated or unmodulated by the glottal airflow waveform. Six vowels are chosen for investigative purposes. The three formants to be used in the vocal tract resonators of Equation (2.9) are selected by the vowel and the gender parameters, as indicated in Table 2.1. Differences in oral and pharyngeal cavity lengths for males and females correlate with different average formant frequencies [73]. The fundamental frequency parameter, f_0, is set for each glottal cycle, and the sampling rate and duration of the vowel are set as desired.

The last three synthesis parameters are DC, OQ, and HNR, which set important attributes of the source signals. DC determines the DC offset on the glottal flow waveform as a fraction of the AC amplitude. OQ indicates the open quotient during a glottal cycle, defined as the ratio of the open-phase to closed-phase duration. Finally, the harmonics-to-noise ratio (HNR) sets the ratio of the powers in the harmonic and noise components computed on the signals after filtering by the vocal tract resonances and the radiation characteristic. HNR is defined as

$$HNR = 10\log_{10}\frac{\sum_{n=0}^{L-1}\left(v[n]\right)^2}{\sum_{n=0}^{L-1}\left(u[n]\right)^2}, \tag{2.11}$$

where $v[n]$ is the harmonic component, $u[n]$ is the noise component, and L is the signal length. See Appendix A for a list of the vowel synthesizer's parameters and Appendix B for a graphical user interface created for developing code and performing simulations with different test parameters.

2.4 Alternative Speech Production Models

The linear source-filter model detailed above, in which the nonlinear modulation is folded into the noise source, is not the only way that one may view the production of voiced speech. Notions of the involvement of non-acoustic components contributing to spectral characteristics of the speech pressure signal were introduced, for example, by Teager [77], further qualitatively evaluated by Kaiser [33], and more recently investigated experimentally by several research groups [3, 39, 49, 52, 71, 81]. The essence of these models of aeroacoustics in speech production rests on the existence of concomitant airflows of vortices in the vocal tract and pharyngeal region.

In one study, measurements of velocity and pressure in a simple mechanical model of the vocal folds and vocal tract seem to indicate the presence of such a non-acoustic component at the source of the mechanical model. The non-acoustic source energy, following a transformation to acoustic energy, is shown to contribute to the power spectrum of the output pressure signal [3, 71]. Evidence thus points to the possibility of aerodynamic influences contributing to the source and to formant shaping [77]. Although aerodynamics and other non-acoustic phenomena must be fully accounted for in a complete model of speech production, implementation is computationally intensive and beyond the scope of this study. The linear source-filter theory provides a flexible paradigm that can be readily adapted for the current study.

2.5 Perception of Aspiration Noise Characteristics

After developing and implementing the vowel synthesizer, it was desired to obtain a flavor for the perceptual salience of different noise characteristics. For this purpose, this section reviews some earlier work as well as our informal evaluation of the perception of these synthesized vowels. In particular, the perceptual experiments performed by Hermes [20] motivated the current preliminary investigation. In his work, Hermes investigates the synthesis of a natural breathy voice quality using an additive model with impulsive and stochastic sources. Hermes documents the perceptual consequences of synthesizing the stochastic source with various characteristics in both the time and frequency domain.

The next three sections briefly investigate time- and frequency-domain characteristics of the aspiration noise source and provides some informal observations of their effect on human perception. Section 2.5.1 comments on differences in perception when the vowel is synthesized either with an unmodulated or modulated noise source. Section 2.5.2 investigates the possible perceptual effects of imposing different modulation functions on the aspiration noise source. Finally, Section 2.5.3 introduces the importance of synchrony between the modulated noise and the periodic excitation, drawing from one of Hermes' experiments [20].

2.5.1 Unmodulated versus Modulated Noise

Hermes investigates the fusion of periodic and noise components when synthesizing breathy vowels and concludes that noise bursts must lie in phase with the glottal pulse excitation for maximum "fusion" with the periodic sound component [20]. References are made to Bregman's theory of auditory scene analysis [5], in which two auditory objects may fuse together only if they both contribute to the overall timbre of the sound. As a consequence, if an unmodulated noise were used for aspiration source synthesis, a percept of two streams may result—one due to the periodic source and the other due to the unmodulated noise source.

Figure 2.8 displays two synthesized sources illustrating the temporal differences between an unmodulated and modulated noise source. In this example, the modulating function is taken to be the glottal airflow waveform, although Hermes did not define a specific shape. Section 2.5.2 will present work on comparing the perception of different modulation functions.

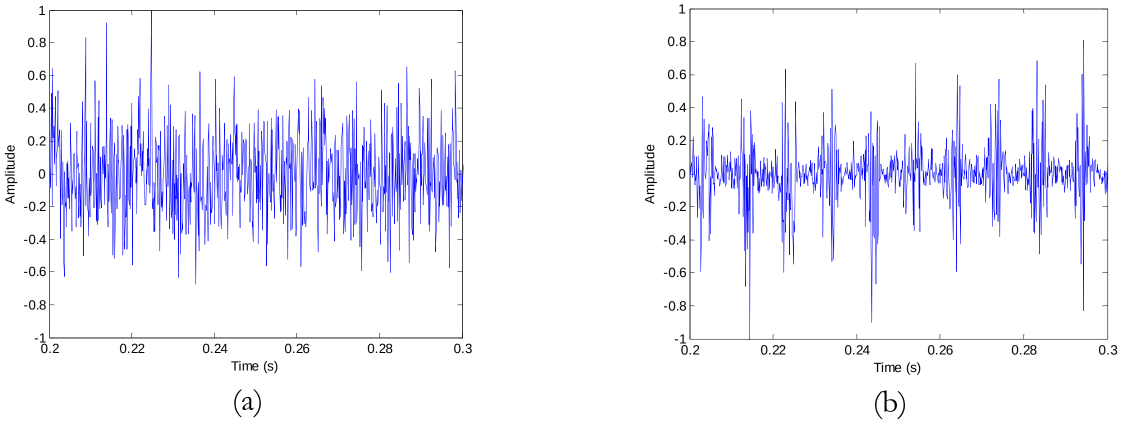

Figure 2.8 The aspiration noise source. (a) Unmodulated white Gaussian noise and (b) noise signal modulated by glottal waveform. Synthesis parameters: f_0= 100 (pitch period = 0.01 s), f_s = 8000, DC = 0.2, OQ = 0.6.

In Hermes' work and in our informal listening, after filtering by the vocal tract formants and radiation characteristic, the vowel's noisy part seems to perceptually integrate better with the periodic component when modulated noise is used as the aspiration noise source. These results indicate that modulation may be important for the synthesis of a natural-sounding vowel but do not reveal how best to select the modulation function.

2.5.2 Modulation Functions

Modulation of the noise component in the time domain seems to be perceptually significant and physiologically plausible, a view adopted by many researchers (e.g., [38]). Klatt, however, states that no evidence supports the use of any specific modulation function, as long as a modulation function exists [36-38]. It is desirable to further explore the perception of different modulation functions on the aspiration noise source.

Four different modulation patterns are chosen for study and illustrated in Figure 2.9. The functions are a rectangle, a sinusoid, and a glottal airflow velocity waveform with and without a DC component. Vowels are synthesized with the noise sources modulated by each function. Informal listening indicates that the glottal airflow waveform provides for the most natural synthesis, with a non-zero DC component slightly preferred to zero DC. Rigorous listening tests, however, would need to be performed to statistically support this conclusion.

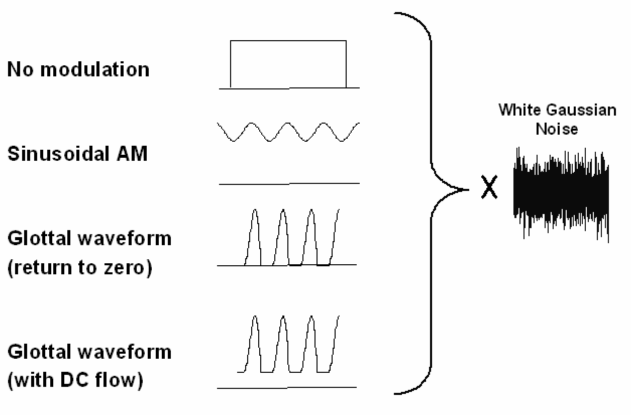
No modulation
Sinusoidal AM
Glottal waveform (return to zero)
Glottal waveform (with DC flow)
X
White Gaussian Noise

Figure 2.9 The four modulation functions imposed on the aspiration noise source. Rectangle (no modulation), sinusoidal amplitude modulation, the glottal waveform with no DC component, and the glottal waveform with a DC component.

2.5.3 Synchrony with Periodic Source

A speculation of Hermes' work is that, to be perceptually fused, the noise bursts at the source lie in a certain phase with the concomitant periodic source [20]. Our work investigates the synchrony issue and takes a step further to use a glottal waveform model (the Rosenberg pulse in Section 2.3.1) to represent the periodic source, unlikely Hermes' impulsive excitation. Figure 2.10 illustrates how the sources would be synthesized when the periodic excitation is in phase or out of phase with the aspiration noise source. The in-phase case synthesizes the sources so that the noise maxima occur near the location of peak air flow, imposed by the modulations of the periodic source.

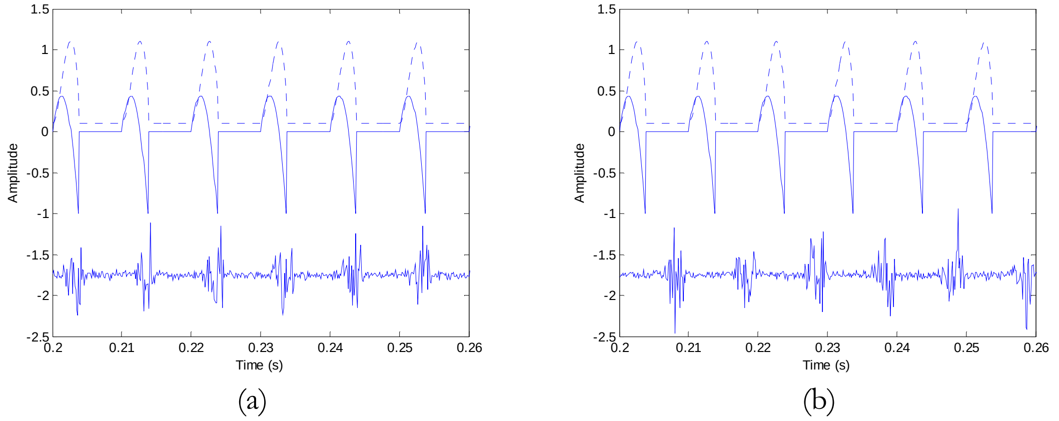

(a) (b)

Figure 2.10 Perception of source synchrony. (a) In-phase and (b) out-of-phase source waveforms. Synthesized glottal waveform (dotted line), derivative of glottal waveform (top solid line), and aspiration noise source (bottom solid line). Synthesis parameters: Noise type = modulated, Vowel = a, f_0= 100, Gender = m, f_s = 8000, Duration = 1, DC = 0.1, OQ = 0.4, HNR = 10. The waveforms are vertically offset for clarity.

The waveforms are then the periodic- and noise-source inputs to the vowel synthesizer of Section 2.3. Note that the pitch is held constant to allow a constant time offset to uniformly shift the entire noise signal so the noise maxima occur in the same phase within each cycle. Our preliminary perception of the two synthesized vowels agree with Hermes' conclusion that there is less roughness in the output signal when the signals in Figure 2.10a are sources. Hermes would say that the listener would hear the out-of-phase sources in Figure 2.10b as two perceptual auditory streams or objects. Indeed, the vowel synthesized from these sources sounds less natural and likely to arise from two distinct sources.

2.6 Summary and Conclusions

In this section, we first described the essential physiological mechanisms of speech production and developed a linear source-filter model to describe the effects of these mechanisms. A vowel synthesizer was implemented in MATLAB [47], and we detailed each stage of processing with equations in Section 2.3. The entire synthesis system resembles the Klatt synthesizer [36, 37], but with a key difference when implementing the aspiration noise source. Instead of selecting an arbitrary modulation function imposed on the noise source, the periodic volume velocity waveform is chosen as the specific modulation function.

Alternative speech models were briefly mentioned in Section 2.4, introducing the importance of aerodynamic parameters. Due to its complexity and its computational load, these models are outside the scope of the current study. Finally, we reviewed earlier work by Hermes [20] and Klatt [38] and made our own preliminary observations on the perception of the natural quality of synthesized vowels with a modulated aspiration noise source. Specifically, we addressed the perceptual salience of noise modulations, the specific modulation function, and the synchrony of the periodic and noise components.

Chapter 2 provides us with a framework within which we can test our analysis and modification algorithms. With knowledge of the input source signals in the synthesizer, we can derive performance measures to assess the accuracy of an analysis tool that extracts the periodic and noise components in speech. Building this harmonic/noise separation algorithm is the subject of Chapter 3.

Chapter 3

Harmonic/Noise Component Analysis

In Chapter 2, we developed an additive noise model to represent the speech signal during phonation as the sum of a periodic or harmonic component and an aspiration noise component. We then developed a vowel synthesizer based on this model that provides access to the waveforms at each stage of synthesis. In Chapter 3, we now develop a tool to analyze the harmonic and noise components of both synthesized and real vowels.

Section 3.1 begins with an overview of current harmonic/noise analysis algorithms and their limitations. We choose one of these algorithms, the pitch-scaled harmonic filter [31], for further analysis and discuss its MATLAB implementation in Section 3.2. Sections 3.3 and 3.4 are devoted to examples of harmonic/noise component analysis on synthesized and real vowels.

3.1 Signal Processing Background

All separation algorithms seek to first estimate the periodic portion of a signal, followed by a temporal or spectral subtraction step. Although some speech processing algorithms assume that the noise and periodic components of voiced speech spectrally overlap, they ultimately simplify the analysis by assuming that the noise component lies solely in a high frequency region [43, 75]. Recently, a number of decomposition techniques have been introduced that show improved accuracy at estimating the harmonic and noise components with accurate spectral and temporal resolution [7, 31, 80]. The resulting signals can then be analyzed for interesting traits in the frequency and time domains.

Three harmonic/noise separation algorithms are described in this section. Section 3.1.1 describes state-of-the-art algorithms for separating the harmonic and noise components of a signal. Section 3.1.2 presents limitations of these algorithms and motivates the selection of one of them for continued analysis and use in our study.

3.1.1 Algorithms

Yegnanarayana et al. [7, 8, 80] propose a decomposition method that incorporates inverse filtering and a cepstral lifter (analogous to a spectral comb filter) to initially separate the harmonic and noise components. The authors take the stance that each DFT coefficient contains a contribution from both a periodic component and a noise component. First, inverse filtering is accomplished by an all-zero whitening filter whose coefficients are calculated using linear prediction. An argument for this first step is that, since both the periodic and noise components are generated at the source level, decomposition should be performed on the excitation signal, or residual signal after inverse filtering. Second, the authors convert the residual excitation signal to the cepstral domain and lifter out the periodic excitation energy in quefrency. This provides initial estimates for the periodic and aperiodic excitation components. Since the resulting aperiodic spectrum contains gaps at harmonic frequencies, an iterative algorithm is developed to converge to an optimized estimate of the aperiodic excitation. Time-domain subtraction from the original residual signal results in the estimate of the periodic component of the source excitation. Each source component is then filtered by an all-pole filter whose coefficients come from the whitening step.

A second decomposition method, by Jackson and Shadle [29-31], provides a purely spectral technique that places a comb filter on the output pressure signal (no inverse filtering) to arrive at the harmonic component of the signal. The approach uses an analysis window duration equal to a small integer number of pitch periods and relies on the property that harmonics of the fundamental frequency fall at specific frequency bins of the discrete short-time Fourier transform. Thus, the pitch at each analysis time instant must be estimated prior to comb filtering. Since the comb filter only passes frequencies in harmonics of the fundamental frequency, the algorithm is referred to as the pitch-scaled harmonic filter (PSHF). To fill in gaps that occur in the residual noise spectrum (as also with the algorithm by Yegnanarayana et al.), spectral power interpolation is performed prior to the inverse DFT. Specifics of the algorithm's implementation are presented in Section 3.2.

Prior to the PSHF, Serra and Smith [70] developed an alternative spectral-based decomposition algorithm. The authors also perform spectral subtraction to separate the periodic and noise components and use the inverse DFT to arrive at the desired extracted signals. An important difference from the PSHF, though, is that Serra and Smith do not restrict the deterministic part of the signal to contain harmonically-related frequency components. This probably results from the authors' interest in analyzing non-harmonic music signals, as well as speech. Instead of filtering each analysis frame whose length depends on the local pitch (as was the case in the PSHF algorithm), Serra and Smith employ a peak-picking algorithm in the short-time spectra to identify energy contributions from the deterministic part of the signal. The algorithm then follows that of the PSHF method, similarly including a interpolation stage to fill in spectral gaps.

A summary of the major features of each of the three algorithms described above is presented in Table 3.1.

Researchers	**Analysis domain**	**Subtraction domain**	**Harmonic constraint?**
Yegnanarayana et al. [7, 8, 80]	CD/FD	TD	Yes
Serra and Smith [70]	FD	FD	No
Jackson and Shadle [29-31]	FD	FD	Yes

Table 3.1 Comparison of harmonic/noise decomposition algorithms. TD = time domain, FD = frequency domain, CD = cepstral domain.

3.1.2 Limitations

The performance of an iterative algorithm like that by Yegnanarayana et al. [7, 8, 80] is pre-disposed to robustness issues. Both the use of a linear predictive analysis front-end and the inclusion of an iterative algorithm have been discounted as being ineffective by Jackson and Shadle [31]. They show the iterative algorithm to ultimately converge to the original residual excitation signal that includes both periodic and aperiodic factors. In addition, whitening by inverse filtering is not viewed as helping improve spectral analysis of the signals, as linear prediction analysis has its own assumptions and limitations. Regarding the Serra and Smith algorithm [70], although harmonicity is not assumed, stochastic variations in the spectrum could lead the system to incorrectly assign a particular DFT bin as deterministic. As a result, the harmonic assumption will be taken in the current study because speech signals tend to behave under this constraint during voicing.

We chose the PSHF since Jackson and Shadle claim that the algorithm can preserve the temporal modulation characteristics of the noise component and approximately isolate the noise component from a voiced fricative signal [29, 31]. Some leakage of harmonicity can be present in the extracted noise component [50], and the presence of shimmer and jitter provides difficulty (see Section 5.1 for a discussion). For shimmer and jitter ranges observed in normal speakers, however, Jackson and Shadle claim that the PSHF can be used as an effective analysis tool [31]. Our implementation of the PSHF and example analyses using the algorithm are described in the following sections.

3.2 Implementation of Pitch-Scaled Harmonic Filter

The pitch-scaled harmonic filter (PSHF) technique was implemented in MATLAB [47] to operate on an input speech signal, $s[n]$. Short-time analysis is performed on a windowed portion of $s[n]$ to result in two signals, a harmonic and a noise component. Overlap-add synthesis is then used to merge together all the short-time segments (see [63] for a discussion on the OLA analysis/synthesis framework). Details of the PSHF can be found in [31], but we present the critical components below.

Every 10 ms, the local pitch period, T_0, is estimated. Pitch estimation is accomplished using the speech signal processing tool Praat [4]. The Praat algorithm arrives at a periodicity measure by a forward cross-correlation analysis [4]. The PSHF imposes an analysis window of length N, which will be shown to be time-dependent. The window employed is the Hanning window, $w[n]$:

$$w[n] = 0.5 - 0.5\cos\left(\frac{2\pi n}{N}\right), \quad 0 \le n \le N-1. \tag{3.1}$$

Using the classic overlap-add analysis method, each short-time segment, $s_w[n,r]$, is thus

$$s_w[n,r] = s[n]w[n - rD + \tfrac{N}{2}], \tag{3.2}$$

where r is the frame number and D is the frame advance. The frame index, r, will be dropped for the moment for clarity and reintroduced during overlap-add synthesis.

Estimation of the periodic component assumes harmonicity and relies on the property that if N is chosen appropriately for each time instant, the harmonics will fall at specific frequency bins of an N-point discrete short-time Fourier transform, $S_w(k)$. See Appendix C for an example analysis on a vowel signal demonstrating this property.

The discrete spectrum of the harmonic component of a frame, $V(k)$, is thus given by:

$$V(k) = \begin{cases} S_w(k), & \text{for } k \in B \\ 0, & \text{otherwise,} \end{cases} \tag{3.3}$$

where $k = 0 \ldots N-1$ is the DFT index and B is the set $\{b, 2b, 3b, \ldots\}$.

After obtaining an estimate for the harmonic component, spectral subtraction is subsequently performed to obtain the spectrum of the noise component estimate, $U(k)$:

$$U(k) = \begin{cases} S(k) - V(k), & \text{for } k \in B \\ S(k), & \text{otherwise,} \end{cases} \tag{3.4}$$

where $S(k)$ is the N-point DFT of the rectangular-windowed single, $s[n]$.

Note that zeroes exist in the discrete spectrum of $U(k)$ at every b th bin. Assuming that the envelope of the power spectrum of the noise is smooth, additional processing interpolates power estimates from neighboring bins to fill in the zeroed frequency regions. A revised harmonic estimate is then obtained by taking into account the interpolated noise power present in the harmonically-labeled bins.

The revised estimates of the harmonic component, $\tilde{V}(k)$, and noise component, $\tilde{U}(k)$, are (from [31]):

$$\tilde{V}(k) = \begin{cases} V(k)\sqrt{1-\lambda^2(k)}, & \text{for } k \in B \\ V(k), & \text{otherwise,} \end{cases} \tag{3.5}$$

$$\tilde{U}(k) = \begin{cases} U(k)+\lambda(k)V(k), & \text{for } k \in B \\ U(k), & \text{otherwise,} \end{cases} \tag{3.6}$$

where

$$\lambda(k) = \frac{L(k)}{\sqrt{|S_w(k)|^2 + L^2(k)}} \quad \text{and} \quad L(k) = \sqrt{\frac{|U(k-1)|^2 + |U(k+1)|^2}{2}}.$$

The time-domain signals of the harmonic and noise components in each frame are obtained by performing an N-point inverse DFT, yielding $\tilde{v}[n]$ and $\tilde{u}[n]$, respectively.

We can reconstruct the entire signals from the short-time segments by re-introducing the time dependence (frame index r) and using overlap-add synthesis [63]:

$$\tilde{v}[n] = \frac{\sum_{r=0}^{Q-1} \tilde{v}[n,r]w[n-rD]}{\sum_{r=0}^{Q-1} w[n-rD]}, \tag{3.7}$$

$$\tilde{u}[n] = \frac{\sum_{r=0}^{Q-1} \tilde{u}[n,r]w[n-rD]}{\sum_{r=0}^{Q-1} w[n-rD]}, \tag{3.8}$$

where Q is the number of segments in each signal. Note that the normalization factor in the denominator is due to window weighting on each short-time segment. The sum of overlapping Hanning windows will not be equal to one, and as a consequence, the overlap-add method divides out the effect of the window sum.

3.3 Performance Evaluation on Synthesized Vowel

This section analyzes a synthesized vowel with a steady pitch. It is instructive to first analyze synthesized vowels since the periodic and noise components are known inputs in the synthesis framework described in Chapter 2. After estimating these components from the overall pressure signal (assuming no knowledge of the input sources), direct comparisons can be made to assess confidence in the decomposition technique. Other example vowels are then analyzed in Section 3.4.

Two assessment measures can be devised for the two outputs of harmonic/noise decomposition. One measure deals with the frequency-domain characteristics and overall power levels. The other, more qualitative, assessment compares the time-domain characteristics of the input and output waveforms. The synthesis framework gives us access to the building blocks of the vowel. The main synthesis parameter that will be varied for performance assessment of decomposition is the harmonics-to-noise ratio (HNR). The HNR serves as an indication of the relative level contributions of the harmonic component and the noise component. HNR is defined as

$$HNR = 10\log_{10}\frac{\sum_{n=0}^{L-1}\left(\tilde{v}[n]\right)^2}{\sum_{n=0}^{L-1}\left(\tilde{u}[n]\right)^2}, \tag{3.9}$$

where $\tilde{v}[n]$ is the estimated harmonic component, $\tilde{u}[n]$ is the estimated noise component, and L is the signal length. Ideally, the HNR value set during synthesis will be equal to the HNR calculated on the extracted components. This allows one to observe any consistent overestimation or underestimation of the power in a specific component.

Table 3.2 displays the results of the analysis of one synthesized vowel. Synthesis parameters are indicated in the caption, with the aspiration noise source being unmodulated. It is noted that due to the stochastic nature of the original signal, it is unreasonable to expect an input random signal to be perfectly reconstructed at the output. The overall statistics, however, are assumed to be unchanged. Table 3.3 calculates performance measures for another synthesized with the same synthesis parameters, except the noise source type is modulated.

HNR_{input} (dB)	HNR_{output} (dB)	ΔHNR (dB)	$Periodic_{input}$ (dB re 1 Volt)	$Periodic_{output}$ (dB re 1 Volt)	$Noise_{input}$ (dB re 1 Volt)	$Noise_{output}$ (dB re 1 Volt)
-20.0	-5.1	+14.9	-42.5	-28.8	-22.5	-23.6
-15.0	-5.0	+10.0	-38.4	-29.5	-23.4	-24.5
-10.0	-2.9	+7.1	-34.4	-28.6	-24.4	-25.7
-5.0	-4.6	+0.4	-29.3	-29.1	-24.3	-24.5
0.0	+2.5	+2.5	-25.8	-25.0	-25.8	-27.6
+5.0	+6.7	+1.7	-22.9	-22.8	-27.9	-29.5
+10.0	+11.2	+1.2	-21.5	-21.6	-31.5	-32.8
+15.0	+15.8	+0.8	-20.9	-20.9	-35.8	-36.7
+20.0	+19.7	-0.3	-20.3	-20.4	-40.3	-40.1
+25.0	+22.7	-2.3	-19.9	-20.0	-44.9	-42.7
+30.0	+23.9	-6.1	-19.7	-19.8	-49.7	-43.7

Table 3.2 HNR measures for harmonic/noise analysis of synthesized vowel with unmodulated aspiration noise source. Noise type = unmodulated, vowel = a, f_0 = 100, Gender = m, f_s = 8000, Duration = 1, DC = 0.1, OQ = 0.6. Parameter is HNR.

HNR_{input} (dB)	HNR_{output} (dB)	ΔHNR (dB)	$Periodic_{input}$ (dB re 1 Volt)	$Periodic_{output}$ (dB re 1 Volt)	$Noise_{input}$ (dB re 1 Volt)	$Noise_{output}$ (dB re 1 Volt)
-20.0	-3.5	+16.5	-45.0	-30.5	-25.0	-27.0
-15.0	-4.7	+10.3	-38.9	-30.1	-23.9	-25.4
-10.0	-4.9	+5.1	-35.0	-31.3	-25.0	-26.3
-5.0	-3.9	+1.1	-30.5	-30.0	-25.5	-26.1
0.0	+2.4	+2.4	-26.2	-25.8	-26.2	-28.2
+5.0	+6.6	+1.6	-24.1	-24.1	-29.1	-30.7
+10.0	+11.3	+1.3	-21.5	-21.4	-31.5	-32.7
+15.0	+16.2	+1.2	-20.9	-20.9	-35.9	-37.1
+20.0	+19.8	-0.2	-20.1	-20.2	-40.1	-40.0
+25.0	+22.6	-2.4	-19.8	-19.9	-44.8	-42.4
+30.0	+23.9	-6.1	-19.7	-19.8	-49.7	-43.6

Table 3.3 HNR measures for harmonic/noise analysis of synthesized vowel with modulated aspiration noise source. Noise type = modulated, vowel = a, f_0 = 100, Gender = m, f_s = 8000, Duration = 1, DC = 0.1, OQ = 0.6. Parameter is HNR.

A plot of output HNR versus input HNR is shown in Figure 3.1, in which the optimal function is a straight line with unit slope. For HNRs between -5 and +20 dB, the relative power levels of the estimated harmonic and noise components lies within about 3 dB of the known input component levels. As HNRs decrease below -5 dB, the output HNR measure stays approximately constant, indicating a ceiling of performance. In these cases, zero regions can be seen in the waveform of the extracted harmonic component. These gaps are partly due to the Praat pitch tracker not being able to calculate a pitch estimate during specific time frames, understandable since the stochastic signal begins to swamp out the harmonic part. Most of the output noise component thus is equal to the input, which contains both harmonic and stochastic elements.

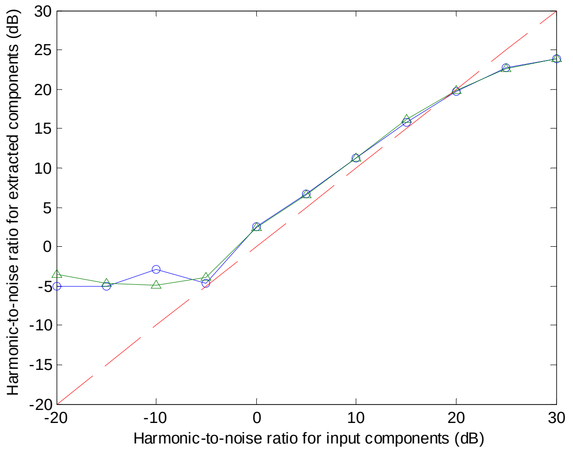

Figure 3.1 Output HNR vs. input HNR. Synthesized noise source is either unmodulated (circles) or modulated (triangles). Dashed line indicates ideal performance with HNR equal at input and output.

Since we are dealing with stochastic signals, we can only estimate their power spectra and try to minimize biases (deviations from the true mean) and variances (deviations from the true variance). Bartlett's procedure [60], a method for averaging periodograms, is used to estimate the power spectra of the above speech-like signals. The periodogram, $I[k]$, for a length-L short-time segment, $x[n]$, windowed with a unit-height rectangle, is proportional to the squared magnitude of the N-point DFT with index k [60]:

$$I[k] = \frac{1}{L}\left|\sum_{n=0}^{N-1} x[n]e^{-j\left(\frac{2\pi}{N}nk\right)}\right|^2 . \tag{3.10}$$

The periodogram itself is a biased estimate of the true power spectrum of noise, with the expected value approaching zero as more sample points are included in the window. For a given data length Q, however, increasing the number of samples per window results in decreasing the number of windows available for averaging. This is a tradeoff, since increasing the number of averaged periodograms reduces the estimate's variance. The parameters of Bartlett's procedure are Q (the entire signal length), L (the window length), and R (the number of samples to advance for each successive window). The number of frames, K, to be averaged falls out of the following equation:

$$K = \text{floor}\left\{\frac{(Q-1)-(L-1)}{R}\right\}, \tag{3.11}$$

where the $\text{floor}\{\ \}$ function finds the largest integer smaller than the argument. In the current analysis, a 50% window overlap was chosen, so that $R = 0.5L$. The assumption of frame independence is not strictly maintained, but the variance of the averaged periodogram has been shown to decrease nevertheless with half-window overlapping [60]. With $r = 0 \ldots K-1$ as the index for each periodogram from Equation (3.10), the averaged periodogram is equal to

$$\bar{I}[k] = \frac{1}{K}\sum_{r=0}^{K-1} I_r[k]. \tag{3.12}$$

In subsequent plots, the individual periodograms are calculated from short-time segments of length 50 ms. For a 1-second vowel sampled at 8000 Hz, the number of frames averaged, K, is 38. Figure 3.2 displays $\bar{I}[k]$ for input and output signals from the PSHF of a synthesized vowel with a modulated noise source. Figure 3.2c shows some harmonic leakage in the periodogram of the noise component, especially in the 1500–2500 Hz frequency region. This leakage is due to small inaccuracies in the estimate of the amplitudes at the harmonic frequencies in Figure 3.2b.

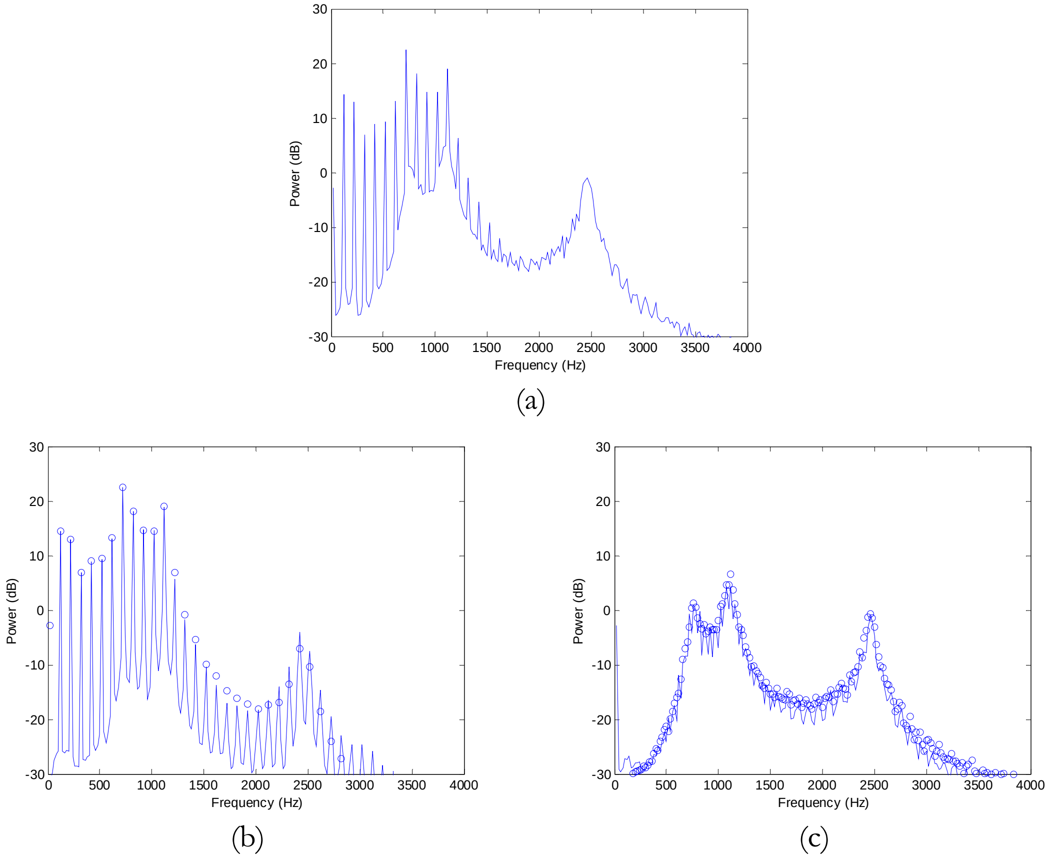

(a)

(b)

(c)

Figure 3.2 Averaged periodograms of (a) synthesized vowel, (b) harmonic estimate, and (c) noise estimate. In (b) and (c), superimposed are DFT magnitudes of the synthesized harmonic and noise inputs, respectively. Synthesis parameters: Noise type = modulated, Vowel = a, f_0 = 100, Gender = m, f_s = 8000, Duration = 1, DC = 0.1, OQ = 0.6, HNR = 10.

In addition to desiring similar spectral characteristics at the input and output, temporal features of the input signals should be appropriately reconstructed in the extracted components. In the vowel synthesizer, the noise source was modulated by the glottal flow velocity function (the Rosenberg model in Figure 2.4), and so to view the modulations in the separated noise component, sample waveforms from the PSHF output are displayed in Figure 3.3 and Figure 3.4.

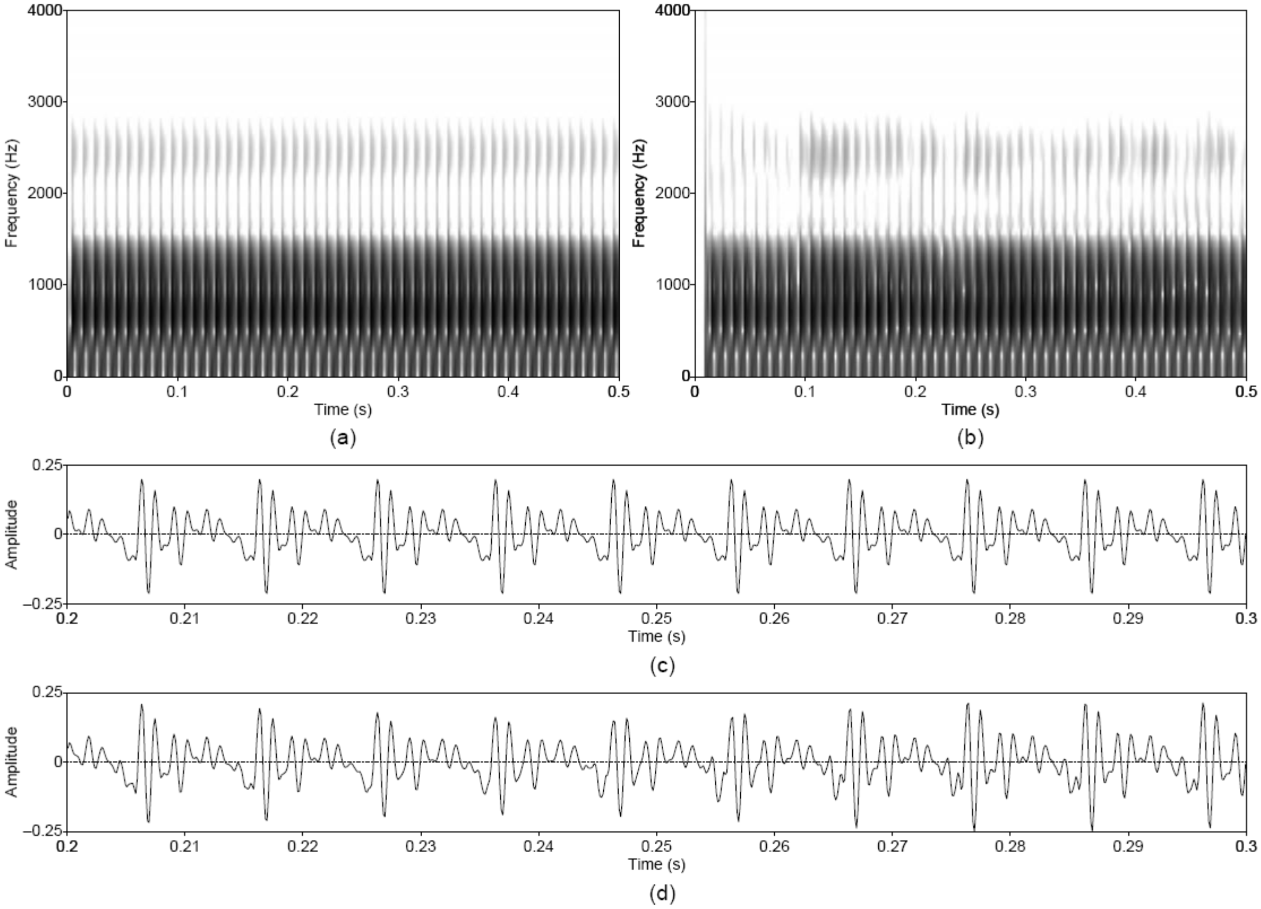

Figure 3.3 Approximate reconstruction of the harmonic component from the synthesized steady-pitch vowel. Wideband spectrograms of (a) synthesized and (b) separated harmonic components, and waveforms of (c) synthesized and (d) separated harmonic components. Waveforms are shown on an expanded time scale. Synthesis parameters: Noise type = modulated, Vowel = a, f_0 = 100, Gender = m, f_s = 8000, Duration = 1, DC = 0.1, OQ = 0.6, HNR = 10.

The output harmonic estimate (Figure 3.3d) lines up in time with the known harmonic signal input into the synthesizer (Figure 3.3c). This verifies the phase of the output. Wideband spectrograms are computed for the synthesized component and estimate in Figure 3.3a and b, respectively. These, and subsequent, spectrograms are computed with 4-ms Hanning analysis windows, half-window overlap, and a 40-dB dynamic range. The variable-length analysis windowing technique in the PSHF results in frequency bin estimates within 1–2 dB of the actual energy in the bin.

Of interest, also, is whether the envelope energy fluctuations of the input white noise source are still present in the extracted noise component at similar time locations. Figure 3.4 displays evidence that the envelope of the output noise estimate contains local maxima and minima that occur at similar times to the envelope of the input noise component.

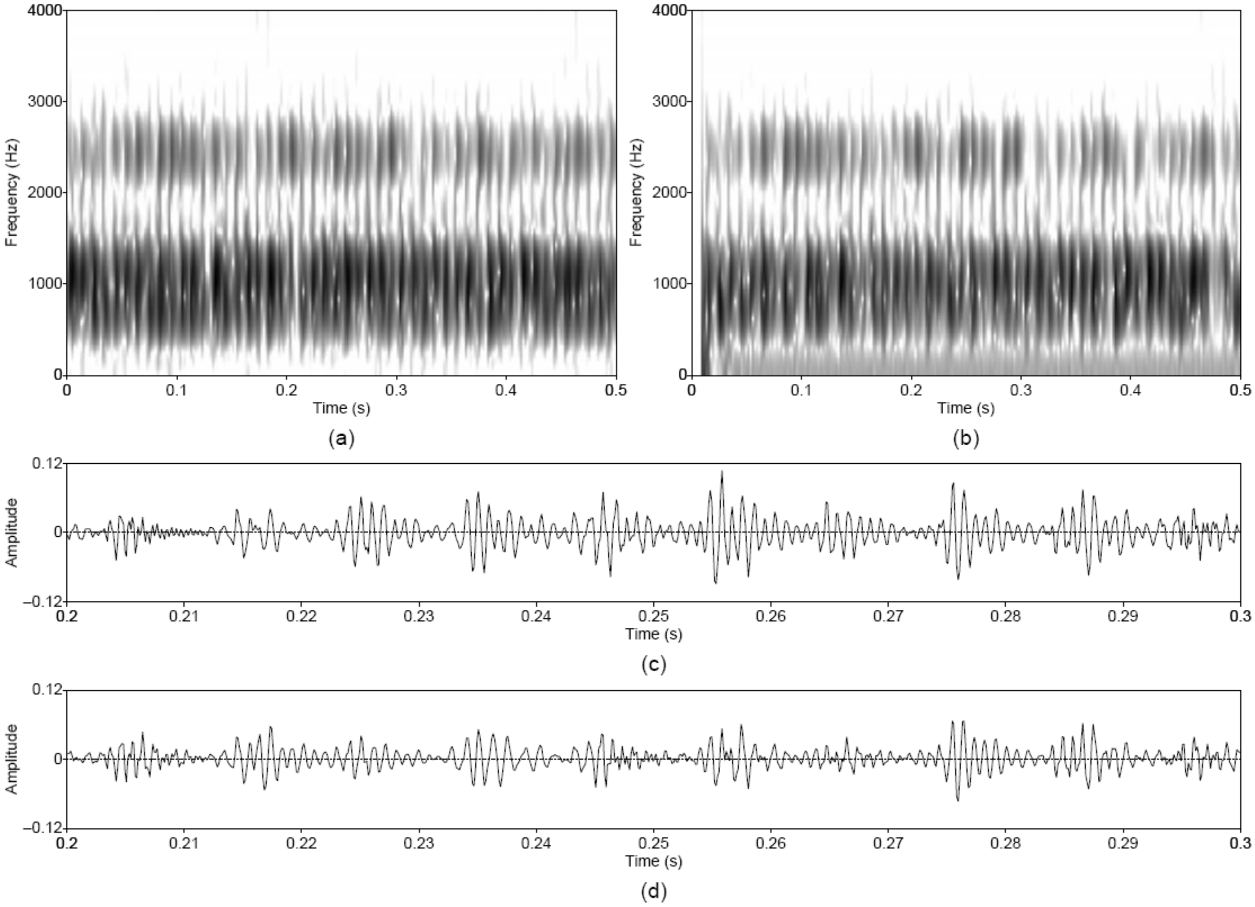

Figure 3.4 Approximate reconstruction of the modulated noise component from the synthesized steady-pitch vowel. Wideband spectrograms of (a) synthesized and (b) separated noise components, and waveforms of (c) synthesized and (d) separated noise components. Waveforms are shown on an expanded time scale. Synthesis parameters: Noise type = modulated, Vowel = a, f_0 = 100, Gender = m, f_s = 8000, Duration = 1, DC = 0.1, OQ = 0.6, HNR = 10.

A time-domain pattern can be observed in the spectrogram of the estimated noise component in Figure 3.4b, reflecting approximate fluctuations of the synthesized aspiration noise in Figure 3.4a. Focusing on an expanded time scale of 100 ms, we can make qualitative remarks on synchrony between modulations in the input and output noise waveforms. The noise modulation pattern in the synthesized waveform (Figure 3.4c) is evident at similar time instants in the noise output of the PSHF algorithm (Figure 3.4d). Due to the stochastic nature of the signal and estimation errors, though, exact reconstruction is not possible and thus noise amplitudes are not identical at input and output.

To explore whether the modulations in the noise output are not merely coincidental artifacts of the decomposition algorithm, a synthesized vowel with unmodulated noise was input into the PSHF analysis algorithm. Figure 3.5 displays wideband spectrograms of the input and output noise components. As expected, regular temporal patterns are not observable in the spectrogram of the synthesized, unmodulated aspiration noise in Figure 3.5a. A closer look at the time structure reveals envelope fluctuations of less regular modulation than the modulated noise example in Figure 3.4, reflecting inherent stochastic fluctuations.

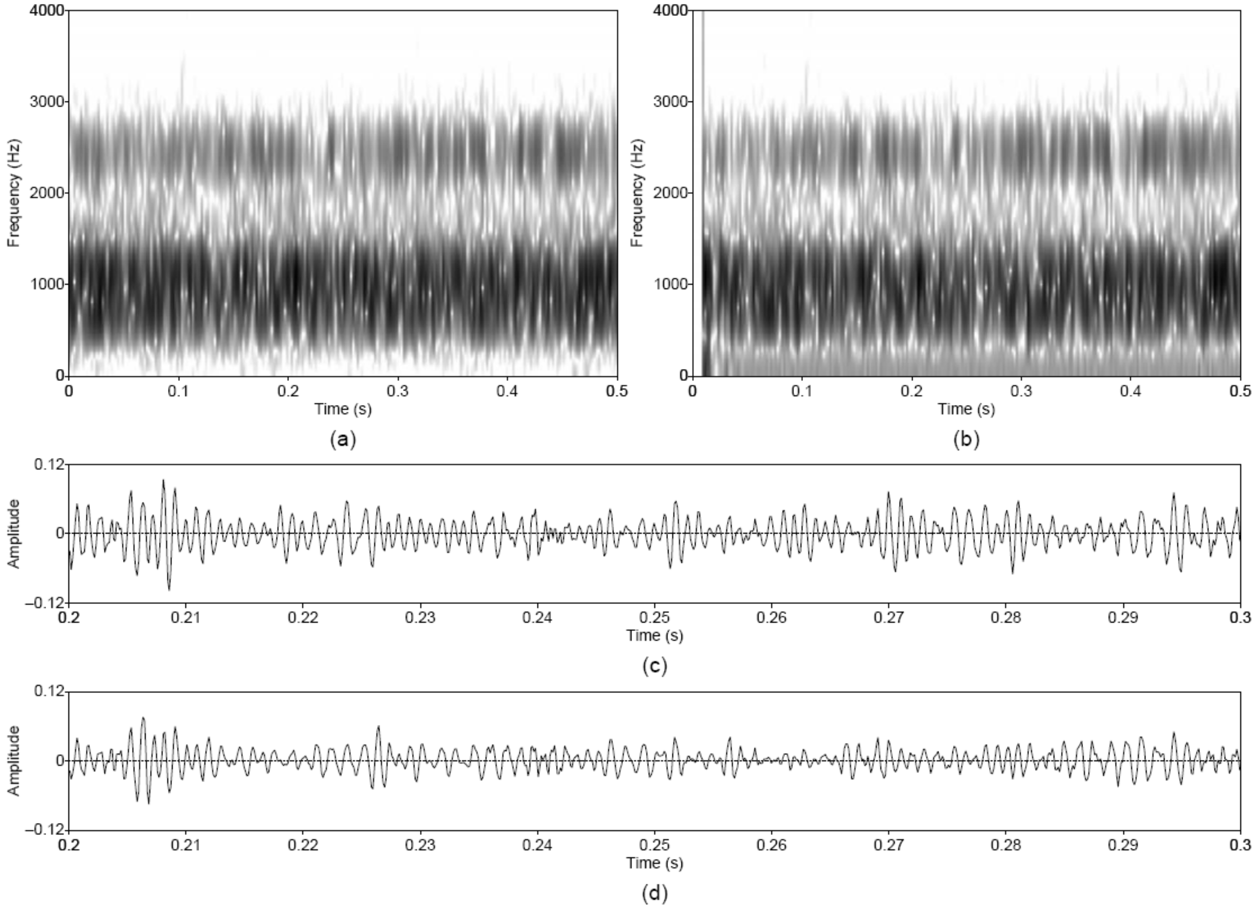

Figure 3.5. Approximate reconstruction of the unmodulated noise component from the synthesized steady-pitch vowel. Wideband spectrograms of (a) synthesized and (b) separated noise components, and waveforms of (c) synthesized and (d) separated noise components. Waveforms are shown on an expanded time scale. Synthesis parameters: Noise type = unmodulated, Vowel = a, f_0 = 100, Gender = m, f_s = 8000, Duration = 1, DC = 0.1, OQ = 0.6, HNR = 10.

Another important issue is whether the modulations in the noise estimate are at the correct phase relationship with the harmonic estimate; that is, the locations of noise source maxima should be present during the open phase of the glottal volume velocity waveform. To better observe these modulations in the noise source of the synthesized vowel, the output noise estimate is inverse filtered to remove the effect of the vocal tract filter. This operation utilizes a short-time whitening filter.

To whiten the spectrum, a Hanning window is applied to a 20-ms analysis frame. Subsequent analysis frames overlap by half the length of the window. Whitening is accomplished in each windowed segment by the following algorithm: (1) estimating an all-pole model representing the vocal tract filter spectral characteristics using linear prediction; (2) inverse-filtering the short-time segment by a finite impulse response filter whose tap weights are equal to the corresponding coefficients in the estimated all-pole model; and (3) synthesis of the resulting signal through an overlap-and-add process. Following the whitening operation, we can observe modulations in the estimate of the noise source along with any synchrony with the periodic component. A more detailed explanation of the whitening algorithm is in Section 4.5.3.

Figure 3.6 displays the output of the whitening process (solid line), representing an estimate of the aspiration noise source. Superimposed (dotted line) is the known modulation function—the synthesized glottal airflow velocity waveform—imposed on the white Gaussian noise source. The desired temporal features are approximately maintained. Maxima in the envelope of the estimated noise source occur during the open phase of the glottal period, the location of the maxima of the modulation function.

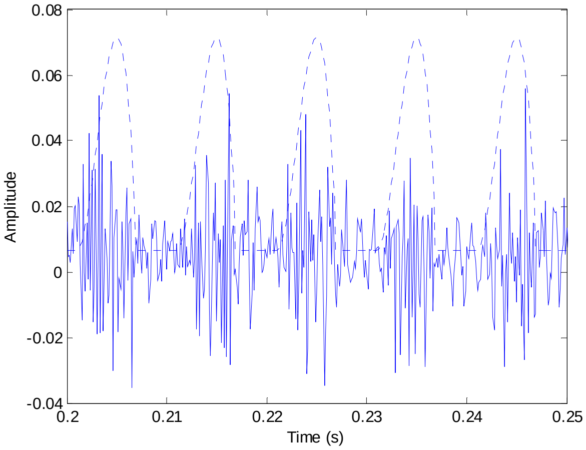

Figure 3.6 Temporal modulation structure approximately preserved by PSHF algorithm. Whitened noise component estimate (solid line) and synthesized glottal waveform (dashed line). Synthesis parameters: Noise type = modulated, Vowel = a, f_0 = 100, Gender = m, f_s = 8000, Duration = 1, DC = 0.1, OQ = 0.6, HNR = 10.

3.4 Examples of Analysis

In their work with the PSHF separation algorithm, Jackson and Shadle analyzed the noise components generated during the production of voiced fricatives [29]. Complementing their work, we analyze a different class of speech sounds, namely vowels that have a noise component generated at the source. In Section 3.4.1, example harmonic/noise component analysis is performed on a synthesized vowel with a time-varying pitch contour. Next, Section 3.4.2 applies the PSHF algorithm on real vowels, one from a normal speaker and another from a database of pathological speakers.

3.4.1 Synthesized Vowel with Time-varying Pitch

To better match the quality of a real vowel, we analyzed a synthesized vowel whose pitch linearly increased from 100 to 140 Hz over a one-second duration. The added pitch complexity tests the time resolution capability of the PSHF algorithm, its ability to track changes in the fundamental frequency of a waveform. Recall that the PSHF utilizes an analysis window of four times the local pitch period, indicating a tradeoff between time and frequency resolution due to the relatively long window length. Figure 3.7 displays the wideband spectrogram, pressure waveform, and pitch contour of the first 0.5 seconds of the synthesized vowel.

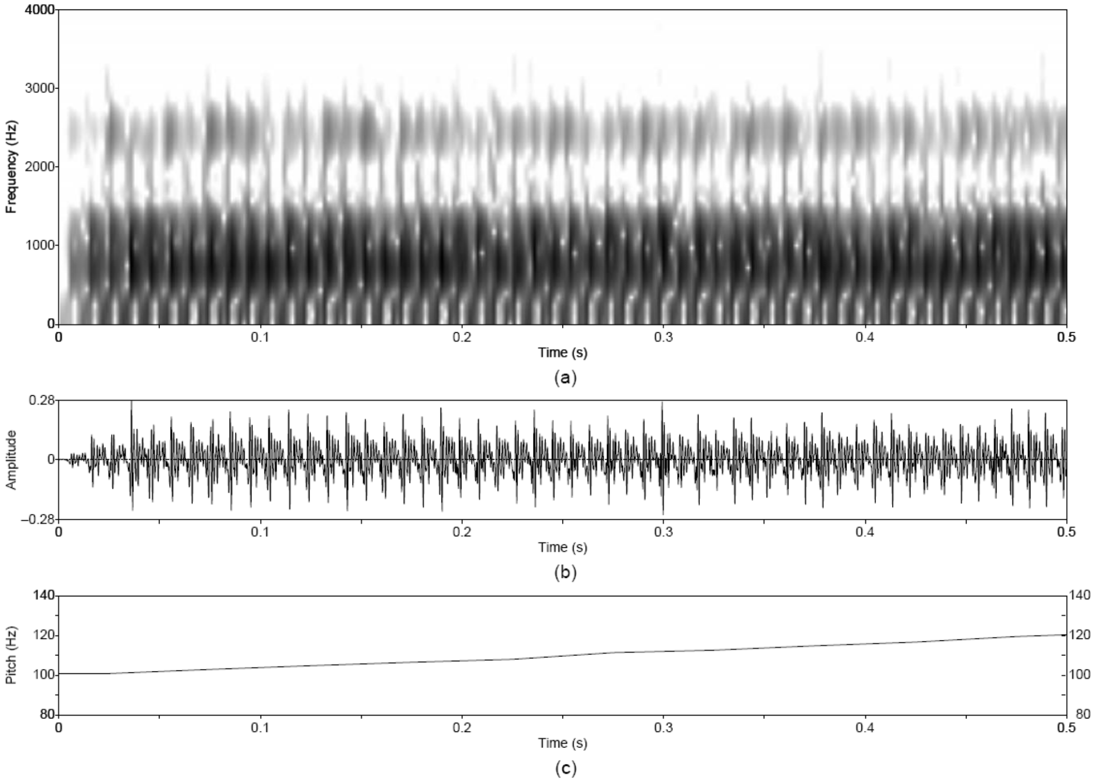

Figure 3.7 Synthesized vowel /a/ with time-varying pitch. (a) Wideband spectrogram, (b) pressure waveform, and (c) pitch contour. Synthesis parameters: Noise type = modulated, Vowel = a, f_0 = 100–140, Gender = m, f_s = 8000, Duration = 1, DC = 0.1, OQ = 0.6, HNR = 10.

Figure 3.8 displays spectrograms and pressure waveforms of the harmonic and noise estimates. As desired, the spectrograms indicate that the harmonic estimate acquires most of the harmonic energy from the input signal (Figure 3.8a and c) and that the noise estimate is stochastic with some patterns in the time domain (Figure 3.8b and d). A critical result lies in the inverse-filtered version of the noise component estimate (Figure 3.8e). Knowing that the aspiration noise source was modulated by an envelope function related to the glottal airflow, this airflow waveform (normalized) is purposely superimposed on the inverse-filtered noise waveform. As expected, the higher noise amplitudes are concentrated in the open phase of the glottal airflow waveform.

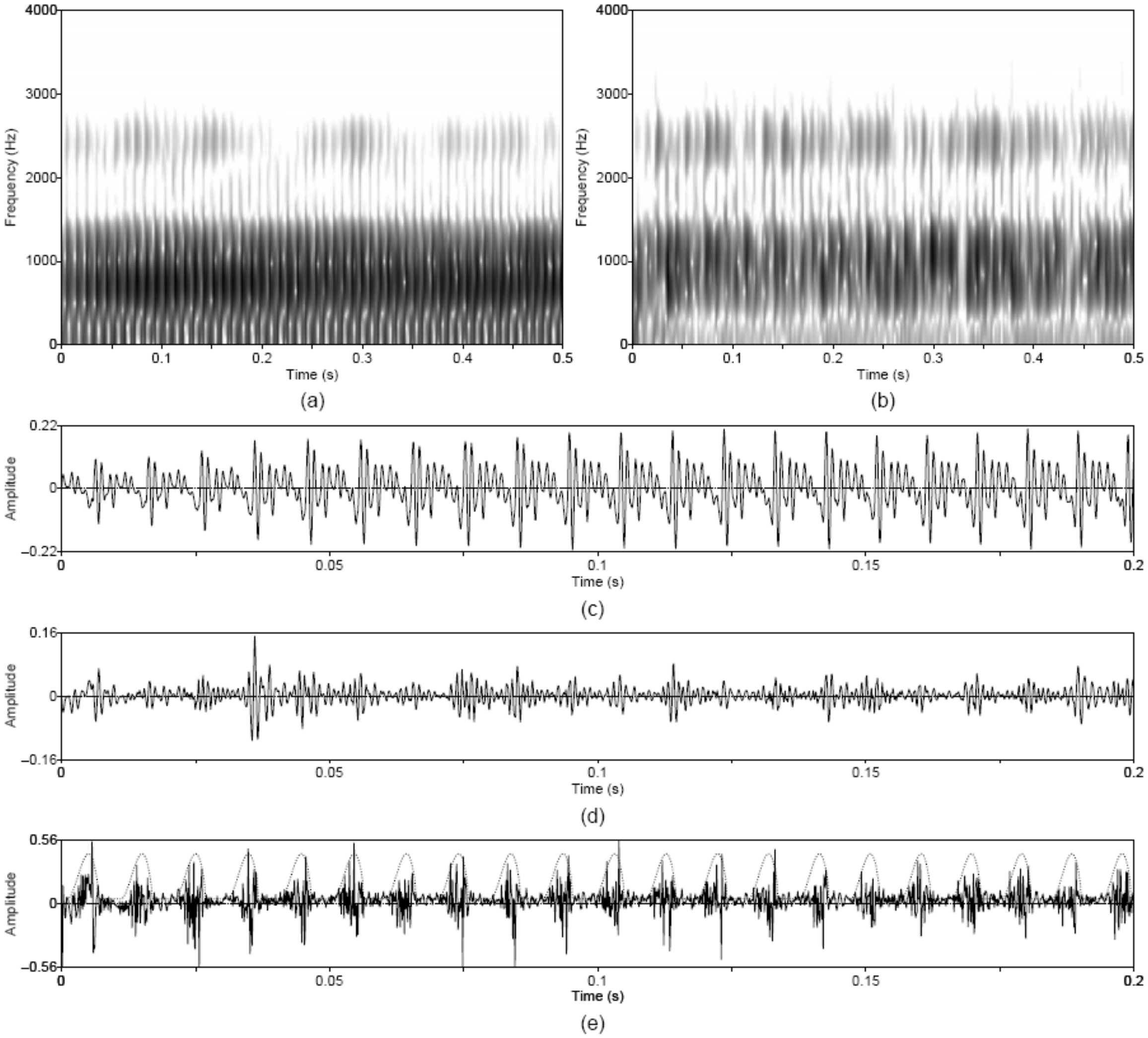

Figure 3.8 Temporal characteristics of harmonic/noise analysis on synthesized vowel with time-varying pitch. Wideband spectrograms of separated (a) harmonic and (b) noise components with pressure waveforms of (c) separated harmonic component, (d) separated noise component, and (e) whitened noise component with synthesized glottal waveform superimposed (dotted line).

3.4.2 Real Vowels

Up until now, the PSHF algorithm was tested on synthesized vowels, where the output separated components could be compared with their known synthesized counterparts. In this section, two real utterances are analyzed, one from a normal speaker and another from a speaker with a diagnosed vocal pathology.

Normal Speaker

The recording analyzed is of a non-pathological, male speaker. The speaker utters the syllable /pæ/, in which the vowel yields a slightly breathy percept. Figure 3.9 displays a wideband spectrogram and pressure waveform of the utterance. Note that the first 0.75 seconds includes the noise bursts due to the plosive release.

Figure 3.10 displays the outputs of the harmonic/noise analysis by the PSHF technique. The separated noise component is notably weaker than the harmonic component, supporting the perception that the breathiness quality is not strong. Again, of note is the presence of modulation patterns in the separated noise component. As was done in the analysis of the synthesized vowels, an inverse-filtered version of the noise component is displayed to estimate the source of the separated noise (Figure 3.10e). Dashed lines superimposed on the pressure waveforms are placed at selected instants of assumed glottal closure. See Appendix D for an explanation of how glottal closure instants are derived from a speech waveform.

The amplitude maxima of the whitened noise waveform occur at these instants; this is in extension to the time instants of noise source peaks in the vowel production model of Figure 2.3, which assumed that noise maxima occurred during the open phase of the glottal cycle. The results of this analysis indicate an additional pattern. The modulation function on the estimate of the noise source is observed to peak at instants of assumed glottal closure, as opposed to at the peak of the open phase. This result extends our vowel production model and the noise source structure in the Klatt synthesizer [36, 37], but consistent with conclusions on source synchrony in [66].

These observations of synchrony between noise bursts and assumed glottal closure are based on selected regions. For normal speaker waveforms, we have observed other modulation patterns that are consistent with the open-phase noise bursts in our vowel production model, as well as patterns that are less distinctive in the estimated noise source waveform.

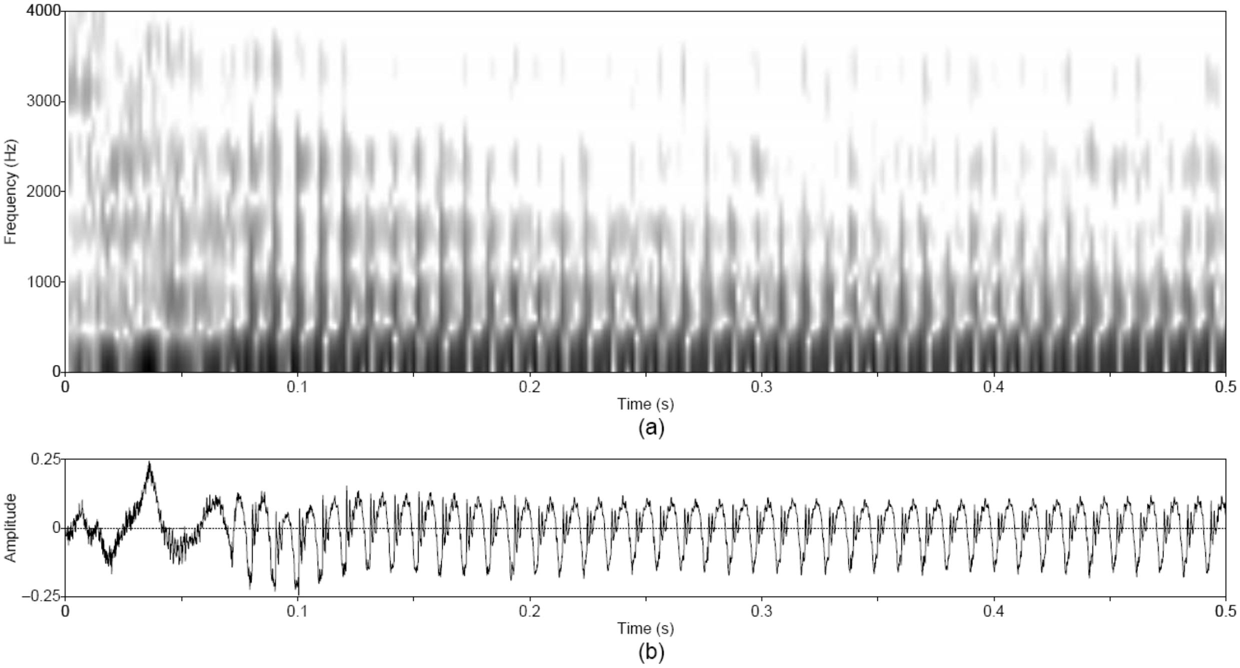

Figure 3.9 Utterance by normal speaker, /pæ/. (a) Wideband spectrogram and (b) pressure waveform.

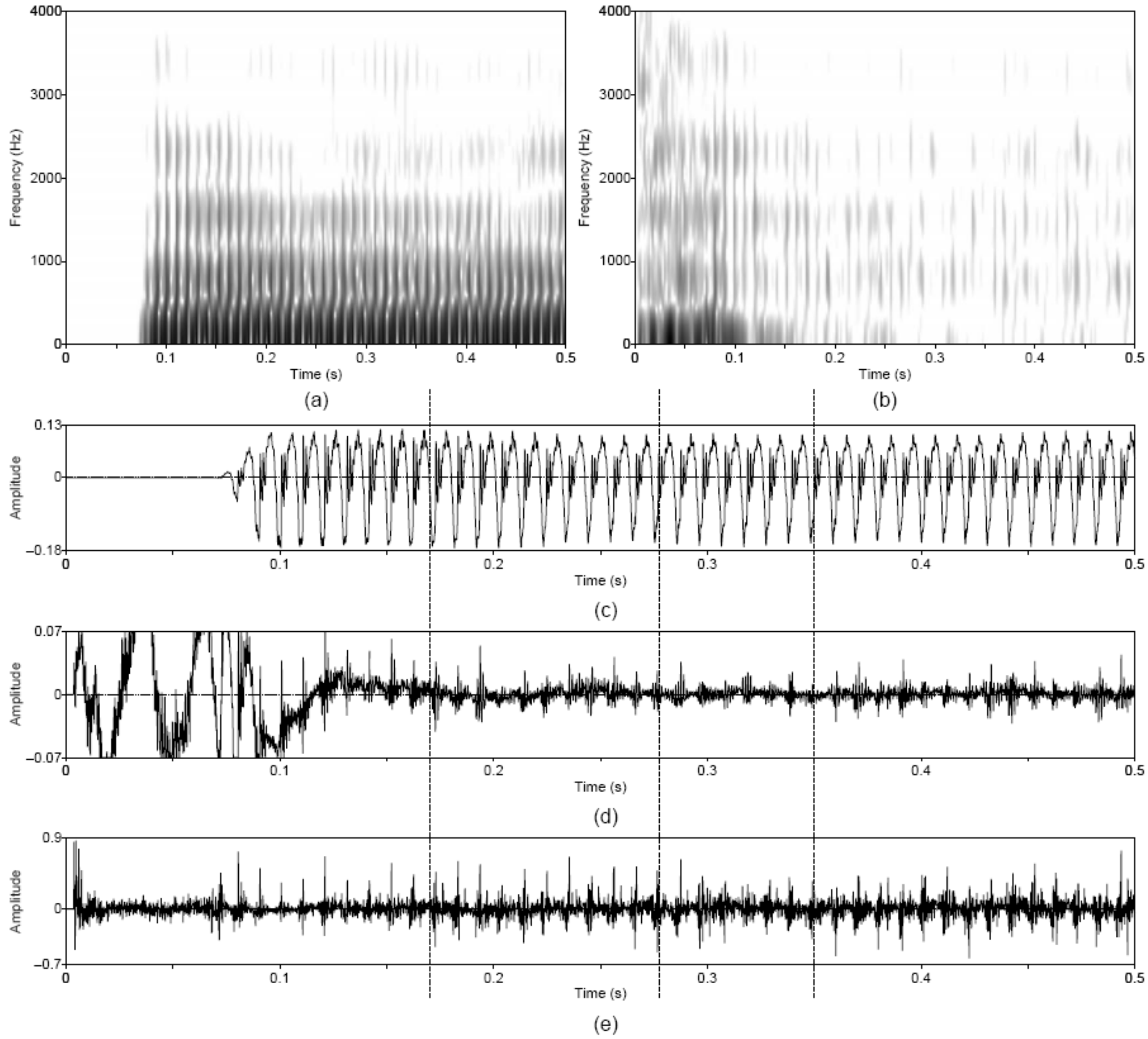

Figure 3.10 Temporal characteristics of harmonic/noise analysis on /pæ/, uttered by normal speaker. Wideband spectrograms of separated (a) harmonic and (b) noise components with pressure waveforms of (c) separated harmonic component, (d) separated noise component, and (e) whitened noise component. Dashed lines indicate sample instants of assumed glottal closure. The plosive burst is vertically clipped in (d) to zoom in on the noise modulations in the vocalic region.

Speaker with Vocal Pathology

We accessed a database of recordings from patients with disordered voice characteristics [1] since aspiration noise in the speech signal has been shown to correlate with certain vocal fold pathologies [23, 25, 26, 28, 40]. Armed with a tool to analyze the harmonic and stochastic components of an acoustic pressure waveform, we can now perform spectral and temporal analysis on the recordings of vowels produced by pathological speakers.

One such recording was selected of a male patient with a laryngeal assessment that indicated hyperfunction, anterior-posterior squeezing, and ventricular compression [1]. These descriptors together mean that the patient unconsciously seems to constrict the structures embodying the laryngeal region, forcing him to "hyperfunction" or compensate by supplying an increased air supply. This patient's case is of particular interest due to the diagnosis of a cyst on his vocal folds [1]. Due to common etiologies of cysts, it is possible that the cyst is positioned on the medial edge of the vocal folds as a scarring reaction to vocal fold trauma. The cyst could obstruct the air supply from the lungs and act as a source of air turbulence. This additional noise source would augment aspiration noise sources that are generated in the normal case. Analysis of this patient's noise source may, thus, lead to acoustic markers of the cyst's presence.

Averaged periodograms were computed over approximately one second of phonation. The original spectrum, along with the spectra of the extracted harmonic and noise components via the decomposition algorithm, is plotted in Figure 3.11. Wideband spectrogram and pressure waveforms are displayed in Figure 3.12. Immediate observations of the separated components yield promising results, but spectral leakage exists. In the spectrum of the harmonic component, the bulk of the energy is harmonic and exists below about 2000 Hz. Above this frequency, however, noise-like energy exists is observed. Similarly, in the noise spectrum, a small degree of harmonic energy is observed below 1500 Hz. These spectral leakages are possibly due to errors in pitch estimation and, most probably, to high values of jitter and shimmer in the original speech signal. The PSHF algorithm breaks down not only at high aspiration noise levels, but also in the face of high jitter and shimmer values. Improving PSHF performance on disordered voices having these perturbations is mentioned as an issue deserving future analysis (Section 5.1).

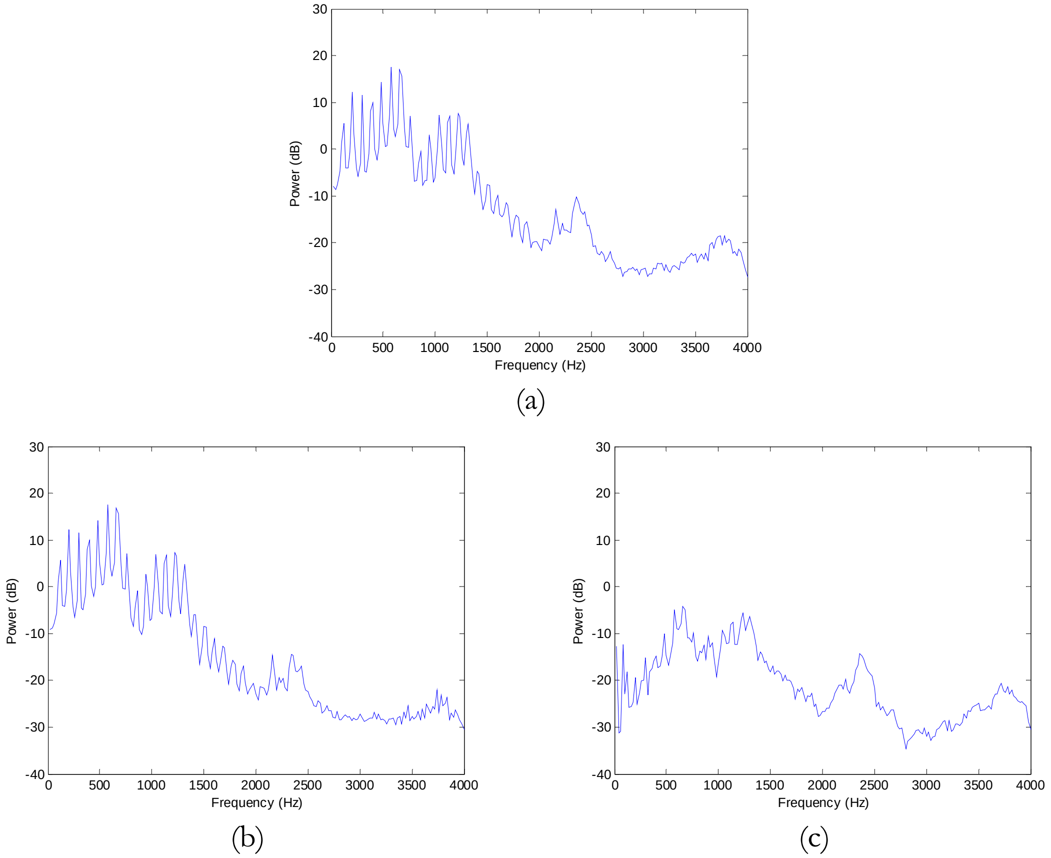

(a)

(b)

(c)

Figure 3.11 Harmonic/noise analysis speaker with vocal pathology. Periodograms of (a) synthesized vowel, (b) harmonic estimate, and (c) noise estimate.

Analysis proceeds in the time domain as was done previously. Figure 3.13 displays sampled sections of the signals output from the decomposition algorithm and an estimate of the source of the noise component. Local peaks in noise amplitude are observed in the noise source estimate. Furthermore, although some of these peaks coincide with the assumed open phase of the glottis (vertical dashed line), other noise peaks occur at times that coincide with the glottal pulse instants (vertical dotted line). Thus, we see modulation phenomena similar to what was seen above in the normal utterance and data that reflect our vowel production model. Fortunately, although our model assumes only modulations with maximum noise amplitude during the open phase, the decomposition algorithm makes no assumptions regarding temporal characteristics of the extracted harmonic and noise estimates.

The aerodynamics interactions at the glottis act as an additional source of noise in the airway, and this was alluded to above owing to the presence of vocal fold cysts. Though these noise modulations have been previously documented in analyses of pathological voices [28], the authors did not inverse-filter the noise component to observe the characteristics of the source waveforms, which we have shown to better illustrate the modulation function.

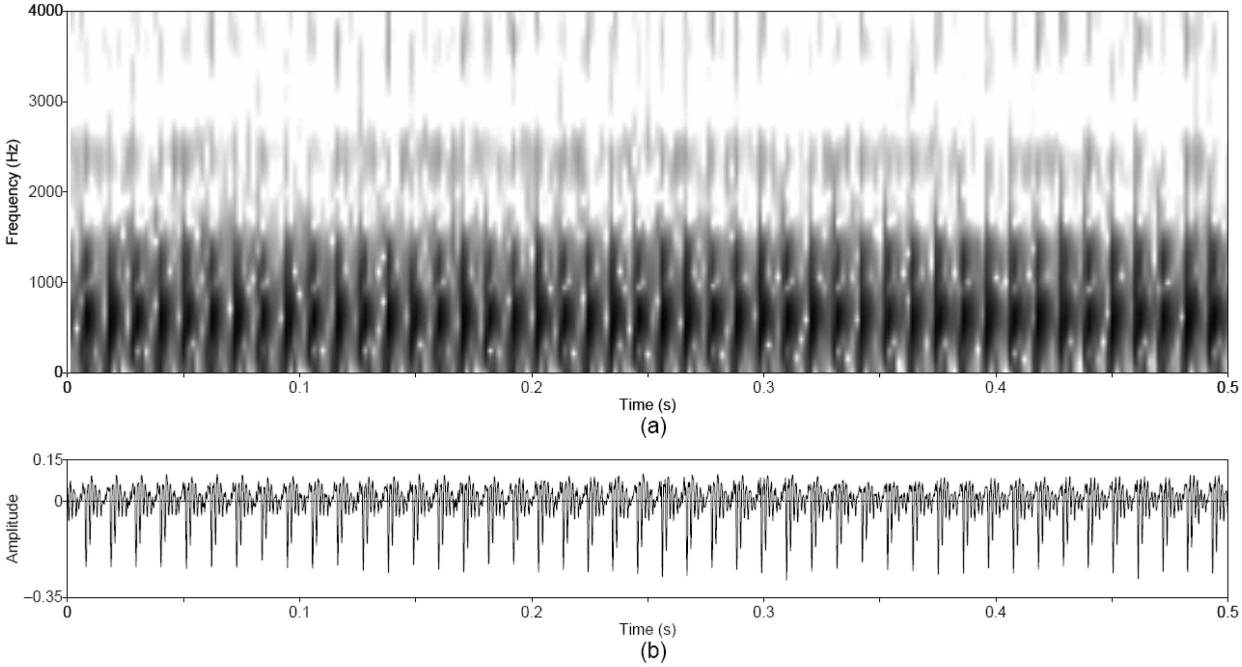

Figure 3.12 Sustained vowel /a/ uttered by speaker with vocal pathology. (a) Wideband spectrogram and (b) pressure waveform.

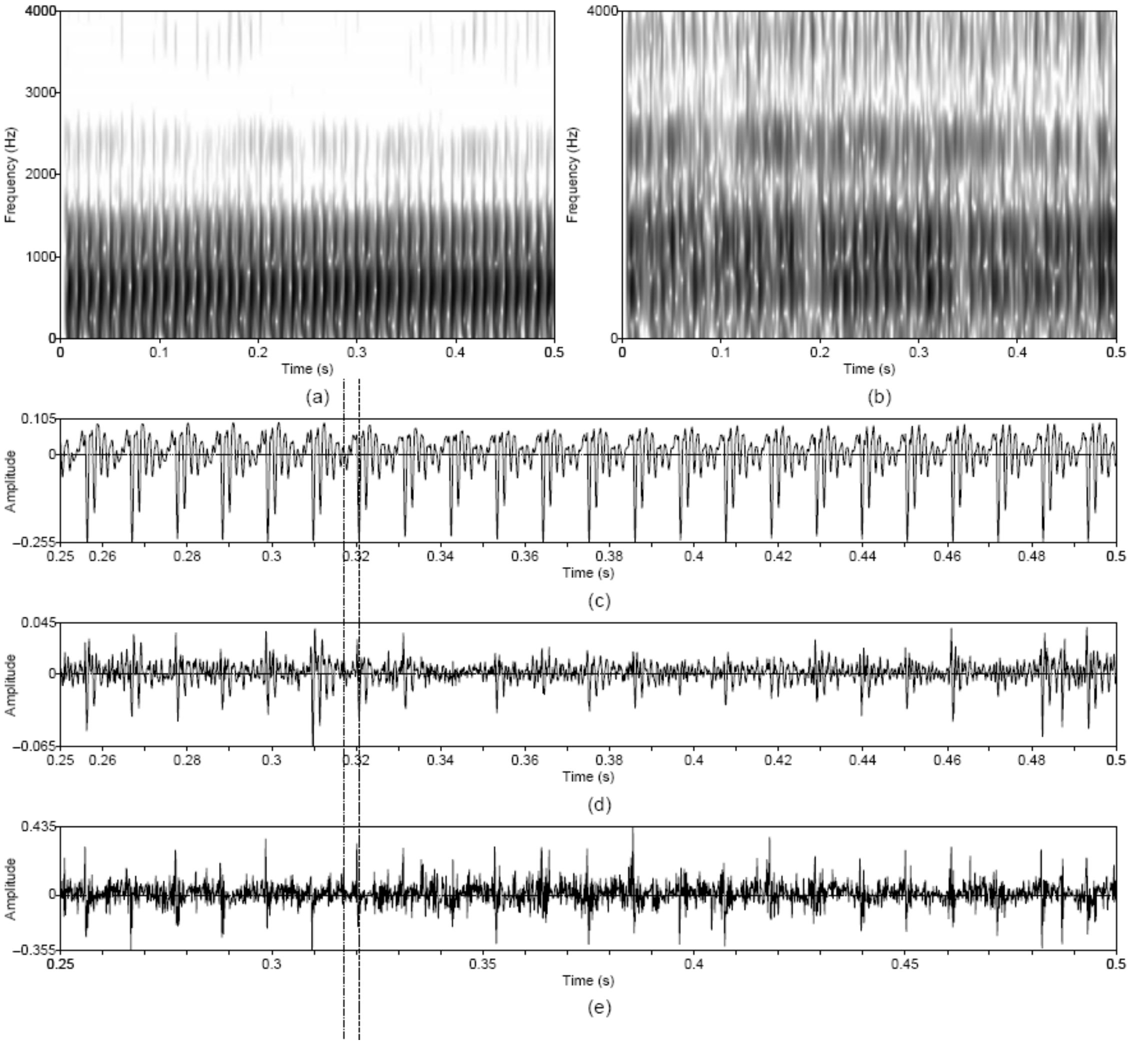

Figure 3.13 Temporal characteristics of harmonic/noise analysis on /a/ uttered by pathological speaker. Wideband spectrograms of separated (a) harmonic and (b) noise components with pressure waveforms of (c) separated harmonic component, (d) separated noise component, and (e) whitened noise component. Left dotted line indicates sample instant of assumed glottal closure. Right dashed line indicates sample instant of assumed peak in open phase of glottal cycle.

3.5 Summary and Conclusions

Following the development of a modeling and synthesis framework in Chapter 2, Chapter 3 dealt with the issue of separating the two additive components in the model—harmonic and noise. A review of three analysis techniques was presented, followed by limitations of these techniques. Based on its published performance and ease of implementation, the pitch-scaled harmonic filter (PSHF) algorithm was selected for further analysis. The algorithm is developed in work by Jackson and Shadle and documented in [29-31]. In Section 3.3, we submitted their algorithm to our own testing using a vowel synthesized, in which all the input source waveforms are known. Finally, Section 3.4 presented analysis of more natural vowels, including one synthesized vowel and two human-produced vowels. One human-produced vowel was from a normal speaker, and the other was from a speaker with a vocal pathology.

Modulations in the noise source waveform and their synchrony with the periodic source were shown to be important for natural-sounding vowel synthesis in Section 2.5, and these modulations were approximately preserved in the output of the PSHF algorithm. Although leakage of noise into the harmonic component estimate was observed, we attribute the deviations to estimation error and excessive levels of jitter and shimmer, a subject for further work (Section 5.1).

From our analysis of real vowels, we speculate that two types of temporal modulations are present in the inverse-filtered version of the separated aspiration noise component. Local peaks in noise amplitude seemed to coincide with (a) the open phase of the glottal cycle and (b) time instants of glottal closure. Thus, we see modulation phenomena that add to the modulation properties in our vowel production model in Figure 2.5. Although the model assumes only modulations with maximum noise amplitude during the open phase, the decomposition algorithm makes no assumptions regarding temporal characteristics of the separated component and can reveal other noise properties.

In Chapter 4, we apply the ideas of physiologically-plausible synthesis from Chapter 2 and the useful harmonic/noise analysis algorithm from Chapter 3 to accomplish high-quality pitch-scale modification of speech.

Chapter 4

Pitch-Scale Modification

In Chapter 3, we presented evidence that modulations occur in aspiration noise during phonation. It is desirable to take advantage of this knowledge in a speech modification system, which can benefit from signal characteristics of perceptual importance. In this section, we apply our modulation model to the development of a pitch-scale modification algorithm. Applications of pitch modification include text-to-speech synthesizers that concatenate acoustical units of speech, batch-mode and real-time voice modification, and audio processing needs in the recording and entertainment industries.

Section 4.1 first describes the approaches of current selected pitch modification algorithms and their limitations. Section 4.2 presents an overview of how humans modify the fundamental frequency of their voice, and this motivates a physiologically-based pitch modification model, discussed in Section 4.3. Section 4.5 details our implementation of pitch-scale modification based on the model. Finally, Section 4.6 presents our results from modifying synthesized and real vowel waveforms.

4.1 Signal Processing Background

The goal of pitch-scale modification is to modify the fundamental frequency of a speech signal without affecting the underlying spectral envelope or its trajectory throughout the utterance. Recall that the fundamental frequency is the vibration frequency of the vocal folds. In the speech signal, the fundamental is usually evident in time-domain periodicity as well as being the lowest harmonic in the spectrum. A survey and comparison of selected state-of-the-art techniques of pitch modification are presented in this section, followed by limitations that motivate the need for an alternate strategy.

4.1.1 Algorithms

The myriad of speech sounds contains many distinct spectral qualities that occur on time scales of milliseconds. An approach that analyzes short-time segments of the speech signal is necessary because one long-time Fourier transform cannot describe the dynamics of the underlying frequency response. A popular approach and framework for processing speech signals, introduced in Chapter 3, is the analysis/synthesis framework termed overlap-add (OLA). This was the framework for the PSHF algorithm implemented in Section 3.2. In a general OLA algorithm, analysis time instants are selected in the original signal at which finite-length windows are centered to obtain short-time frames. The central assumption of stationarity requires that the spectral characteristics do not rapidly vary within the frame, thus allowing for the use of the Fourier transform on a short-time basis.

In our short-time world, we will focus on algorithms that assume that the original signal is based on the linear source-filter model of speech similar to our vowel production model developed in Section 2.2. The types of algorithms are categorized into non-parametric and parametric classes. Parametric methods attempt to fit the speech signal to a given model before modifying the model's physical parameters. Non-parametric methods instead process the speech signal without fitting to a specific model. Within these two categories, we will see that modifications can be performed in the time or frequency domain.

Non-Parametric Methods

Several non-parametric methods have been developed for pitch modification [54]. A sampling of these methods is chosen to give a flavor for the different approaches. These methods fall into two categories, depending on whether the analysis instants are at a fixed or variable rate. Recall that the original signal, $s[n]$, is segmented by windowing overlapping sections, centered on the analysis instants, d:

$$s[n,r] = s[n]w[n - d + \tfrac{N}{2}], \tag{4.1}$$

where $w[n]$ is the analysis window and N is the window length. Processing is thus done on a frame-by-frame basis.

In a fixed-rate analysis system, $d = rD$, where D is the fixed distance between analysis instants and r is the frame index. To perform pitch modification, these algorithms follow a series of steps involving (1) source estimation, (2) resampling the source signal, and (3) re-imposing spectral characteristics. Source estimation, though, is not unique to fixed-rate systems, but it is a common way to avoid modifying spectral properties due to the vocal tract resonances. This first step assumes an impulsive excitation model of voiced speech and attempts to whiten the speech signal to estimate the source. Whitening often involves inverse-filtering the poles of the spectrum using linear prediction analysis [63]. Alternative methods of source estimation achieve a flat source spectrum by either dividing the magnitude spectrum by an estimate of its envelope or by an estimate of an all-pole fit to the zero-phased envelope [54]. Armed with an estimate of the source, the second step resamples the time-domain waveform to modify the excitation times to fit the new fundamental frequency contour. The third and final step re-imposes the spectral characteristics on the modified source waveform.

In a variable-rate analysis system, d in Equation (4.1) can represent sample times that are not necessarily a fixed distance apart. In a popular technique termed pitch-scale overlap-add (PSOLA), the analysis time samples are set at instants of glottal closure that are estimated from $s[n]$. (See Appendix D for our definition of glottal closure instant.) Short-time frames of length N are centered on these instants, where N is an integer multiple of the local pitch period.

In a frequency-domain PSOLA implementation (FD-PSOLA), N is usually equal to 4 times the local pitch period length, giving the required spectral resolution. The modified harmonics are calculated by resampling the discrete Fourier transform and interpolating between samples if necessary [53, 54]. In a time-domain implementation (TD-PSOLA), N is chosen to be smaller (two times the period) for better time resolution. The new pitch contour is computed, and then the synthesis time instants are calculated based on the new pitch contour. The next step, unique to TD-PSOLA, maps the analysis frames to synthesis time instants or discards them entirely depending on the pitch scale [53, 54]. A more complete description of TD-PSOLA is presented in Section 4.5.2. As suggested above, source estimation can also be performed as a first step in variable-rate methods, including linear-predictive PSOLA, or LP-PSOLA [78]. Overlap-add synthesis then merges the modified frames together after vocal tract filtering.

Parametric Methods

Table 4.1 compares the features of three parametric methods of pitch modification. The features indicate whether the researchers chose a time-domain or frequency-domain processing strategy, whether a spectral voiced/unvoiced decision was made, and whether harmonicity of the signal was assumed.

Researchers	TD or FD modification	Boundary frequency	Harmonic constraint
Quatieri and McAulay [64, 65]	FD	Yes	No
Macon and Clements [46]	FD	No	No
Stylianou et al. [74, 75]	FD	Yes	Yes

Table 4.1 Comparison of pitch-scale modification algorithms. TD = time-domain, FD = frequency-domain.

McAulay and Quatieri have developed a speech modification system [64, 65] based on an analysis/synthesis system that models all speech sounds as a sum of sinusoids [48]. Even fricative sounds and plosive bursts are modeled using sinusoids. Each sinewave has a time-varying amplitude and time-varying phase associated with it:

$$s(t) = \sum_{k=1}^{M} A_k(t) \cos[\theta_k(t)], \tag{4.2}$$

where M is the number of sinusoids, $A_k(t)$ is the amplitude associated with the k th sinewave, and $\theta_k(t)$ is the cosine phase of the k th sinewave. A degree of voicing measure sets a boundary frequency in the speech spectrum, below which voiced speech is assumed and above which noise is assumed. The sinewave frequencies themselves are chosen using a peak-picking algorithm in which the frequencies are not constrained to be harmonically-related. After this analysis stage, the sinewave-based system accomplishes pitch modification by scaling the frequencies of the sinusoids in the voiced region by the desired pitch scale ratio, while maintaining the spectral envelope. Re-synthesis of the sinusoids completes the technique.

Similarly, another sinusoidal modeling technique by Macon and Clements [46] represents speech as a sum of possibly non-harmonic sinusoids to represent both harmonic and noise components. To better handle the modification of noise components, a degree of voicing index is used to set the phase characteristics of the speech spectrum. Instead of specifying a cutoff frequency (as above by McAulay and Quatieri), the voicing index leads to a phase randomization that supposedly synthesizes better noise characteristics.

Stylianou, Laroche, and Moulines have detailed their development of a modification algorithm based on their "harmonic + noise model" of speech [43, 74, 75]. The crux of their model is sinewave-based, where time-domain estimation over two periods of a voiced signal is employed to determine amplitude, frequency, and phase parameters:

$$s(t) = \sum_{k=1}^{M} A_k(t)\cos\left[k\omega_0 t + \phi_k(t)\right]. \tag{4.3}$$

The main difference with the previous algorithms is that these parameters are computed only for a harmonic estimate of the signal. A boundary frequency in the spectrum separates the speech spectrum into harmonic and noise regions. Energy below this boundary frequency is assumed to be harmonic, and energy above is considered due to noise sources. The harmonics are modified by resampling the spectrum at the new fundamental frequency and its harmonics up to the boundary frequency.

An enhancement in this technique is that the noise component is modified also, which was not done in the previous two algorithms. The noise component is assumed to be concentrated during the open phase of the periodic glottal cycle and not present over the entire pitch period duration. To take this into account, a triangular envelope is imposed on a re-synthesized noise signal to result in the aspiration noise component. Note that the envelope is imposed after the noise has been filtered by the vocal tract characteristic, whose all-pole model is estimated by linear prediction analysis (linear prediction of a stochastic signal is described in Appendix E).

4.1.2 Limitations

To increase the pitch in most non-parametric fixed-rate methods, the source signal is downsampled, and a high-frequency portion of the spectrum is discarded. To regenerate the high frequencies, spectral folding or copying must be used to fill in this range [54]. Perceptually, this is sub-optimal, especially for speech signals sampled at low rates (8kHz). Other drawbacks of fixed-rate methods include the difficulty in using linear prediction to effectively estimate the vocal tract filter with an all-pole model. Nasals, with their added spectral zeros [73], are not handled well, and high-pitched speech also present problems since the all-pole model may incorrectly model each harmonic as a pole.

Drawbacks to the TD-PSOLA method include the generation of pseudo-periodicity of noise due to the replication of pitch periods and the requirement of accurate estimates of glottal closure time instants. The method also does not allow for separate control and modification of the noise signal if desired, which is an advantage for parametric techniques. The success of TD-PSOLA, however, lies in its ability to smoothly duplicate or eliminate parts of the speech signal at a pitch-synchronous rate [54].

In the sinewave-based systems above [46, 64, 65], the researchers fit the speech to a sum of sinusoids without regard to temporal features of the aspiration noise source, namely the modulations that were observed in Section 3.4. An advantage of sinewave modeling, though, is that all signals are fit to the same model, and modifications of different signal components do not have to be aligned. In addition, sinewaves may better represent sharp vowel onset attacks and plosive noise bursts than a white noise model, as was done by Stylianou et al. [63] A tonal character, however, has been heard while perceiving modified stochastic signals in the sinewave-based systems [63]. In addition, the peak-picking process in sinewave analysis removes much of the energy of the aspiration component present in the voiced region of the original spectrum. Finally, the boundary frequency is sometimes inaccurate, thus under- or over-estimating the voiced spectral region.

Parametric modification by Stylianou et al. [74, 75] attempts to take into noise modulations in speech and maintain the modulations at the modified pitch rate. Estimation of the noise component is done by picking a high frequency region. Since aspiration noise has been shown to exist across the spectrum and not just at certain frequencies (recall Sections 2.2 and 3.4.2), a fullband decomposition technique like that in Chapter 3 would better estimate the noise component. In addition, though the authors appropriately address the need for noise modulations, the modulation function imposed is on the noise component itself and not on the source waveform, which would be more consistent with our vowel production model (Figure 2.3). Also, contrary to arbitrarily selecting a triangular shape as the modulation function, we feel that a non-parametric method of estimating the true modulation function will result in a more accurate noise representation.

The impetus for a novel pitch modification stemmed from an interest in improving on the above speech signal processing systems, which perform sub-optimally on voiced speech that contains an aspiration noise component.

4.2 Physiology of Pitch Control

In Section 2.1 above, we described the view of the voice source mechanism through a myo-elastic aerodynamic theory [73]. Once the subglottal pressure increases passed threshold of vibration, the airflow from the lungs reduces the differential pressure at the glottis, and Bernoulli forces bring the vocal folds together. In opposition, the stiffness and compliance of the vocal folds act to force the structures apart. Thus, a pseudo-periodic oscillation occurs. At quiet sound production levels, only a superficial layer or "cover" vibrates, while at normal and loud levels, both the cover and a deeper "body" layer vibrate [58]. A simplified view is to model the system as a vibrating string with fundamental frequency, f_0 (from [57]):

$$f_0 = \frac{1}{2L}\sqrt{\frac{\sigma}{\rho}}, \tag{4.4}$$

where L is the length of the string, σ denotes stress, and ρ is the string density. A similar, but certainly more complex scenario, can model the relationship between fundamental frequency and the physical properties of the vocal folds.

The main factor determining f_0 is tension, which is dictated by properties of the vocalis muscles of the vocal folds. The stiffnesses of the body and cover of the vocal folds are largely due to the activity of the thyroarytenoid and cricothyroid muscles [58]. Since these muscles act more or less independently from modifications of the vocal tract shape, we view the source mechanism as independent and decoupled from the filter. In reality, however, humans change the pitch of their voice with concomitant changes in jaw, lip, and tongue movements. This observation of coupling between pitch and formants is explored for future improvements in Section 5.1.4.

Barring this caveat, pitch-scale modification of speech signals can be performed by changing the source excitation properties without affecting the spectral characteristics due to the vocal tract filter. Of particular interest is how the generation of turbulent noise is affected during a pitch change. The signal processing approach below assumes that modulations of the aspiration noise source follow the glottal waveform at the new fundamental frequency; that is, according to the vowel production model in Figure 2.3, pitch modification needs to preserve the time-domain coupling between the airflow volume velocity waveform and the aspiration noise source.

4.3 Pitch Modification Model

When performing pitch modification, the system should recognize any modulations present in the aspiration noise source component and preserve synchrony between the periodic and noise components. In this way, speech processing attempts to emulate the way that we modify the pitch of our voice physiologically. Our model of pitch modification is displayed in Figure 4.1. Note that the only difference between this model and the vowel production model in Figure 2.3 is the change in the pitch period of the periodic glottal airflow waveform. The source at Pitch 1 has a fundamental frequency equal to $\frac{1}{T_0}$ Hz, where T_0 is the duration between successive glottal closure instants (Appendix D). Pitch 2 in the model represents a periodic source at a higher rate and thus having a higher fundamental frequency equal to $\frac{1}{T_0^{'}'}$ Hz. Also note that changing the glottal flow rate simultaneously affects the modulation function on the white noise aspiration source. Filtering mechanisms that act on the source are assumed unchanging during pitch modification.

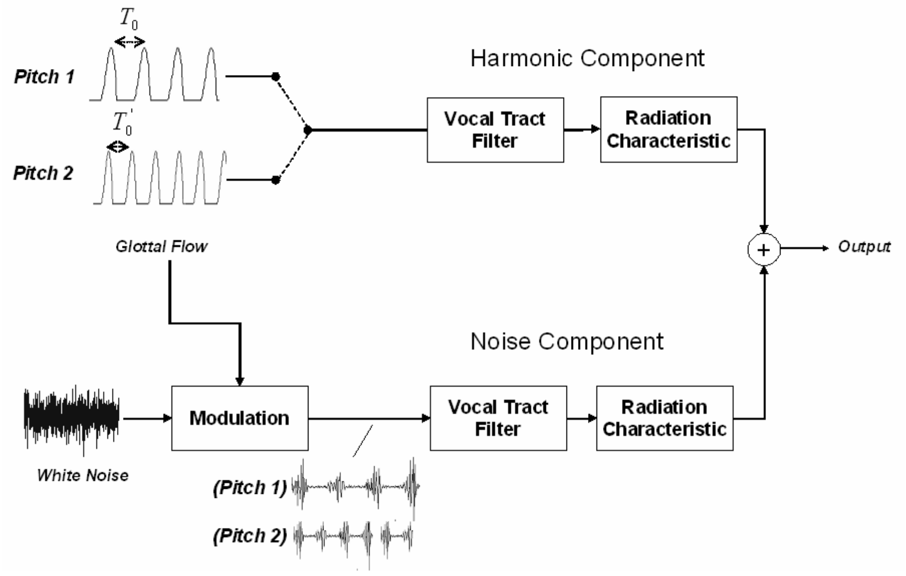

Figure 4.1 Pitch modification model.

Recall the waveforms generated in synthesizing a vowel signal, $s[n]$:

$$\begin{aligned} s[n] &= \left(x_p[n]*r[n]\right)+\left(x_n[n]*r[n]\right) \\ &= \left(u_g[n]*h[n]*r[n]\right)+\left(q[n]u_g[n]*h[n]*r[n]\right) \\ &= \left(p[n]*g[n]*h[n]*r[n]\right)+\left(q[n]u_g[n]*h[n]*r[n]\right). \end{aligned} \tag{4.5}$$

The periodic portion of voiced speech is represented by the expression $\left(p[n]*g[n]*h[n]*r[n]\right)$, where $p[n]$ is the impulsive excitation spaced by a pitch period to a chain of linear time-invariant filters with impulse responses $g[n]$, $h[n]$, and $r[n]$. These filters represent the glottal waveform shape, vocal tract acoustic filter, and radiation characteristic, respectively. The aperiodic or noise portion of voiced speech is represented by the expression $\left(q[n]u_g[n]*h[n]*r[n]\right)$, where $q[n]u_g[n]$ is the stochastic excitation to the same filters $h[n]$ and $r[n]$, $q[n]$ being the multiplicative modulation function and $u_g[n]$.

4.4 Proposed Approach

The pitch modification system developed in this study is non-parametric and estimates the envelope of the estimated noise source without assuming a specific shape for the envelope. In addition, the inherent speech noise is not re-synthesized with an arbitrary white Gaussian noise source (as was done by Stylianou et al. [43, 74, 75]). To approach the problem of accurate pitch modification, we attempt to reverse-engineer the physiological pitch modification model of Figure 4.1. A diagram outlining our pitch-scale modification algorithm is shown in Figure 4.2.

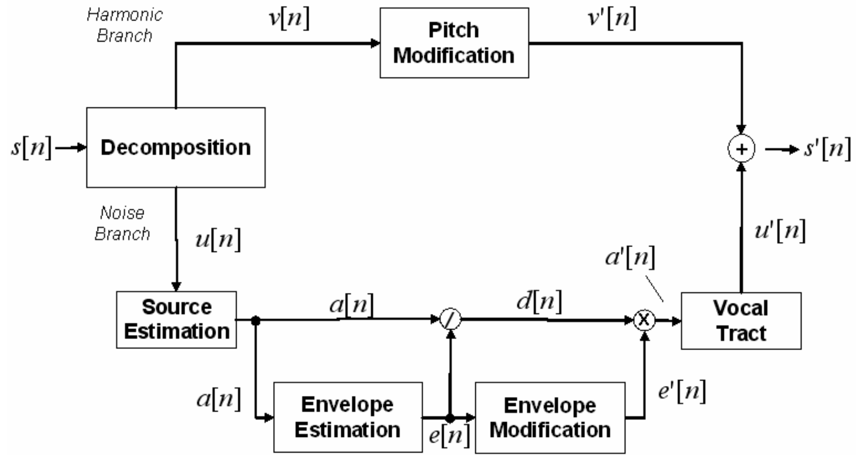

Figure 4.2 Block diagram of approach to pitch-scale modification.

The aim of the Decomposition block is to reverse the summation step and decompose the signal into periodic and noise components. With this decomposition, any changes made to the periodic portion of speech can be balanced by modifications in the aspiration noise component. We denote the input speech signal as $s[n]$, and the harmonic and noise estimates from the Decomposition block $v[n]$ and $u[n]$, respectively.

The flow diagram then splits the processing stages into two branches: the Harmonic Branch and the Noise Branch. In the Harmonic Branch, standard techniques can be applied to scale the pitch of the harmonic component estimate. The harmonic component at the new fundamental frequency, $v'[n]$, is then summed to the modified noise component, $u'[n]$. This additive model is identical to the vowel production model of Figure 2.3.

The Noise Branch in Figure 4.2 warrants more complex signal processing. To preserve temporal synchrony between traits of the periodic and noise sources (see discussion in Section 2.6), a mechanism is designed to estimate the aspiration noise source from the aggregate noise component estimate, $u[n]$. Algorithms that would usually be applied in a one-step Pitch Modification block, as in the Harmonic Branch, would not work in the Noise Branch. These algorithms traditionally need to be able to compute correlations for pitch determination, which is prohibitive in white noise signals. Thus, complexity is added to modify the noise component in the Noise Branch.

Modification of the aspiration noise source is accomplished by first removing the spectral effects of the vocal tract filter and radiation characteristic in the Source Estimation block. The output signal, $a[n]$, can be viewed as the source estimate from the aspiration noise signal, $u_g[n]$. For instance, if a linear filter with impulse response $h^{-1}[n]$ were designed for this block, we would utilize the following equation:

$$a[n] = u_g[n] * h^{-1}[n]. \tag{4.6}$$

The result is an estimate of the aspiration noise source, which is related to the noise source waveform, $q[n]u_g[n]$. The waveform, $a[n]$, thus has features of a white noise signal with a modulation function imposed on it. Since modifying the fundamental frequency of the harmonic component involves shifting the time instances of glottal excitation (recall Section 4.1), and since the noise component contains modulations that occur at certain times within the glottal cycle (recall Section 3.5), the noise modulations must be modified in the same manner. The approach we take is to de-modulate and re-modulate the noise source with a new modulation function scaled by the pitch modification factor.

The Envelope Estimation block computes $e[n]$, a waveform related to the glottal flow waveform (recall the coupling between the two sources in Figure 4.1). With the modulation function computed, we divide out the effect of the envelope to result in an estimate of the de-modulated white noise estimate, $d[n]$:

$$d[n] = \frac{a[n]}{e[n]}. \tag{4.7}$$

The remaining intermediate waveforms in our flow diagram are "prime" versions of waveforms described so far. The "prime" indicates that the waveform is at the new fundamental frequency. The Envelope Modification block in Figure 4.2 changes the rate of the modulation function so that modulations in the noise source are now synchronized with the modified harmonic component, $v'[n]$. The new envelope, $e'[n]$, is a pitch-scaled version of $e[n]$. The modified aspiration noise source, $a'[n]$, is derived from the de-modulated noise source and the new envelope to generate the new aspiration noise source, $a'[n]$:

$$a'[n] = e'[n]d[n]. \tag{4.8}$$

This new source is then filtered by the inverse of $h^{-1}[n]$ to represent the vocal tract resonance properties and radiation characteristic. The impulse response, $h[n]$, is convolved with the new aspiration noise source to produce the pitch-modified version of the aspiration noise component, $u'[n]$:

$$u'[n] = a'[n] * h[n]. \tag{4.9}$$

The overall pitch-modified speech signal, $s'[n]$, is then re-synthesized by adding the modified harmonic and noise components:

$$s'[n] = v'[n] + u'[n]. \tag{4.10}$$

Section 4.5 next describes the implementation of this approach to pitch modification and discusses the selection of specific algorithms.

4.5 Implementation of Proposed Pitch-Scale Modification

As mentioned above, the proposed approach to pitch modification essentially attempts to reverse-engineer the pitch modification model to modify the aspiration noise source characteristics. The following sections describe implementation of each block in Figure 4.2.

4.5.1 Harmonic/Noise Component Analysis

The output of the PSHF method by Jackson and Shadle [31] is used as the first stage in the pitch modification algorithm. Implementation of the PSHF method was described above in Section 3.2. The outputs of the PSHF method used in the pitch modification algorithm are chosen to be the outputs after spectral interpolation, $\tilde{v}[n]$ and $\tilde{u}[n]$ for the harmonic and noise component estimates, respectively. The reconstructed harmonic component is sent through the Harmonic Branch, and the reconstructed noise component passes to the Noise Branch in the modification scheme of Figure 4.2.

4.5.2 Harmonic Branch

Pitch modification of the harmonic component estimated by the PSHF algorithm can be accomplished by any of the algorithms introduced in Section 4.1. The drawbacks of many of the methods are circumvented if they are used to process only the periodic component of a vowel. We implemented our own version of TD-PSOLA in MATLAB [47] for a simple modification scheme that we will consistently use. The TD-PSOLA is diagrammed in Figure 4.3 and involves the following steps (from [54]):

1) **Determination of analysis pitch marks.** These are times of the time instants of glottal closure that must be determined. The Praat speech analysis tool [4] is used to estimate the analysis pitch marks.
2) **Formation of short-time segments.** Each segment is formed by a Hanning window centered on the analysis pitch marks and two pitch periods in length.
3) **Determination of synthesis pitch marks.** The first synthesis pitch mark is fixed to be at the same time as the first analysis pitch mark. The next synthesis pitch mark is located one pitch period away, where this pitch period is derived from the new local pitch. For simplicity, the pitch modification factor is constant across the entire speech segment, and the pitch contour is modeled to be piecewise-constant.
4) **Mapping of analysis windows to synthesis pitch marks.** At each synthesis pitch mark, an analysis frame is inserted. In the case of pitch decreases, an analysis frame may not be associated with a synthesis pitch mark and thus discarded. Likewise, when increasing the pitch, analysis frames may be replicated at more than one synthesis pitch marks. See Figure 4.4 for a schematic of how analysis frames are chosen.
5) **Overlap-add synthesis.** The short-time segments at the new pitch are merged together.

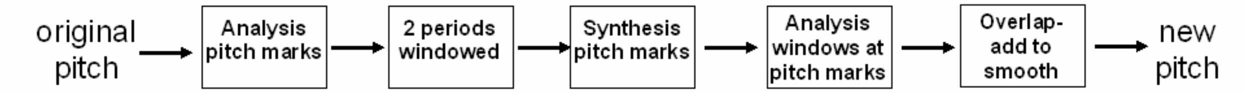

Figure 4.3 Block diagram of TD-PSOLA algorithm.

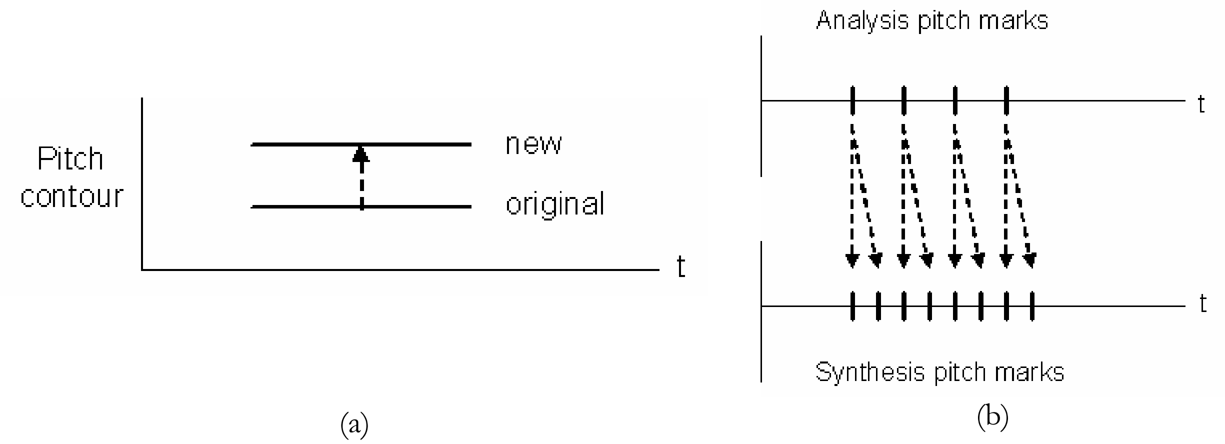

Figure 4.4 Example schematic of TD-PSOLA algorithm, pitch scale = 2. (a) Original and new pitch contours and (b) replication of analysis frames centered at glottal closure instants.

The TD-PSOLA method is less practical on stochastic speech sounds since pitch estimators (e.g., autocorrelation techniques [4] or frequency-domain peak-picking [65]) cannot estimate a modulation rate in the aspiration noise source. Consequently, the proposed pitch modification algorithm treats the noise component output of the PSHF differently from the periodic component estimate. Pitch modification of the noise branch in the algorithm (Figure 4.2) is described in the next section.

4.5.3 Noise Branch

The crux of the algorithm lies in the processing of the noise component estimated by the Decomposition block Figure 4.2. The Source Estimation stage obtains an estimate of the noise source itself. In other words, inverse filtering is performed prior to envelope estimation so that modulations in the aspiration noise may be modified as they appear prior to vocal tract filtering.

Source Estimation

The Source Estimation block estimates the underlying source waveform. Joint estimation algorithms could be inserted here, in which the decoupling of source and filter is not assumed [32]. We choose, on the other hand, the linear source-filter assumption of speech production, utilizing linear prediction analysis to remove the effects of the linear time-invariant filters $h[n]$ and $r[n]$

(recall Figure 2.3). It is tempting to estimate the modulation function, $u_g[n]$, by only inverse filtering by $h[n]$ the periodic component of speech, $u_g[n]*h[n]*r[n]$. In this case, however, the result would approximate the derivative of the glottal waveform, $u_g'[n]$, and make it impossible to estimate the DC component of the glottal airflow waveform.

Instead, recall that the aspiration noise estimate is modeled by $\left(q[n]u_g[n]*h[n]*r[n]\right)$. We then estimate the modulation function, $u_g[n]$, so it may be modified and re-imposed on the noisy excitation waveform, $q[n]$. The immediate goal of the Source Estimation stage is to analyze the noise component estimate, remove the effects of the filters $h[n]$ and $r[n]$, and estimate $q[n]u_g[n]$.

The choice of using linear prediction to estimate the aspiration noise source requires several assumptions. Wide-sense stationarity (WSS) is a constraint for linear prediction to be effective; therefore analysis must be performed on short-time frames of the aspiration noise estimate. Since WSS implies that the mean and variance of the underlying random process are unchanging, the duration of the windowed frame must be short enough to ensure WSS but long enough to afford a fair amount of spectral resolution.

After the whitening computation, it is assumed that any modulations in the resulting white noise are preserved. Implied by linear predictive analysis is that the linear filters acting on the stochastic process are of all-pole forms. The all-pole assumption is valid for many voiced sounds, except for nasals, which are produced with a closed side branch at the mouth and excessive losses due to the compliance of the nasal passage walls [73]. The all-pole assumption also does not adequately handle the radiation characteristic, which was modeled as a single zero from the first-difference filter in Equation (2.10). Our use of linear predictive analysis relies on the fact that this single zero may be approximately modeled by several poles [63].

Whitening of the input signal, $u[n]$, is implemented as follows. Overlap-add analysis utilizes a 20-ms Hanning analysis window (length N) with half-window overlap:

$$u_w[n,r] = u[n]w[n - rD + \tfrac{N}{2}], \tag{4.11}$$

where r is the frame number, D is the frame advance, and $w[n]$ is the Hanning window in Equation (3.1). See Appendix E for a derivation of the inverse filter, $h^{-1}[n,r]$, using linear prediction analysis of stochastic signals. The rth inverse filter is applied to the rth windowed frame, $u_w[n,r]$:

$$a[n,r] = u_w[n,r] * h^{-1}[n,r]. \tag{4.12}$$

We can reconstruct the entire source estimate from the short-time segments using overlap-add synthesis [63]:

$$a[n] = \frac{\sum_{r=0}^{Q-1} a[n,r]w[n-rD]}{\sum_{r=0}^{Q-1} w^2[n-rD]}, \tag{4.13}$$

where Q is the number of segments. Note that the normalization factor takes into account the weighting effects of the analysis and synthesis windows.

Figure 4.5 displays an example case of the whitening process performed on the aspiration noise component of a synthesized /a/ vowel. The aspiration noise source is either modulated with the glottal waveform or unmodulated. When modulated, function is at a constant 100-Hz rate. As desired, the whitening process approximately preserves the time-domain modulation characteristics of the aspiration noise source.

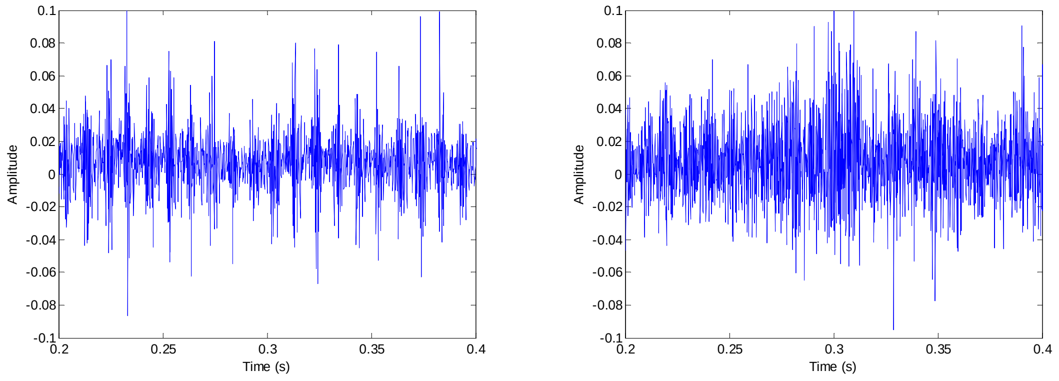

(a) (b)

Figure 4.5 Inverse filtering the noise component estimate of a synthesized vowel. Whitened noise estimate plotted where the synthesized aspiration noise source was either (a) modulated or (b) unmodulated. Synthesis parameters: Noise type = modulated, Vowel = a, f_0= 100, Gender = m, f_s = 8000, Duration = 1, DC = 0.1, OQ = 0.6, HNR = 10.

Envelope Estimation

The result of the Envelope Estimation block in Figure 4.2 uncovers the noise modulations generated by the glottal airflow undulations. In other words, armed with an estimate of $q[n]u_g[n]$, envelope detection can estimate the modulation function, $u_g[n]$. We have chosen a method based on the Hilbert transform. (See Appendix F for a comparison of two envelope detection methods.)

The Hilbert transform method is schematized in Figure 4.6. The discretized estimate of the aspiration noise source, $a[n]$, is related to the output envelope, $e[n]$ by:

$$e[n] = \left| a[n] + j\left(a[n] * r_Q[n]\right)\right| * l[n], \tag{4.14}$$

where $r_Q[n]$ is the discrete impulse response of the quadrature filter in Figure 4.6 and $l[n]$ is a 50-tap finite impulse response low-pass filter with a 3-dB cutoff frequency set as a parameter of the algorithm (see parameter list in Appendix A).

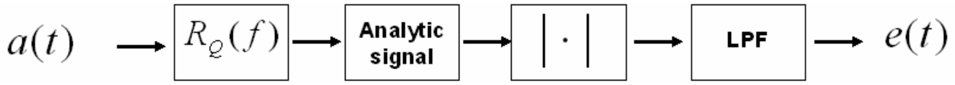

Figure 4.6 Hilbert transform method of envelope detection, in continuous time. $R_Q(f)$ is the frequency response of the quadrature filter that outputs the Hilbert transform of the input real signal. The complex analytic signal is then formed, with its real part equal to $a(t)$ and its imaginary part equal to its Hilbert transform. Next, the magnitude of the analytic signal is taken. Finally, a low-pass filter acts on the signal.

Envelope Modification

After uncovering the envelope of the noise source estimate, $e[n]$, the algorithm re-modulates the glottal noise source with a new scaled envelope. To perform this envelope modification in our preliminary work, resampling was performed on the envelope of the whitened modulated noise signal [50]. This method, however, was only applicable to pitch scale factors less than one. To also provide for pitch increases, the TD-PSOLA technique detailed above in Section 4.5.2 is used.

Dividing out the envelope from the noise source estimate, we obtain the demodulated signal, $d[n]$:

$$d[n] = \frac{a[n]}{e[n]}. \tag{4.15}$$

The new envelope, $e'[n]$, is then imposed on $d[n]$ to form a modified source signal:

$$a'[n] = e'[n]d[n]. \tag{4.16}$$

Spectral Coloring

The Spectral Coloring block re-imposes the spectral effects of the vocal tract and the radiation characteristic on the aspiration noise source. In the process of pitch modification, the pitch scale only affects the source characteristics, while the movements of the speech articulators are assumed unchanged. This assumption stems from the model of a decoupled voicing source and vocal tract filter.

The input to the block is the modified aspiration noise source, $a'[n]$, and the output is its spectrally-shaped version, $u'[n]$. The newly-modulated white noise component, $a'[n]$, is filtered by the radiation characteristic filter and an all-pole vocal tract filter model with filter coefficients taken from the short-time segments chosen in the Source Estimation stage. Overlap-add analysis results in the short-time segments, $a'_w[n,r]$:

$$a'_w[n,r] = a'[n,r]w[n - rD + \tfrac{N}{2}], \tag{4.17}$$

where N is the frame length, r is the frame number, D is the frame advance, and $w[n]$ is the Hanning window from Equation (3.1).

The processing stage to obtain the spectrally-colored short-time segment, $a'_w[n,r]$:

$$a'_w[n,r] = a'_w[n,r] * h[n,r], \tag{4.18}$$

where the vocal tract/radiation filter, in the z-domain, $H(z,r)$, is

$$H(z,r) = \frac{A}{1 - \sum_{k=1}^{P} \alpha_k[r] z^{-k}}, \tag{4.19}$$

and the coefficients, $\alpha_k[r]$, are taken from the r th frames in the Source Estimation stage.

Overlap-add synthesis eliminates the index r and completes the reconstruction of $u'[n]$:

$$u'[n] = \frac{\sum_{r=0}^{Q-1} a'_w[n,r]w[n - rD]}{\sum_{r=0}^{Q-1} w^2[n - rD]}, \tag{4.20}$$

where Q is the number of short-time segments, and normalization is included due to both analysis and synthesis window weightings.

4.5.4 Parameters

Finally, the modified aspiration noise, $u'[n]$, is then summed with the modified harmonic component, $v'[n]$, to yield the output at the new pitch, $s'[n]$. Three parameters are defined for the pitch modification algorithm: pitch scale, LPC order, and LPF cutoff. The pitch scale indicates the constant ratio by which the original pitch contour is multiplied. For example, a pitch scale of 1.2 indicates a pitch increase by a factor of 1.2. For a vowel with a time-varying pitch linearly increasing from 100 to 120 Hz, the algorithm would modify the pitch contour to 120–144 Hz. The LPC order refers to the number of linear prediction coefficients to be used in the Source Estimation stage (P in Appendix E). The LPF cutoff is the 3-dB frequency parameter of the low-pass filter in the Envelope Estimation stage of Figure 4.6. (See Appendix A for a tabulation of the modification parameters and Appendix B for a MATLAB GUI that integrates the algorithms into a visual representation.)

4.6 Examples of Modification

In Sections 3.3 and 3.4, we presented sample analyses on synthesized and real vowels. These same vowels are now input into our pitch-scale modification algorithm. The goal is to appropriately modify both the fundamental frequency of the periodic component of speech and any modulations in the aspiration noise source.

4.6.1 Synthesized Vowels

Steady Pitch

Figure 4.7 and Figure 4.8 step through the process of pitch modification using the new algorithm. Figure 4.7 displays the block diagram of the algorithm with unique letters indicating the waveform resulting from a specific stage in processing. These letters correspond to the waveform labels in Figure 4.8. Synthesis parameters are: Noise type = modulated, Vowel = a, f_0 = 100, Gender = m, f_s = 8000, Duration = 1, DC = 0.1, OQ = 0.6, HNR = 10. Modification parameters are: Pitch scale = 0.8, LPC order = 10, LPF cutoff = 350. The salient parameters are the input pitch and the pitch scale. The pitch of the input synthesized vowel is 100 Hz, static across the entire signal. The output waveform is a pitch-modified version of the input, where the pitch scale is equal to 0.8, indicating a desired pitch of 80 Hz at the output.

Each step breaks down the signal into its constituent components, allowing for specific analysis of the aspiration noise source. The underlying assumption to be kept in mind is that the pitch change of an individual only affects the source characteristics at the glottal level of the speech production system. As a result, pitch modification of aspiration noise must solely modify the aspiration noise source waveform. This is the critical processing stage. Before- and after-modification waveforms of the aspiration noise source are displayed in Figure 4.8g and h, respectively.

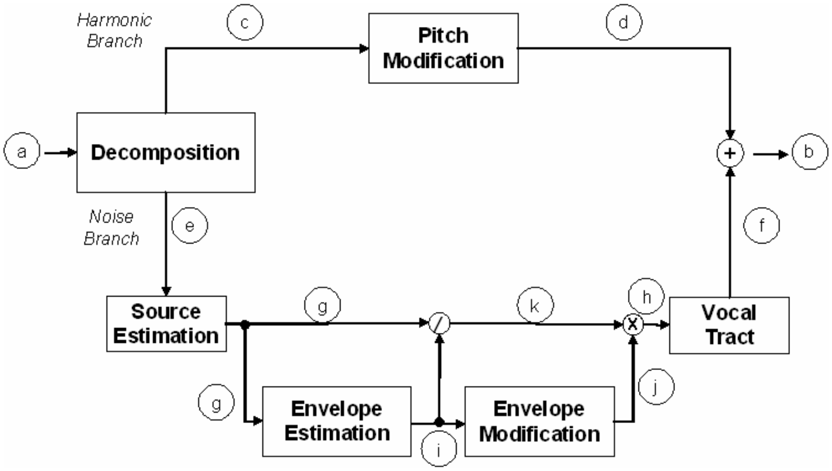

Figure 4.7 Block diagram for pitch modification example. Letters denote the speech waveform at a specific instance during processing. (a) Synthesized vowel, (b) modified vowel output, (c) extracted harmonic component, (d) modified harmonic component, (e) extracted noise component, (f) modified noise component, (g) aspiration noise source estimate, (h) modified aspiration noise source, (i) envelope of aspiration noise source, (j) modified envelope, and (k) demodulated aspiration noise source.

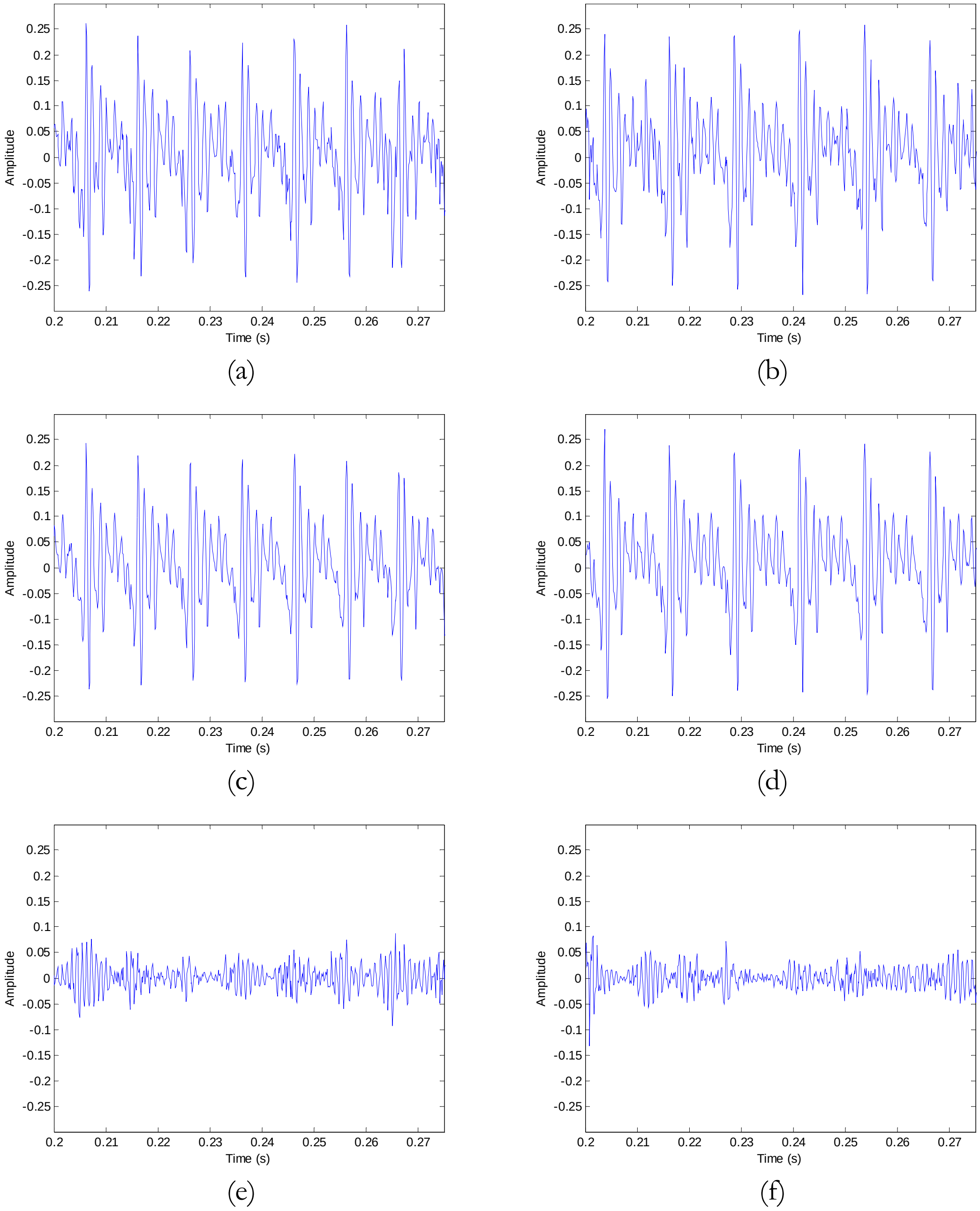

(a) (b)

(c) (d)

(e) (f)

Figure 4.8 Pitch modification example, synthesized vowel. Original and modified waveforms are placed side-by-side for ease of comparison. (a) Synthesized vowel, (b) modified vowel output, (c) extracted harmonic component, (d) modified harmonic component, (e) extracted noise component, and (f) modified noise. See Figure 4.7 for the waveform's location in the algorithm (letters correspond to waveforms in this figure). Synthesis parameters: Noise type = modulated, Vowel = a, f_0 = 100, Gender = m, f_s = 8000, Duration = 1, DC = 0.1, OQ = 0.6, HNR = 10. Modification parameters: Pitch scale = 0.8, LPC order = 10, LPF cutoff = 350.

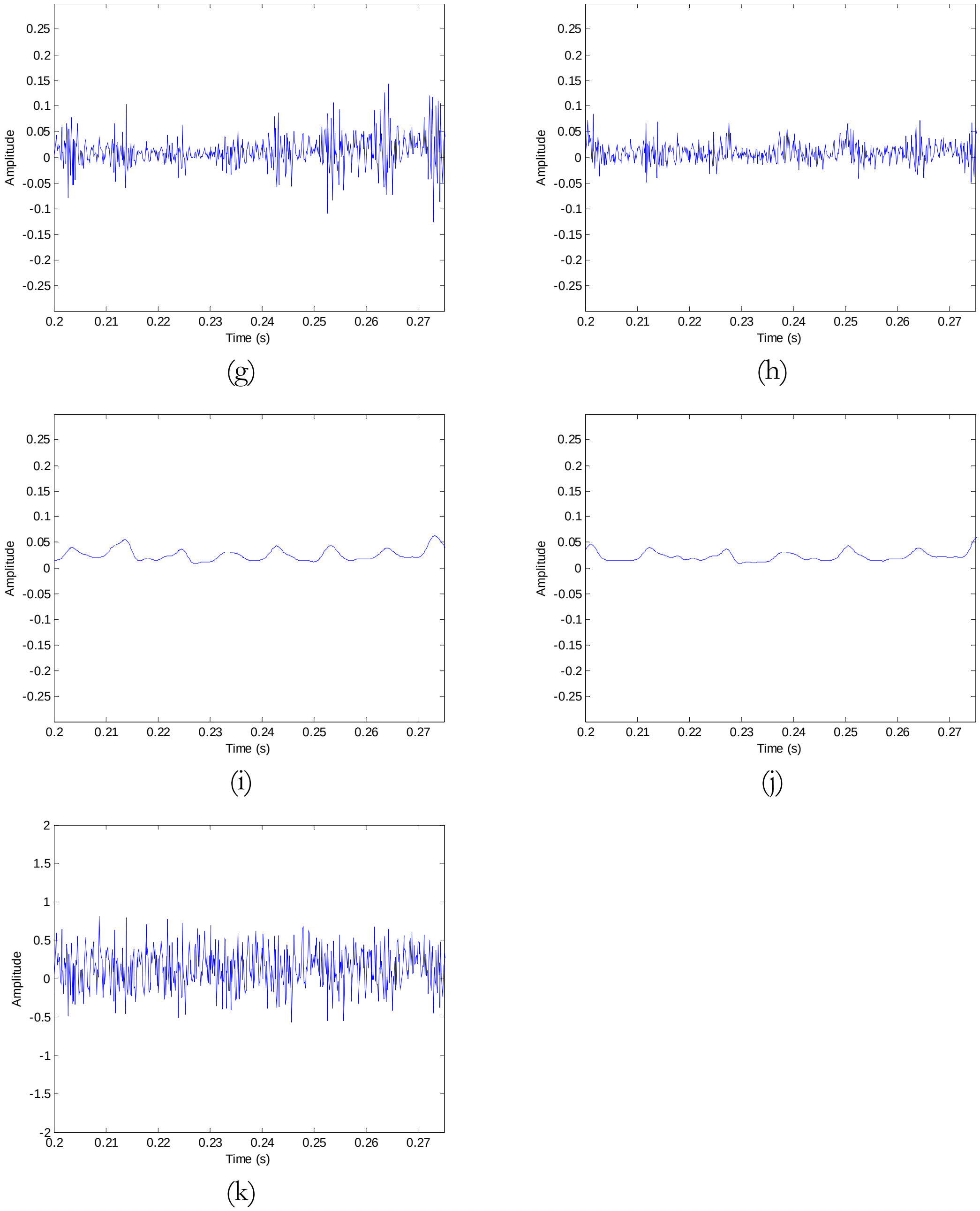

Figure 4.8 continued… **Pitch modification example, synthesized vowel. Original and modified waveforms are placed side-by-side for ease of comparison. (g) Aspiration noise source estimate, (h) modified aspiration noise source, (i) envelope of aspiration noise source, (j) modified envelope, and (k) demodulated aspiration noise source. See Figure 4.7 for the waveform's location in the algorithm (letters correspond to waveforms in this figure). Synthesis parameters: Noise type = modulated, Vowel = a, f_0 = 100, Gender = m, f_s = 8000, Duration = 1, DC = 0.1, OQ = 0.6, HNR = 10. Modification parameters: Pitch scale = 0.8, LPC order = 10, LPF cutoff = 350.**

This example involved pitch modification of a synthesized vowel, where we have access to all waveforms that serve as building blocks for the vowel. Comparisons of waveforms at the various stages of the pitch modification algorithm may be made with waveforms from the stages of vowel synthesis. The idea of reverse-engineering the model has already been mentioned, and its benefits are evident here. The example stepped through in Figure 4.8 can be viewed from a synthesis point of view. To simulate the decrease in pitch from 100 Hz to 80 Hz, we can simply synthesize two vowels with fundamental frequencies of 100 Hz and 80 Hz, respectively. We can compare waveforms from the synthesized vowels with the waveforms during each stage of processing in the pitch modification algorithm.

Figure 4.9 shows the vowel production model with labels indicating waveforms at each stage of vowel synthesis. Corresponding waveforms at each stage of synthesis for different-pitched vowels are displayed side by side in Figure 4.10. The left waveforms are from the 100-Hz vowel, and the right waveforms are from the 80-Hz vowel. The general characteristics of the modified noise and source waveforms are preserved. Compare Figure 4.8e, f with Figure 4.10e, f. However, the corresponding envelopes (compare Figure 4.8i, j with Figure 4.10i, j) differ due to the stochastic nature of the envelope in the presence of aspiration noise. (See discussion in Section 5.1.3).

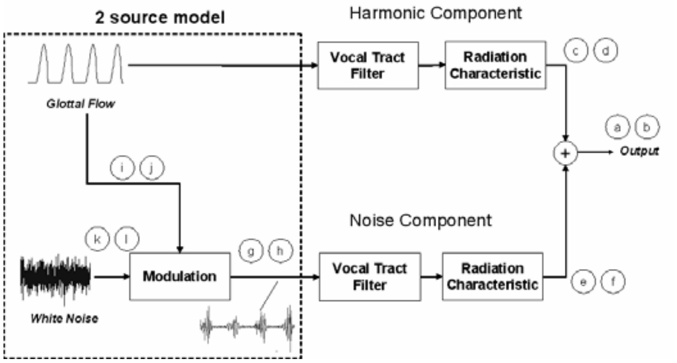

Figure 4.9 The vowel production model with labels at each stage. Letters denote the speech waveform at a specific instance during processing. At each step, the first letter indicates vowel synthesis at one pitch; the second letter indicates vowel synthesis at another pitch. (a, b) Synthesized vowel, (c, d) harmonic component, (e, f) noise component, (g, h) aspiration noise source, (i, j) envelope of aspiration noise source, (k, l) aspiration noise source before modulation.

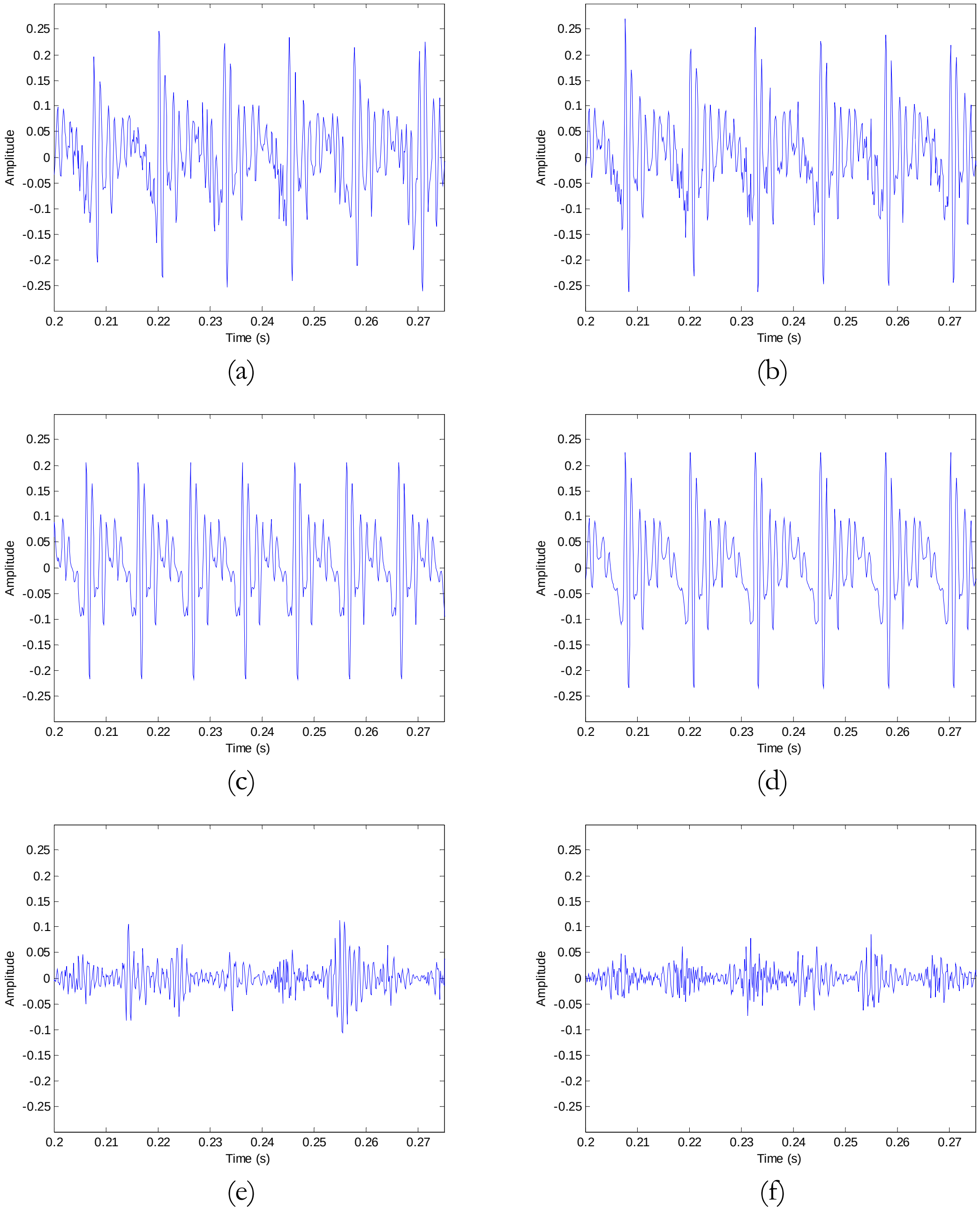

(a)

(b)

(c)

(d)

(e)

(f)

Figure 4.10 Vowel synthesis of two vowels, simulating a pitch change from 100 Hz to 80 Hz. (a, b) Synthesized vowel, (c, d) harmonic component, and (e, f) noise component. See Figure 4.9 for the waveform's location in the algorithm (letters correspond to waveforms in this figure). Synthesis parameters: Noise type = modulated, Vowel = a, f_0 = 100, Gender = m, f_s = 8000, Duration = 1, DC = 0.1, OQ = 0.6, HNR = 10.

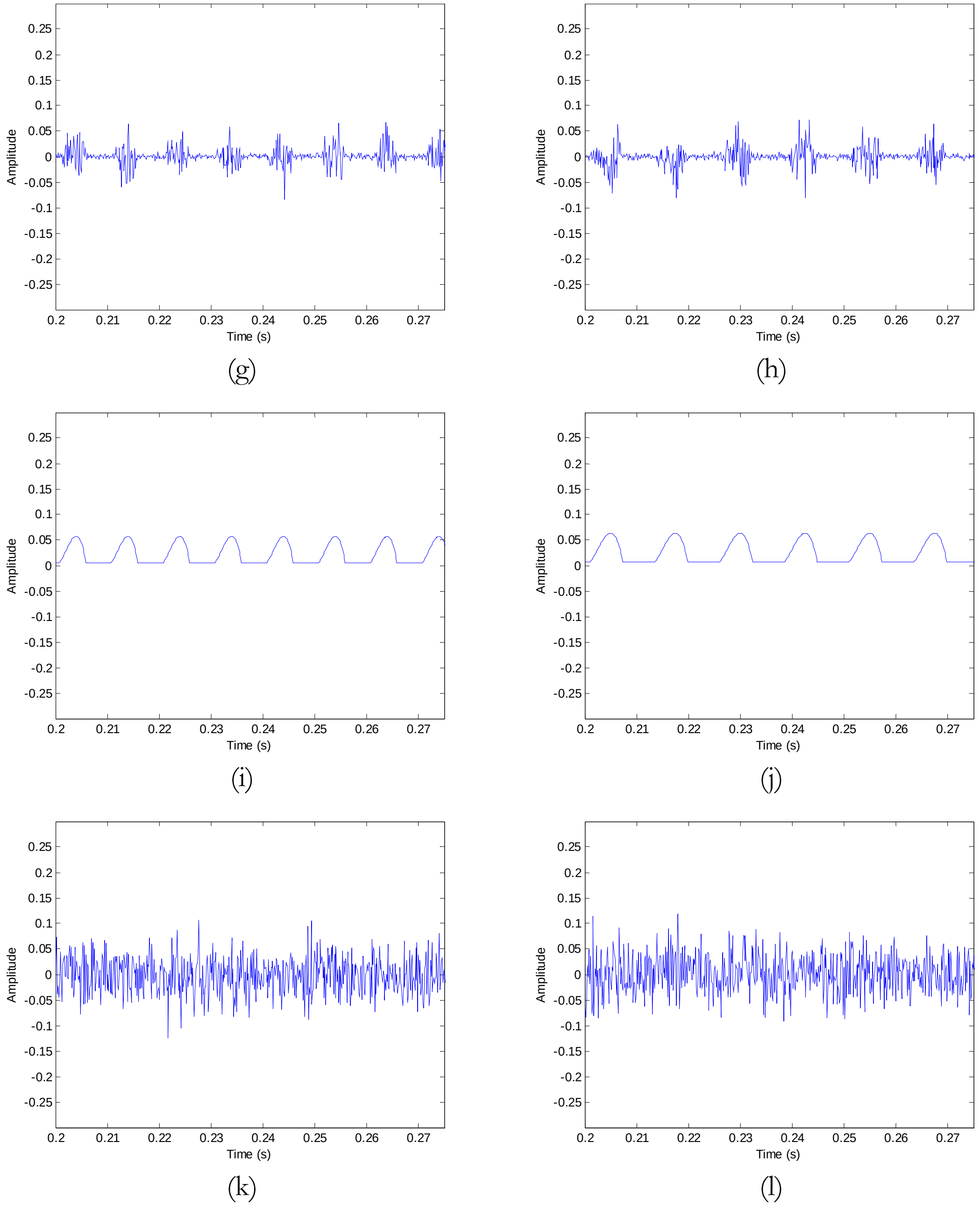

Figure 4.10 continued… Vowel synthesis of two vowels, simulating a pitch change from 100 Hz to 80 Hz. (g, h) Aspiration noise source, (i, j) envelope of aspiration noise source, (k, l) aspiration noise source before modulation. See Figure 4.9 for the waveform's location in the algorithm (letters correspond to waveforms in this figure). Synthesis parameters: Noise type = modulated, Vowel = a, f_0 = 100, Gender = m, f_s = 8000, Duration = 1, DC = 0.1, OQ = 0.6, HNR = 10.

Time-varying Pitch Contour

We analyzed and decomposed a vowel into its harmonic and noise components in Figure 3.8 above, which was synthesized with a linearly increasing pitch from 100 to 140 Hz over one second.

We now apply our pitch modification algorithm to scale the pitch by a fixed factor of 1.2, shifting the endpoints of the contour to 120 and 168 Hz. Figure 4.11 displays a wideband spectrogram of the pitch-modified vowel along with the original and modified pitch contours. An autocorrelation pitch estimation technique [4] was used to compute pitch values every 5 ms.

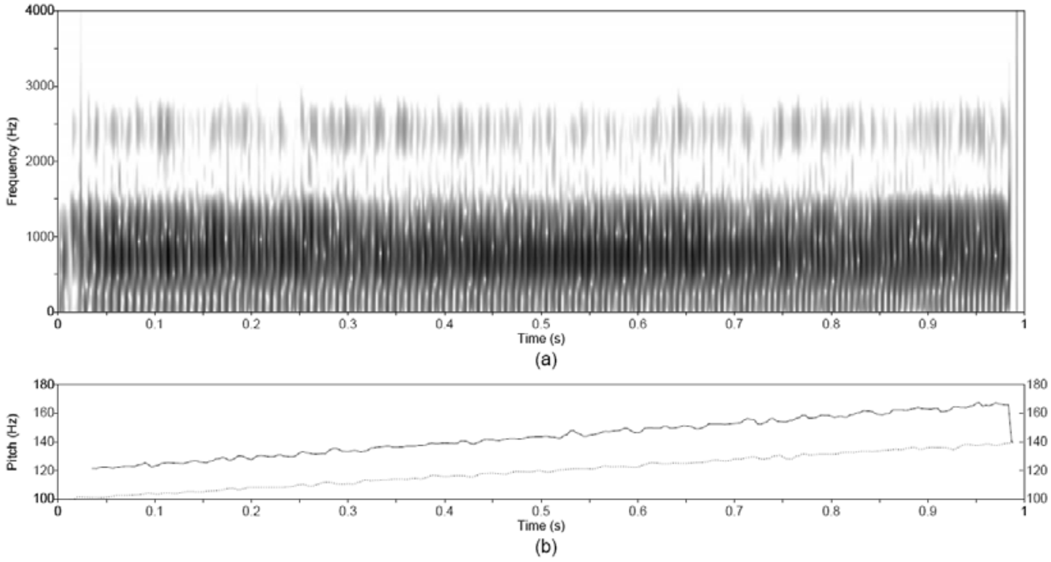

Figure 4.11 Synthesized vowel with time-varying pitch, 100-140 Hz, over one-second duration, shown in Figure 3.7. (a) Wideband spectrogram and (b) original (dotted line) and modified (solid line) pitch contours. Synthesis parameters: Noise type = modulated, Vowel = a, f_0 = 100–140, Gender = m, f_s = 8000, Duration = 1, DC = 0.1, OQ = 0.6, HNR = 10. Modification parameters: Pitch scale = 1.2, LPC order = 10, LPF cutoff = 350.

Figure 4.12 displays the modified components of the vowel, and Figure 4.12c indicates that the TD-PSOLA algorithm works effectively on the harmonic component to decrease the original pitch periods. A 0.1-s sample waveform of the modified envelope is displayed in Figure 4.12a, superimposed on the modified noise source waveform. The modified noise component, re-constructed by applying spectral coloring due to the vowels formants, is displayed in Figure 4.12b.

The desired synchrony is that maxima in the noise source envelope occur during the open phase of the glottal waveform. To observe this property, the modified envelope is superimposed as a dotted line on the modified periodic waveform in Figure 4.12c. The peaks in the modified envelope function lie just prior to the instants of glottal closure, during the open phase of the glottal cycle. An advantage of the modification algorithm is its approximate preservation of the original synchrony between the noise source modulations and the periodic component.

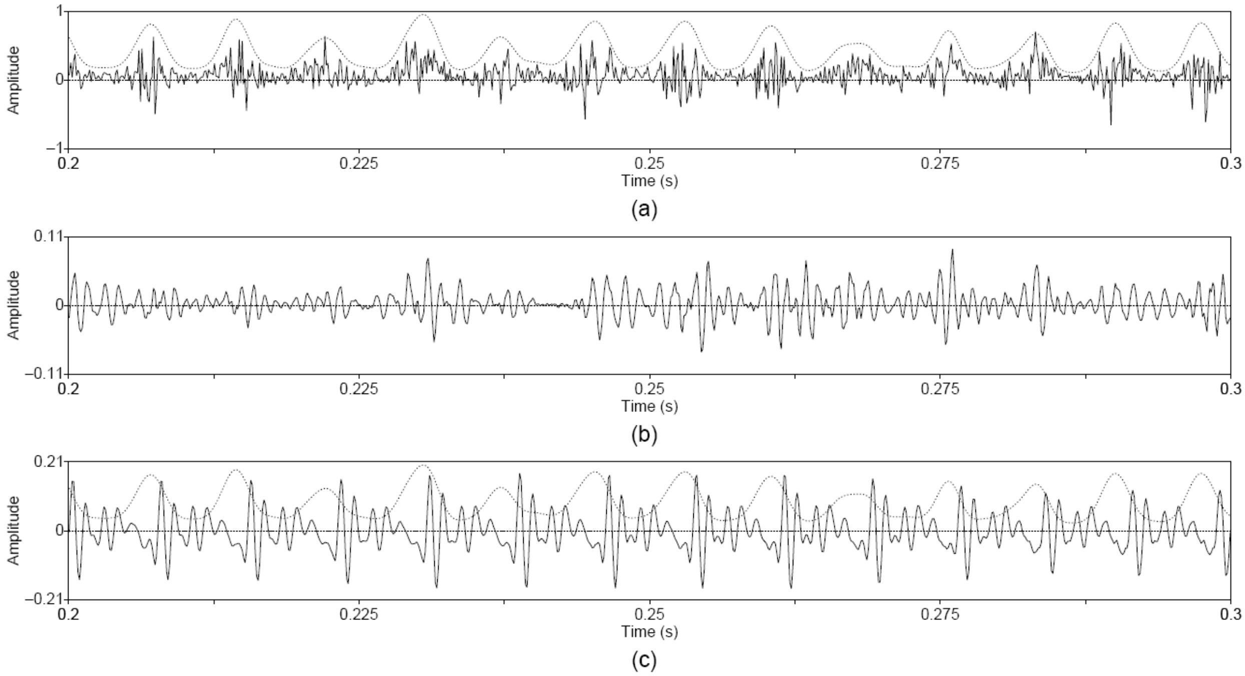

Figure 4.12 Modified components of synthesized vowel. (a) Modified aspiration noise source with modified envelope (dotted line), (b) modified noise component, and (c) modified periodic component with modified noise source envelope (dotted line).

4.6.2 Real Vowels

Normal Speaker

Recall that the spectrogram and waveform of the syllable /pæ/ were displayed in Figure 3.9. Again, we apply our modification algorithm to scale the pitch by 0.8. The spectrogram and input and output pitch contours are displayed in Figure 4.13, indicating the change in fundamental frequency from about 100 to 80 Hz. Further temporal analyses are performed as was done in Section 4.6.1. Waveforms of the newly modulated noise source, modified noise component, and modified harmonic component are displayed in Figure 4.14 for a 0.1-s time range. Recall that in the separated aspiration noise component, Figure 3.10 showed that noise bursts appeared at instants of assumed glottal closure (see Appendix D for glottal closure assumption). Synchrony between the modified components is consistent with this observation. Figure 4.14c illustrates the synchrony by superimposing the modified noise source envelope on the modified periodic component.

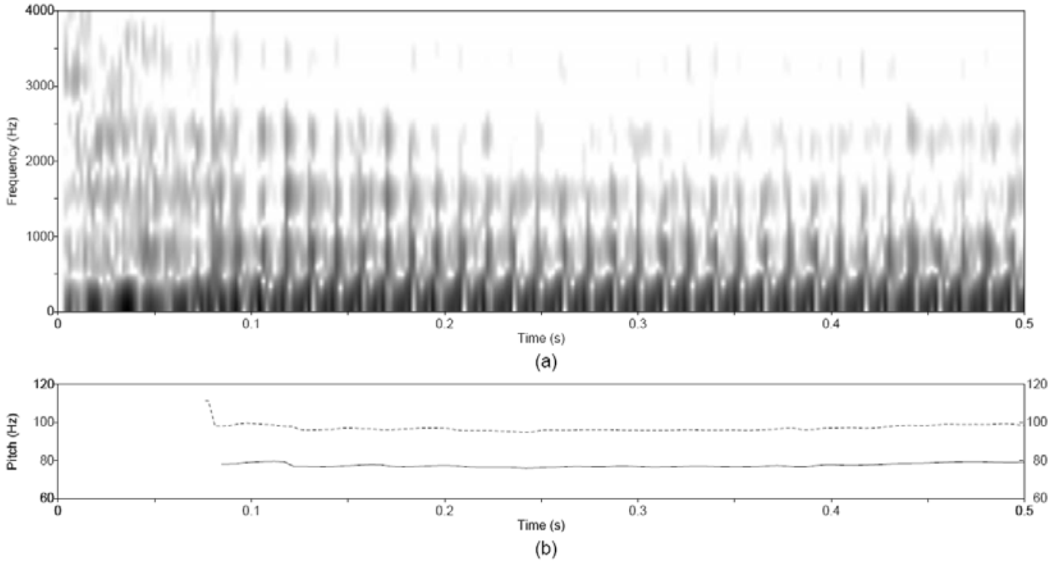

Figure 4.13 Utterance by normal speaker, /pæ/, as in Figure 3.9. Pitch scale = 0.8. (a) Wideband spectrogram and (b) original (dotted line) and modified (solid line) pitch contours.

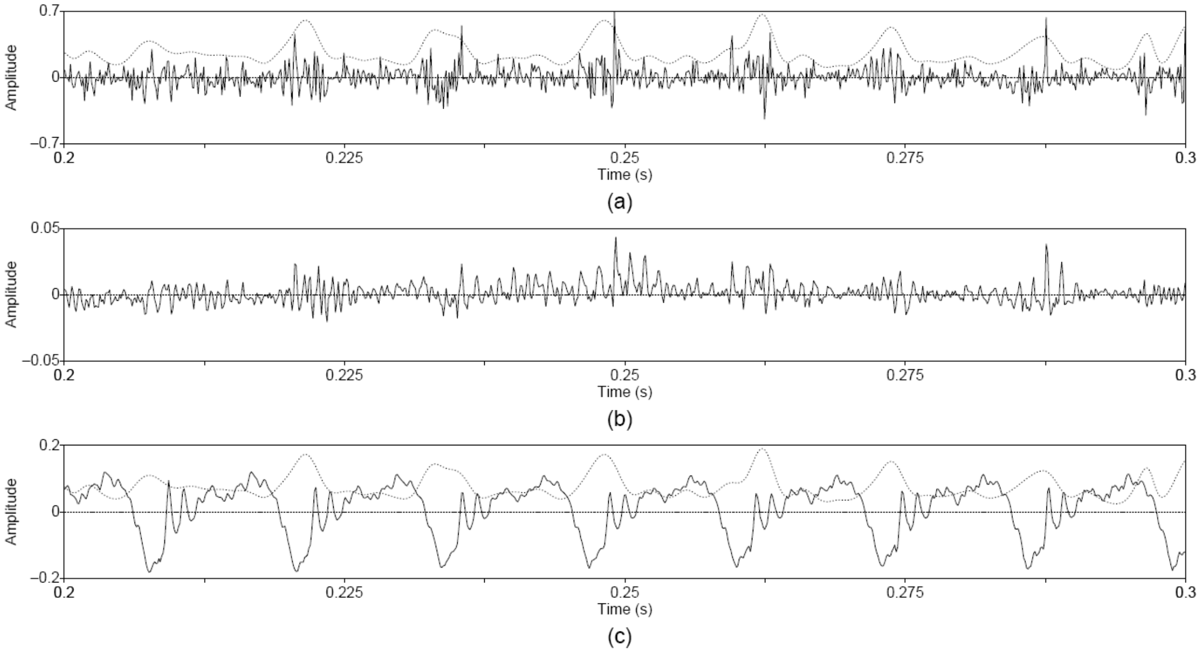

Figure 4.14 Modified components of normal speech. (a) Modified aspiration noise source with modified envelope (dotted line), (b) modified noise component, and (c) modified periodic component with modified noise source envelope (dotted line).

Pathological Speaker

We introduced the sustained /a/ vowel by the pathological speaker in Figure 3.12. The patient was diagnosed with vocal fold cysts and constricted structures in the laryngeal region. To compensate for his weaker voice, the patient "hyperfunctioned" by forcing larger volumes of air through the vocal apparatus.

Recall that we observed maximum amplitudes in the envelope of the estimated aspiration noise source occurring at both the assumed glottal open phase and the glottal closure instant. The modified envelope should aim to preserve the synchrony of the original harmonic and noise components. Figure 4.16 steps through the reconstruction of the modified noise component using our algorithm. The envelope of the whitened noise signal shows the relatively variable nature of the modulations in the pathological vowel. It is then instructive to view the modified harmonic waveform along with the envelope of the modified noise source. Some amplitude maxima in the envelope coincide with the assumed open phase of the periodic component, but other maxima occur at other phases within the glottal cycle. This possibly illustrates the various source mechanisms of aspiration noise during phonation when uttered by a speaker with vocal fold pathology.

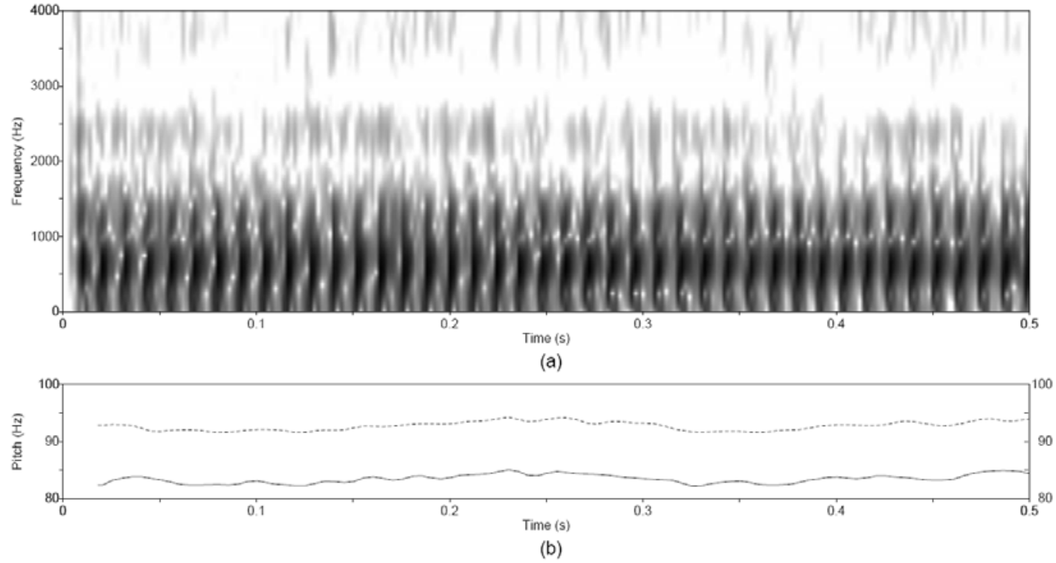

Figure 4.15 Vowel by speaker with voice disorder, as in Figure 3.12. Pitch scale = 0.9. (a) Wideband spectrogram and (b) original (dotted line) and modified (solid line) pitch contours.

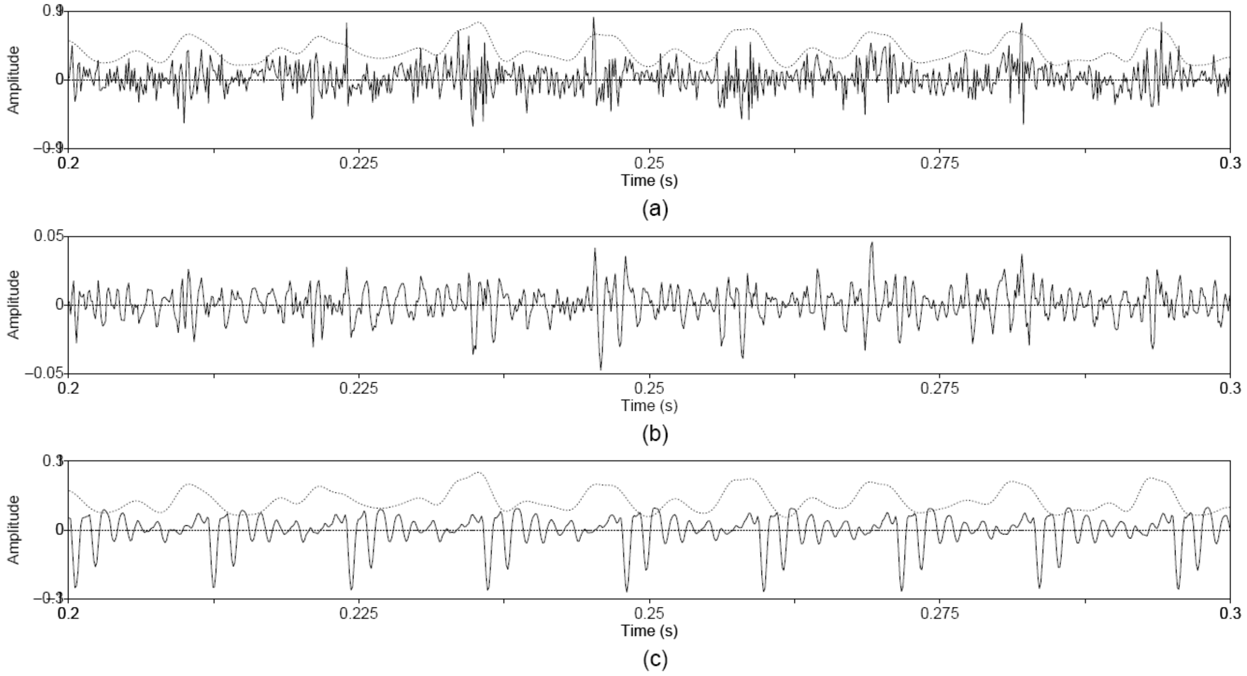

Figure 4.16 Modified components of disordered speech. (a) Modified aspiration noise source with modified envelope (dotted line), (b) modified noise component, and (c) modified periodic component with modified noise source envelope (dotted line).

4.7 Observations on Signal Quality

Ultimately, we are interested in judging aurally the signal quality of the proposed approach against standard methods outlined in Section 4.1. Such an evaluation, including judgment of the naturalness of the aspiration component, and how it is perceived to blend with its corresponding periodic component, requires a rigorous listening test that is beyond the scope of the current effort. Nevertheless, our informal listening shows promise for the technique for a variety of pitch-scale factors and synthesized vowels with steady and varying pitch contours, as well as for real vowels. In these modified signals, the periodic component was altered by either TD-PSOLA or by a sinewave-based approach [64, 65], and the noise component was modified by our proposed method. For these signals, we observed that the pitch-modified aspiration noise typically reflects the aspiration in the original signal and suffers less from artifacts of the two implemented standard techniques, such as those due to voicing errors in the sinewave-based approach and glottal-closure estimation errors in TD-PSOLA. Further discussion of a future study in the context of continuous-speech processing and its extension to a more rigorous evaluation are given in Section 5.1.5.

4.8 Summary and Conclusions

Chapter 4 presented an alternative strategy to pitch-scale modification that aims to preserve temporal characteristics in the aspiration noise source that were observed in the analysis of Chapter 3. Inspired by the physiology of pitch change in speech production, the proposed strategy took a dual processing approach to pitch modification. The harmonic and noise components of the speech signal were separately analyzed, modified, and re-synthesized, so that temporal synchrony was approximately maintained between the sources of each component. Current algorithms take different approaches to implementing pitch modification. Some process the signal as a whole, while others first obtain an estimate of the source before modifying the fundamental frequency. Some function in the spectral domain, while others operate on time-domain waveforms. None, however, addresses temporal synchrony between the periodic and noise source signals.

The proposed approach is a non-parametric analysis and modification strategy that does not assume any specific modulation pattern such as in the noise modulation model. The TD-PSOLA method was selected to modify the harmonic component of speech because of its high time resolution properties and its relative success in perceptual quality. Due to the modeled coupling between the harmonic and aspiration noise components, processing the noise component was more involved. Modification of the fundamental period of the periodic component was balanced by modifications in the temporal features of the noise component. Although our vowel production model assumed one type of noise source modulation, decomposition of real vowels demonstrated that noise bursts seem to appear in more than one phase of the glottal cycle.

The algorithm's implementation and parameters were described in Section 4.5, and example cases of pitch-scale modification were presented in Section 4.6. Results are promising, providing evidence that our algorithm appropriately analyzes the aspiration noise component and attempts to preserve noise modulations in the modified speech signal.

Chapter 5

Future Work and Conclusions

This thesis concludes with a look into improving the algorithms of the current study. The following sections discuss possible ways and take initial steps toward adding robustness and flexibility to the vowel synthesizer of Chapter 2, the harmonic/noise analysis algorithm of Chapter 3, and the pitch-scale modification strategy of Chapter 4.

Section 5.1.1 introduces the perturbation effects of jitter and shimmer that are ubiquitous in running speech and extends the synthesizer flexibility to include these parameters. The effects of the perturbations on the performance of the separation algorithm are discussed. As a result, Section 5.1.2 presents the possible advantages of SEEVOC [61], an alternate strategy for resolving the periodic portion of speech when perturbations are present.

Section 5.1.3 discusses the issues inherent in estimating a modulation function from a broadband stochastic carrier signal. Section 5.1.4 challenges our pitch modification model in Figure 4.1, which assumed a strict decoupling between the control of fundamental frequency and formant resonances in the vocal tract. Finally, Section 5.1.5 and 5.1.6 present preliminary investigations into extending the developed algorithm to process continuous speech and provide future directions on perceptual ratings of different algorithms.

5.1 Future Work

5.1.1 Effects of Jitter and Shimmer

When observing the results from both normal and disordered voices, often the analysis of the aspiration noise component is confounded by perturbations to the signal other than randomness due to aspiration noise sources. In the PSHF decomposition algorithm, the noise component is simply assumed to be the residual after stripping the speech waveform of its estimated harmonic component. In the residual, aspiration noise is a major contribution, but so are the effects of frequency jitter and amplitude shimmer. These perturbations may have their root in physiological mechanisms of neural or muscular origin. Currently, the decomposition algorithm can handle low levels of these perturbations while still performing adequately. Refinement and extension of the algorithm to eliminate the jitter and shimmer influences in the aspiration component estimate is a goal of future research.

To illustrate the jitter/shimmer issue, implementation of the vowel production model was extended to allow synthesis of perturbed source components. A common measure of jitter is its percent deviation from the nominal pitch period value. During synthesis, the glottal flow waveform is generated during each pitch period and concatenated with successive waveforms. Recalling that the duration of the cycle corresponds to the pitch period T_0, we have control over the period of each cycle in the synthesized vowel. For example, we can modify the synthesis of a steady-pitch vowel by adding jitter and shimmer into the pitch period parameter.

During each glottal cycle, the nominal pitch period, T_0, is perturbed using the following equation (from [31]):

$$T_0 = T_0 \pm \frac{\eta_J}{100} T_0 (2x - 1), \tag{5.1}$$

where η_J is the maximum jitter percentage and x is a random variable with uniform distribution between 0 and 1. The $(2x-1)$ factor serves to transform the uniform random variable into one with zero mean and extremes dependent on the maximum jitter percentage parameter. Similarly, shimmer is applied as a cycle-to-cycle variation in the amplitude of the source excitation. The equation for each cycle's perturbed amplitude, A, is

$$A = A \pm \frac{\eta_S}{100} A(2x - 1), \tag{5.2}$$

where η_S is the maximum jitter percentage and x is the random variable defined above.

To observe the individual effects of jitter and shimmer, PSHF separation of harmonic and noise components is performed on a synthesized vowel with HNR = ∞ dB (idealized as a voiced source with no aspiration noise energy). Synthesis parameters are listed in the caption of the following illustrative figures. Figure 5.1 displays the extracted aspiration noise component when the input vowel was synthesized with a maximum jitter percentage of 1%. The percept of the vowel is one of slight roughness. A sampling rate of 48000 Hz is chosen to minimize undersampling effects. Note that a significant, although small, noise component has leaked into the output of the decomposition algorithm. The current study assumes any output energy at this stage is due to turbulent noise sources at the glottis. The result of the simulation in Figure 5.1 shows that a significant jitter contribution can confound the subsequent pitch modification algorithm. The algorithm would attempt to uncover modulations inherent in the aspiration noise component, even though the signal itself is known not to be due to aspiration noise.

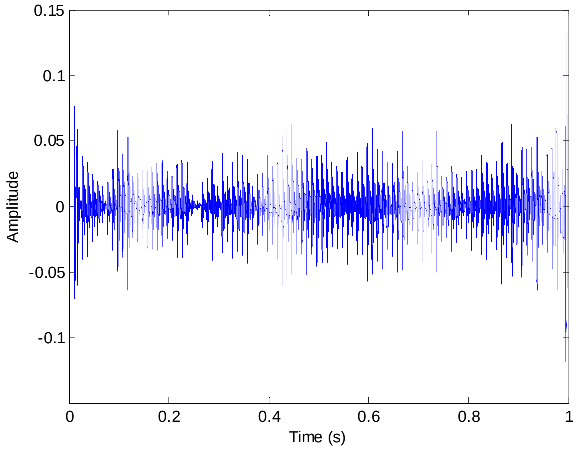

Figure 5.1 Noise waveform estimated from purely periodic vowel with jitter. Synthesis parameters: Noise type = modulated, Vowel = a, f_0 = 100, Gender = m, f_s = 48000, Duration = 1, DC = 0.1, OQ = 0.6, HNR = 500, jitter = 1, shimmer = 0.

Similar observations of non-aspiration noise sources leaking into the extracted noise component are seen when adding a shimmer factor with no jitter and aspiration noise contributions. Although not as much leakage is observed for a 10% shimmer parameter (Figure 5.2), the result is still perceptible and can easily degrade the performance of the pitch modification algorithm. With each additional stage of processing, errors accumulate and can be potentially magnified. Compensation for these perturbations warrants novel signal processing techniques.

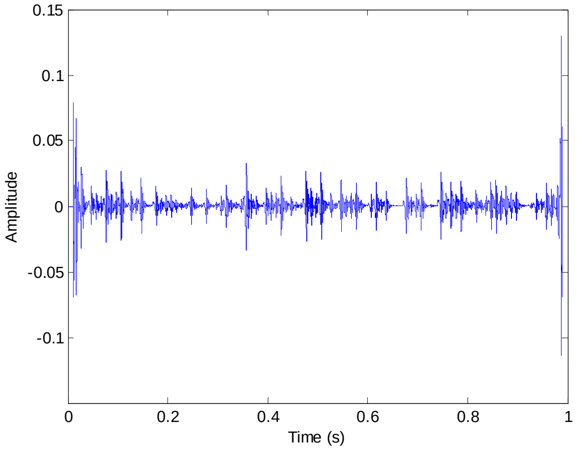

Figure 5.2 Noise waveform estimated from purely periodic vowel with shimmer. Synthesis parameters: Noise type = modulated, Vowel = a, f_0 = 100, Gender = m, f_s = 48000, Duration = 1, DC = 0.1, OQ = 0.6, HNR = 500, jitter = 0, shimmer = 10.

5.1.2 Periodic Component Estimation with SEEVOC

SEEVOC, standing for spectral envelope estimation vocoder, was developed in the early 1980s for the low-bit rate coding field to provide for an efficient method of parametrically representing the spectral envelope of short-time speech segments [61]. Applications of the SEEVOC algorithm include background noise estimation, noise suppression, and, most relevant to this study, high-quality pitch estimation. For our purposes, we use the SEEVOC algorithm to help handle jitter and rapid pitch changes that occur in voiced speech.

In the present PSHF algorithm, both stationarity and strict harmonicity are assumed over the analysis window of four pitch periods in duration. To estimate the signal's harmonic component, the PSHF simply samples the frequency spectrum at integer multiples of the local pitch estimate. Over the duration of the analysis window, however, there may be deviations in the frequency location of particular harmonics due to rapid fluctuations or more subtle perturbations in the pitch period. This movement is effectively averaged out when the discrete Fourier transform is taken. With such pitch fluctuations, harmonic energy can lie at frequency bins of the DFT other than bins that are harmonically spaced apart. In a way, a pseudo-harmonic filter could be applied to determine the energy attributed to the periodic component, and this is what SEEVOC attempts to do.

The SEEVOC algorithm models the periodic source as an impulse train that is filtered by the spectral properties of the vocal tract resonances. In the spectral magnitude domain, this model dictates that the envelope is sampled by line spectra at integer multiples of the fundamental frequency. The strictness of this spectral sampling assumption is relaxed. Instead of blindly selecting the harmonic bins of the discrete Fourier transform, SEEVOC uses frequency ranges centered on harmonic bins and looks to the left and right of the bin by half the fundamental frequency. The algorithm then utilizes a peak-picking technique within this range to determine the spectral bins that correspond to the periodic source. Frequency errors are avoided by bootstrapping each search from the previous frequency estimate. To connect the dots of the spectrum, linear interpolation is performed in the log frequency domain. Finally, a minimum-phase constraint is applied before calculating the inverse DFT to yield the spectral envelope's impulse response.

For our purposes, we can directly apply the SEEVOC algorithm up to the final steps. Once the periodicity bins are identified from the magnitude of the DFT, we can revert to the DFT's complex coefficients and perform an inverse DFT of the pseudo-comb filter to arrive at an estimate of the periodic component. To reconstruct the aperiodic component due to the aspiration noise source, we can take the inverse transform of the remaining frequency bins, or first interpolate across the zeroed bins as was done in the PSHF method.

5.1.3 Estimating the Envelope of a Noise Signal

One of the critical steps in the proposed pitch-scale modification algorithm is Envelope Estimation in the Noise Branch of Figure 4.2. This stage estimates the slow-moving amplitude of the modulated noise signal that represents the aspiration noise source. We mentioned the magnitude of the analytic signal derived using the Hilbert transform is known to reconstruct an envelope that was imposed on a narrowband carrier signal. When imposed on a broadband signal such as white noise, the reconstructed envelope results in a suboptimal estimate. Here, we briefly explore the cause of this estimation difficulty.

As an example case, an aspiration noise source waveform is synthesized with an assumed periodic source at a fundamental frequency of 100 Hz. This means that a white Gaussian noise signal is multiplied by the glottal airflow velocity waveform. Short-time spectral and temporal features of these waveforms are displayed in Figure 5.3. As expected, the spectrum of the periodic source shows peaks at zero due to the DC offset and at multiples of 100 Hz. The spectrum of the modulated noise source waveform is distinctly broadband in nature and notably dominates the periodic component above about 1300 Hz. One DFT was computed to estimate the noise spectrum, justifiably translating into a high variance estimate that is not perfectly flat.

The challenge is how to reconstruct the imposed modulation function from the modulated noise signal. The Hilbert transform method used in our study gives this initial estimate. Recall that the magnitude of the analytic signal is smoothed by a low-pass filter with a 3-dB cutoff frequency of 350 Hz. The resulting envelope estimate is displayed in Figure 5.3 at a normalized amplitude with the known modulation function. The AC structure and DC offset measures are qualitatively preserved, though the gain fluctuates from period to period.

Further improvements for the Envelope Estimation stage are warranted. It may be possible to develop a comb filter method, similar to that done in the PSHF decomposition algorithm, where the bins of the comb are placed at harmonics of the local fundamental frequency. Judging from the spectra in Figure 5.3, the comb filter would be ineffective on the modulated noise source and better suited on the output of the first-pass envelope estimate. Jitter and shimmer issues similar to those encountered when processing the overall pressure signal will complicate the processing. Even with an effective comb filter, energy above the 6th harmonic is already lost in the envelope estimate's spectrum. (See Appendix F for more discussion on envelope estimation.)

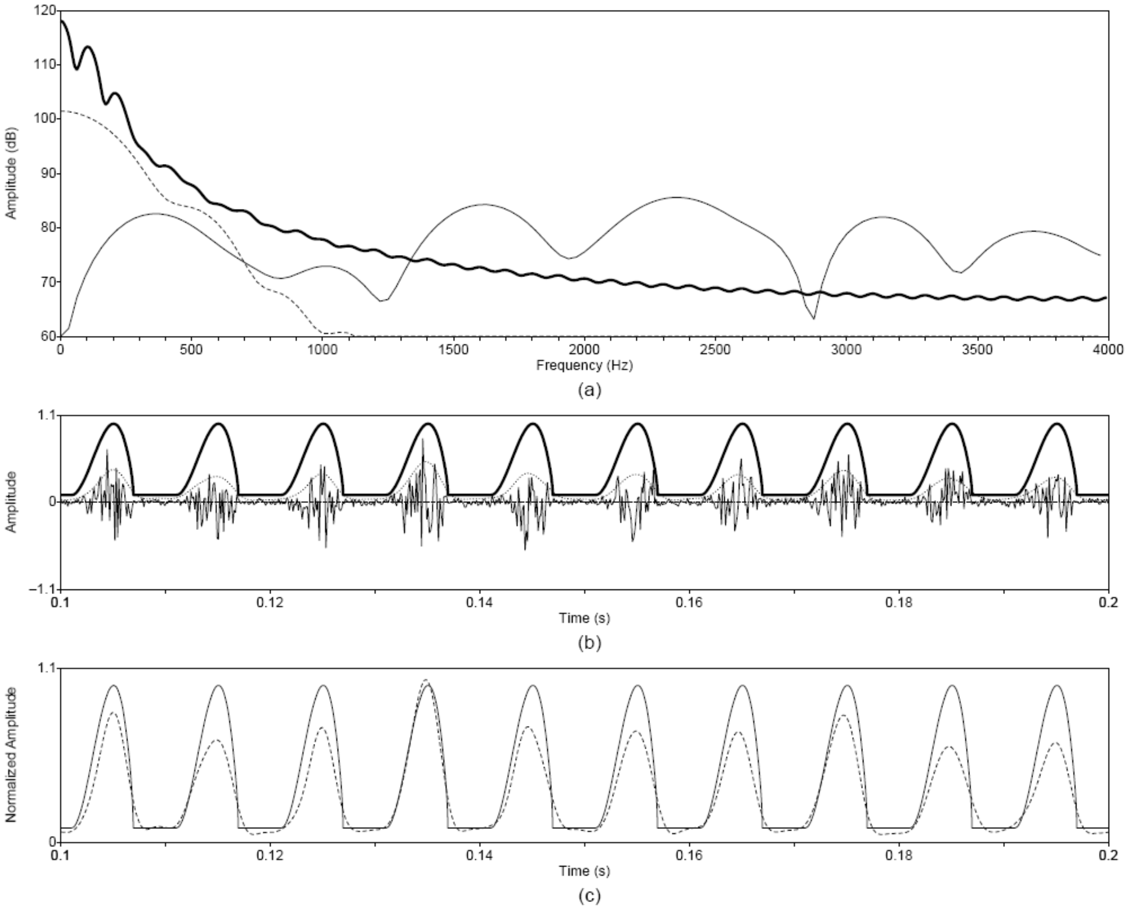

Figure 5.3 Difficulty estimating an envelope from a noise signal. (a) Short-time spectra, (b) waveforms, and (c) envelope waveforms with normalized amplitudes. Line types indicate the glottal airflow velocity (thick line), noise source modulated by glottal waveform (thin line), and noise source envelope estimated by Hilbert transform method (dotted line). Synthesis parameters: Noise type = modulated, f_0= 100, f_s = 8000, DC = 0.1, OQ = 0.6, HNR = 10.

5.1.4 Coupling between Pitch and Formants

In this study, the classic decoupled source-filter theory is assumed as the model for the production of vocalic speech sounds. In this view, the vocal apparatus can independently control the frequency of vibrations of the vocal folds and the shape of the supraglottal cavities. In addition, the acoustic impedance of the glottal orifice is assumed to be much larger than the impedance of the vocal tract, further supporting the decoupled theory [73]. As explained in the physiology of pitch control in Section 4.2, the fundamental frequency of vocal fold oscillation is largely due to the stiffness of the vocalis muscle and vocal fold tissue density, where the stiffness can be modulated by external laryngeal muscles. Thus, each vowel's associated formants, dependent mainly on the position of the tongue, can thus be realized at a continuous array of pitches.

In reality, though, this simple model has been shown to be incomplete by several studies investigating the coupling effect of formant frequencies and the frequency of vocal fold vibrations. Perhaps the best evidence for coupling is found in studies that simply analyze vowel acoustics across many speakers and languages of the world. Peterson, Barney, and Lehiste have documented what is referred to as the "intrinsic pitch of vowels," where high and low vowels are observed to be produced with higher and lower pitches, respectively [44, 62]. The difference in pitches vary anywhere from 4 to 25 Hz, and the difference has been shown to be significant across different languages and testing settings [79]. Though not a physiological verification of source-filter coupling, the evidence that humans tend to co-vary their pitch with vowel formants demonstrates the existence of a natural coupling phenomenon.

Turning to the speech production of the singing voice, a commonly cited predicament is how soprano vocalists sing a vowel in which the first formant frequency (F1) is lower than the fundamental frequency. In this case, the percept of F1 is nonexistent, since the spectral envelope due to the vocal tract resonances is effectively sampled at integer multiples of the fundamental frequency. Sundberg has shown that, at high pitches, soprano vocalists alter their tongue position to match F1 to the fundamental frequency [76]. One possible cause given for this formant matching phenomenon is the need for the vocalist to maximum his or her vocal efficiency. Thus, placing F1 at the location of the desired pitch will maximally amplify the energy at the fundamental frequency.

Finally, in an interesting study by Rothenberg, it was shown that the amplitude of the vocal fold vibrations can be affected by changes in the vocal tract acoustics [69]. Again, the effect was only observed when the subjects, female professional vocalists, produced vowels at pitches greater than 600 Hz. Briefly, the experimental setup consisted of a Rothenberg mask [68], an electroglottograph (EGG), and a cylindrical tube whose variable position could be controlled by a electromechanical transducer. Within a trial, the subject sustained a vowel while the tube was dynamically pushed to the lips and pulled away. Adding the tube effectively increased the acoustic length of the vocal tract and forced a downward shift in F1. Rothenberg analyzed the EGG signals and concluded that the amplitude of the vocal fold vibrations was decreased during the times when the tube extended the length of the vocal apparatus.

Again, detailed aerodynamic and mechanical measurements have not been made yet on the extent to which formant frequencies and pitch co-vary. The results of these studies, however, point to an alternative pitch modification model that provides for constant feedback between the periodic source waveform and the resonance properties of the vocal tract acoustic filter.

5.1.5 Processing Continuous Speech

In the analysis above, sustained vowels and vowels with time-varying pitch were the speech signals of interest. Taking a broader view, we are interested in continuous speech. Toward this objective, we have developed a preliminary pitch-scale modification system that handles both voiced and unvoiced speech by processing voiced speech with our proposed system and then concatenating unprocessed unvoiced speech with our pitch-modified voiced speech.

Figure 5.4a displays the original and modified waveforms of continuous speech spoken by a non-pathological female speaker. The utterance is "As time goes by." The pitch scale is set to 0.8 and the original and modified pitch contours are shown in Figure 5.5. A signal comparison is made in Figure 5.4 between outputs from our proposed modification algorithm and from the sinewave transformation system (STS) discussed in Section 3.1 [64, 65]. Both algorithms adequately modify the pitch contour by the desired ratio. Using STS, the noise component is perceived as somewhat tonal and more perceptually separate from the periodic component. Harmonicity in the narrowband spectrogram in the 1–1.25 s window above 2500 Hz is overestimated by the STS algorithm in Figure 5.4b. This effect is due to the degree of voicing index that selects a boundary frequency between periodic and stochastic spectral regions. In the time between 1 and 1.25 s, it appears that the degree of voicing is overestimated and the perceived speech is removed of aspiration noise.

The output signal from the proposed algorithm is perceived to contain a breathier quality, consistent with the quality of the original waveform. Specifically, the signal characteristics displayed in Figure 5.4c tends to preserve the fullband aspiration noise features from the original signal. The signal modified with the proposed algorithm is free of artifacts and discontinuities that may appear in standard modification techniques. When performing preliminary analysis on running speech, however, it is observed that the decomposed noise estimate sometimes contain leakage from the harmonic components. This harmonicity in the noise spectrum, also observed when decomposing isolated vowel waveforms, is also perceptually significant. The time-varying nature of natural vowels, in addition to the effects already mentioned regarding jitter and shimmer, may contribute to the suboptimal performance of the separation technique because of inaccurate pitch estimation. Possible solutions may employ more advanced signal processing methods to help create perturbation-free waveforms and to better estimate the pitch contour of continuous speech.

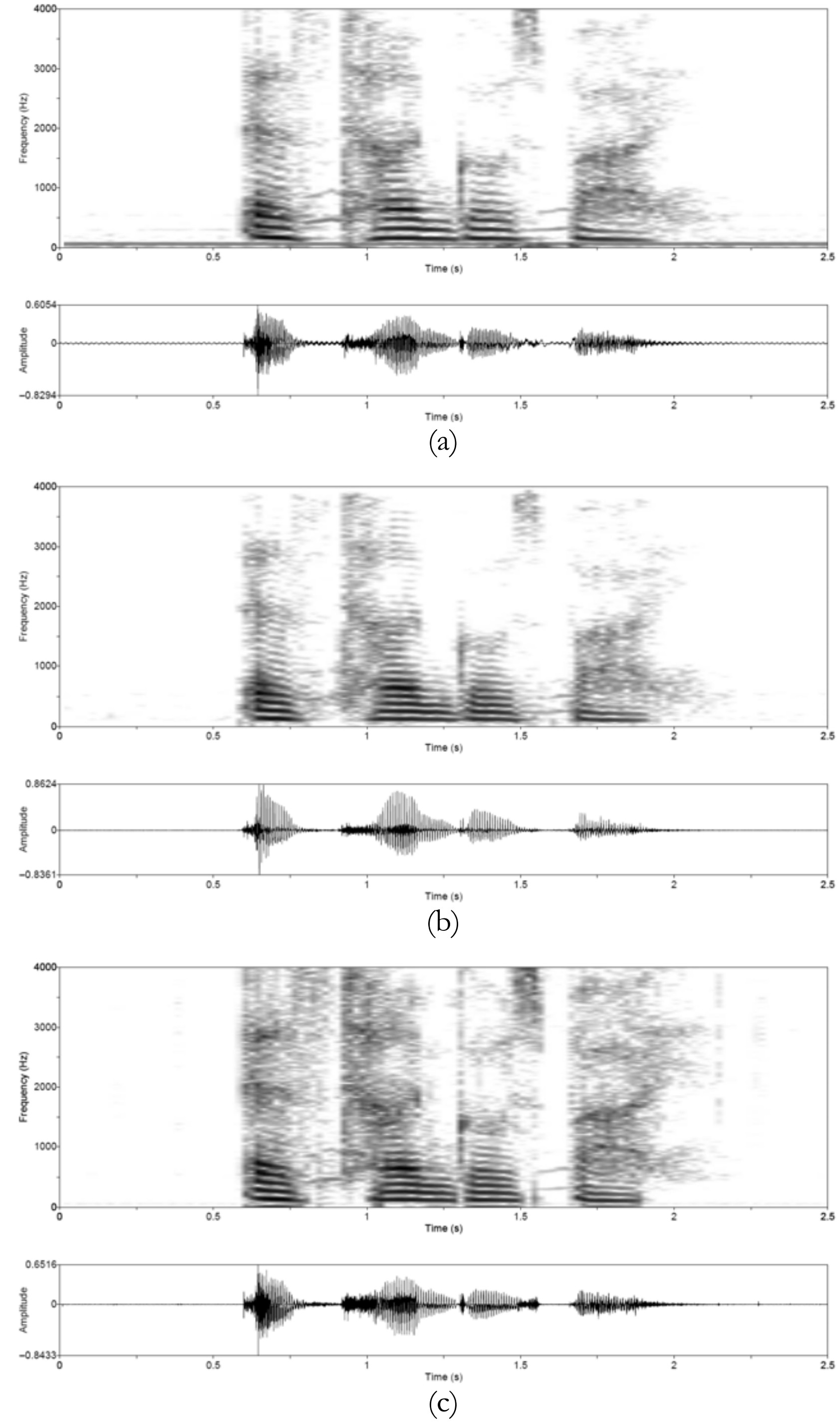

Figure 5.4 Comparing pitch-scale modification algorithms. Utterance by a normal speaker saying: "As time goes by." (a) Original signal, (b) modified by STS, and (c) modified by our proposed algorithm. Narrowband spectrograms (upper plot) and time-domain waveforms (lower plot) plotted for each signal. Modification parameters: Pitch scale = 0.8, LPC order = 10, LPF cutoff = 350.

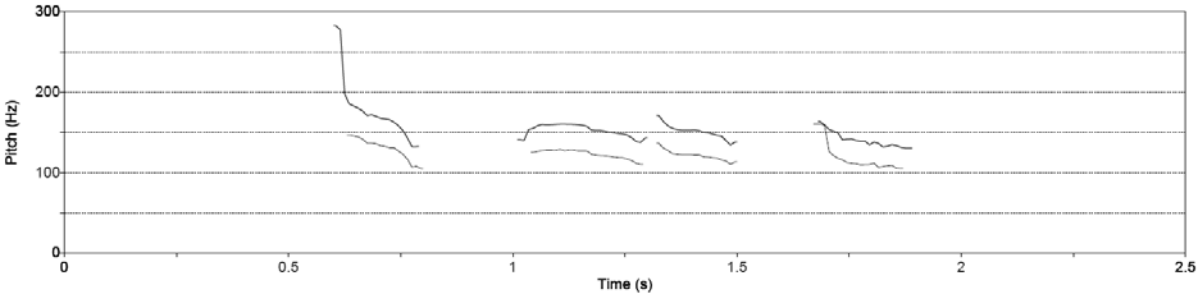

Figure 5.5 Original (thick line) and modified (thin line) pitch contours of continuous speech example in Figure 5.4. Pitch contours similar for outputs of proposed algorithm and STS.

5.1.6 Formal Listening Evaluation

We have made informal listening observations in both Sections 4.7 and 5.1.5, indicating promise to our proposed modification approach on both vowels and continuous speech. Formalizing the evaluation procedure is a direction of future work. Perceptual ratings of pitch-modified speech may be performed using the mean opinion score (MOS) as the quality index. To determine the MOS, listeners rate the quality of the speech signals pitch-modified by different algorithms. Listeners give each signal a quality rating ranging from 1 to 5: (1) unsatisfactory, (2) poor, (3) fair, (4) good, and (5) excellent [35]. The MOS is the arithmetic mean of all the individual scores. This assessment would provide for a statistical significant way of evaluating our algorithm against baseline algorithms.

5.2 Conclusions

In this study, we approached the problem of high-quality speech synthesis and pitch-scale modification in the context of vocalic speech sounds containing an aspiration noise component. We first developed a vowel production model that follows the classic linear source-filter speech model, in which both a periodic and stochastic source excite the acoustic filter in the vocal tract. Inspired by physiological observations, we assumed an additive model, in which both speech sources are coupled together, so that the stochastic excitation, or aspiration noise source, is temporally modulated by the periodic source waveform due to gating of turbulent airflow by vocal fold vibrations. The glottal airflow velocity waveform, modeled by the Rosenberg pulse [67], serves as the multiplicative modulation function that acts on the aspiration noise source. Based on our model, we implemented a vowel synthesizer allowing us to explore the salience of these modulations, specifically revealing the importance of temporal synchrony between noise bursts and the periodic glottal airflow waveform. This is consistent with previous research on the perception of natural-sounding vowel synthesis [20, 36, 66].

To estimate the actual patterns of the noise modulations in the aspiration noise signal, we turned to signal processing algorithms that analyze a speech signal and separate its periodic and noise components. After qualitatively reviewing state-of-the-art algorithms and quantitatively evaluating one in particular, we chose to use the pitch-scaled harmonic filter [31] because of its simplicity and ability to approximately preserve temporal modulation features present in the noise component of a synthesized vowel waveform. Due to the stochastic nature of aspiration noise, the envelopes of the noise modulations could only be estimated to a certain degree, but show varying levels and types of modulation patterns in normal and pathological speakers. Results of our analysis on real vowels indicate that noise bursts can occur at several time instants within the glottal cycle. In particular, after estimating the source of a noise component, we observed noise amplitude maxima during the open phase of the assumed glottal cycle and at time instants around glottal closure.

Finally, to enhance the natural quality of pitch-scale modification algorithms, we designed a strategy to take into account the observed patterns of modulation and temporal synchrony between the harmonic and noise components in a voiced speech sound. We showed that advanced modification algorithms have taken several different approaches to altering the fundamental frequency of a speech signal and that we aimed to take the effective parts from each strategy to develop a more physiologically-based algorithm. Inspired by the physiology of pitch control in human speakers, our approach was designed to preserve temporal and spectral features in the original speech signal. Assuming our vowel production model, a change in pitch affected the fundamental frequency of the periodic source and the modulation function imposed on the turbulent airflow sources. Thus, after separating the original signal into its harmonic and noise components, we focused on maintaining the inherent qualities of the noise by implementing a non-parametric processing structure that estimated the envelope of the modulated noise source and re-modulated the source with a pitch-modified version of the envelope. Due to an inverse filtering stage by linear prediction and a noisy envelope estimation procedure, certain assumptions and caveats must be satisfied before effectively making use of the proposed algorithm. For the given examples, however, the reconstructed modified signal was perceptually natural-sounding and gives promise and direction toward a more accurate pitch-scale modification system.

Appendix A

Parameter Lists

Synthesis parameter	Units (if applicable)	Possible values	Default value	Purpose
Noise type		unmodulated, modulated	modulated	Indicates whether the noise source is modulated by the periodic glottal waveform or not.
Vowel		i, e, ae, a, o, u	a	Indicates formant values. See Table 2.1.
f_0	Hz	Any positive number	100	Pitch track for synthesized vowel.
Gender		m, f	m	Selects set of formant values. See Table 2.1.
f_s	Hz	Any positive number	8000	Sampling rate
Duration	seconds	Any positive number	1	Duration of vowel
DC		Any rational number between 0 and 1, inclusive	0.1	Only relevant if modulated noise is chosen. This parameter controls the amount of noise during the closed phase. The minimum flow at the open phase is increased depending on DC flow.
OQ		Any rational number between 0 and 1, inclusive	0.6	The open quotient. Dictates the open phase duration (OQ/f_0) within a glottal cycle.
HNR	dB	Any rational number	10	Sets the harmonics-to-noise power ratio. $10\log_{10}\left(\frac{\text{Harmonic power}}{\text{Noise power}}\right)$

Table A.1 Parameters of vowel synthesizer.

Modification parameter	**Units (if applicable)**	**Possible values**	**Default value**	**Purpose**
Pitch scale	Hz	Any positive, rational value	0.8	Pitch modification factor. For example, if the input pitch is 100 Hz, the output pitch will be equal to 0.8(100) = 80 Hz.
LPC order		Any positive whole number.	10	Indicates order of all-pole model in the linear prediction analysis of the inverse filtering stage. *P* in Equation (E.2).
LPF cutoff	Hz	Any positive number	350	3-dB cutoff frequency for low-pass filter used in the Envelope Estimation stage (see Figure 4.6).

Table A.2 Parameters of proposed pitch-scale modification algorithm.

Appendix B

MATLAB Graphical User Interface

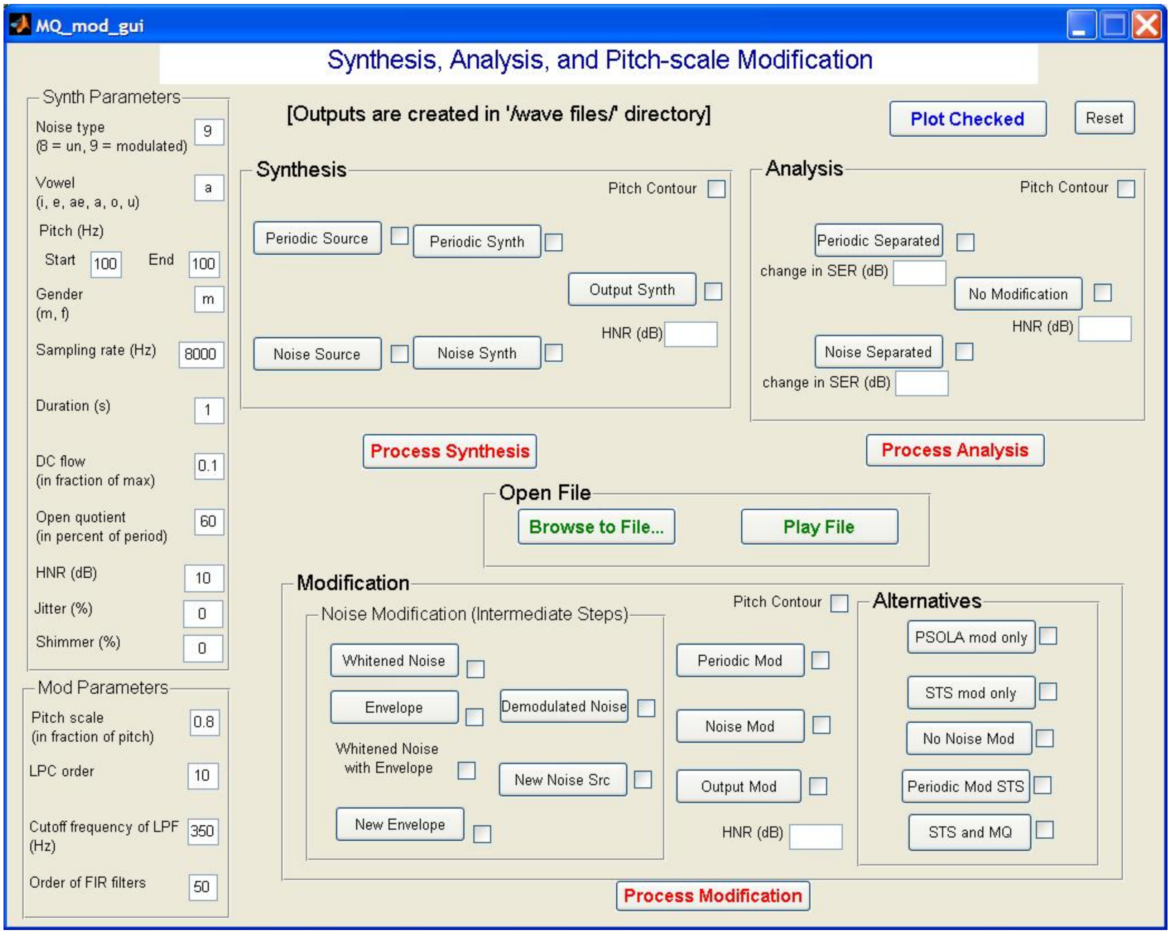

[Outputs are created in '/wave files/' directory]

Synth Parameters

Noise type (8 = un, 9 = modulated) 9

Vowel (i, e, ae, a, o, u) a

Pitch (Hz) Start 100 End 100

Gender (m, f) m

Sampling rate (Hz) 8000

Duration (s) 1

DC flow (in fraction of max) 0.1

Open quotient (in percent of period) 60

HNR (dB) 10

Jitter (%) 0

Shimmer (%) 0

Mod Parameters

Pitch scale (in fraction of pitch) 0.8

LPC order 10

Cutoff frequency of LPF (Hz) 350

Order of FIR filters 50

HNR (dB)

change in SER (dB)

HNR (dB)

change in SER (dB)

HNR (dB)

Figure B.1 MATLAB GUI.

The parameters from the tables above were integrated into a graphical user interface (GUI) in MATLAB [47] for rapid prototyping of speech signal synthesis, analysis, and modification. A screen shot of the GUI is displayed in Figure B.1. Chapter 2 discussed the background and development leading up to the code behind the Synthesis GUI panel. Chapter 3 led the reader through the implementation behind the Analysis panel that decomposes the input signal into harmonic and noise components. Finally, Chapter 4 discussed the pitch-scale modification sections.

The GUI layout was designed for easy access to the waveforms during intermediate processing stages of each algorithm. Each button can be depressed to play the waveform out to the PC soundcard, and checkboxes are available to select waveforms to be plotted. The left column allows user input to control the parameters of vowel synthesis and pitch-scale modification. Note that no parameters are needed for running the harmonic/noise decomposition algorithm. In the future, it would be instructive to view the effects of varying the analysis window duration. Presently, the embedded duration is fixed at four times the local pitch period. Note that the harmonic-to-noise (HNR) measures are calculated for the synthesized, analyzed, and modified signals to allow for comparison of relative energy contributions. The "change in SER" value is analysis performance measure from [31] that was not used in this thesis.

In the Modification panel, alternative outputs are generated that allow for analysis on the differences between different algorithms. In the GUI, the overall signal is processed by the TD-PSOLA algorithm and the sinusoidal transformation system (STS) based on the sinewave representation of McAulay and Quatieri [64, 65]. In addition, No Noise Mod refers to a modified output whose periodic component was modified using TD-PSOLA and noise component was unmodified. Periodic Mod STS is a similar waveform, except that the periodic component was processed using the STS method. STS and MQ refers to a fusion of algorithms: the periodic component being modified by STS and the noise component modified by the author's proposed approach from Section 4.4. Finally, Output Mod refers to the proposed modification algorithm, in which the periodic component is processed by TD-PSOLA and the noise component is modified as in our implementation (Section 4.5.3). Note also that intermediate steps in the proposed pitch modification algorithm are identified and allowed to be plotted in the GUI.

Finally, since our analysis encompasses both synthesized and real vowels, the Open File button provides the ability for the user to access any wave file containing a spoken utterance. In the case of the analysis of a wave file, any changes to the synthesizer parameters are ignored and the Synthesis panel outputs are meaningless. Processing can then be continued via the Analysis and

Modification panels. Microsoft WAV files are created for each waveform and stored in a local "wave files" folder for easy access and portability.

Appendix C

Pitch-Scaled Harmonic Filter

To gain insight into the pitch-scaled harmonic filter, we step through the derivation for an example frame, where N is the window length, f_s is the sampling rate in Hz, and T_0 is the assumed pitch period, in seconds. We start by knowing that the frequency spacing between bins of the N-point DFT is $\frac{f_s}{N}$ Hz [60], which is the reciprocal of the window duration, $\frac{N}{f_s}$ seconds. If N is chosen to be an integer multiple of the pitch period in samples, then we have $N = b \cdot T_0 \cdot f_s$, where b is a positive integer. The DFT bin spacing, in Hz, can then be written as $\frac{f_s}{N} = \frac{f_s}{b \cdot T_0 \cdot f_s} = \frac{1}{b \cdot T_0}$. Since the pitch, in Hz, is $\frac{1}{T_0}$, each bin is spaced apart by $\frac{1}{b}$ of the pitch. For example, if b is 4, the bin spacing would be one-fourth of the pitch, and every fourth Fourier coefficient would contain power at harmonics of the fundamental frequency.

Figure C.1 displays an example of a purely periodic vowel signal and its analysis by the pitch-scaled harmonic filter. The vowel, with a steady pitch of 100 Hz, has a pitch period length of 80 samples (f_s = 8000 Hz). The factor b is 4, and the 320-point DFT is taken of a windowed segment of length 320 samples. The magnitude spectrum shows that the harmonic energy is concentrated at every fourth DFT bin, a direct result of the bin spacing being one-fourth of the pitch, or 25 Hz.

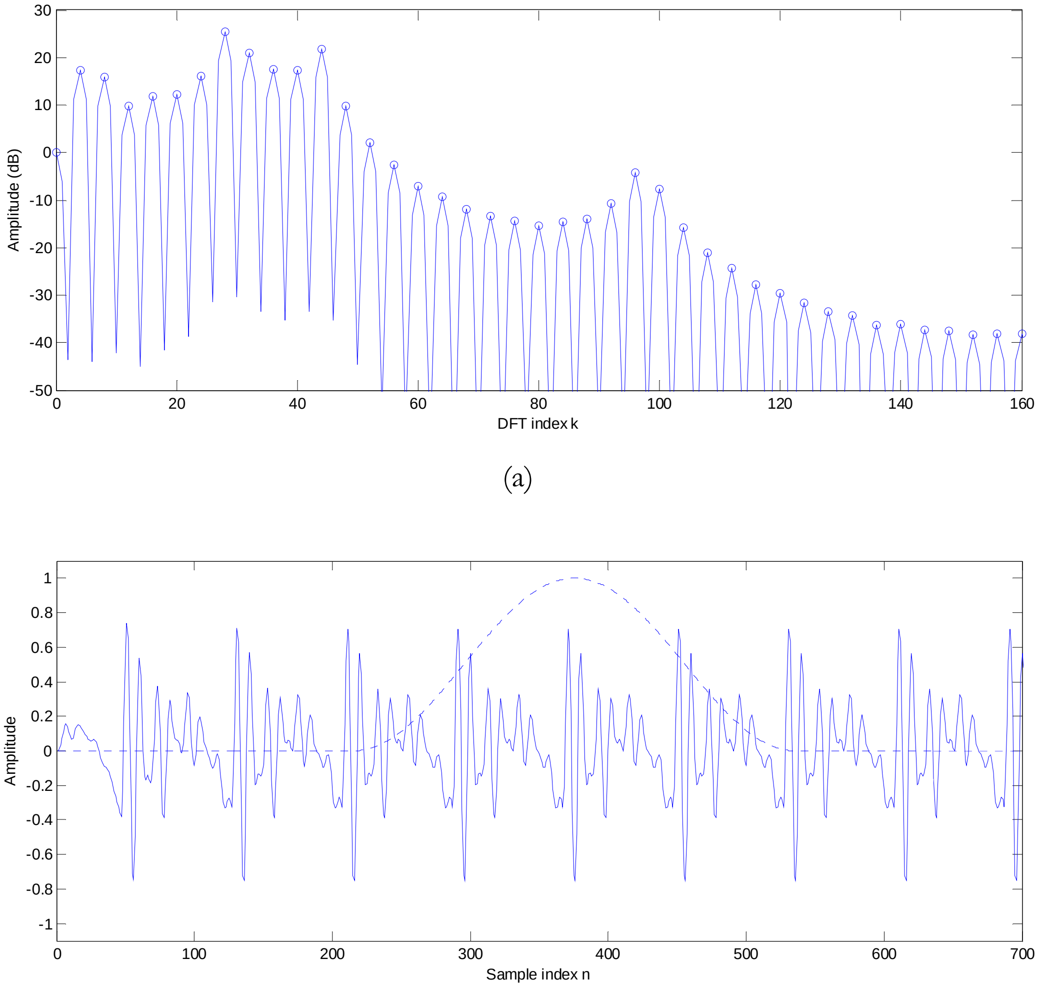

(a)

(b)

Figure C.1 Example of the pitch-scaled harmonic filter on a windowed segment. (a) DFT of short-time signal from vowel signal in (b), windowed by a Hanning window (dotted line). Circles in (a) indicate DFT magnitude at every fourth DFT index. Synthesis parameters: Vowel = a, f_0= 100, Gender = m, f_s = 8000, DC = 0.1, OQ = 0.6.

Appendix D

Defining Glottal Cycle Properties

Figure D.1 summarizes our definition of closed phase, open phase, and glottal closure within a glottal cycle, or pitch period. The closed phase is the time during which the membranous vocal folds are in contact and no AC component exists. The open phase is the remaining duration of the pitch period when airflow velocity is modulated by the vocal fold vibrations. The glottal closure instant is the time when the open phase becomes the closed phase. Note that the open quotient measure is the ratio between the open and closed phases.

In our analyses in Sections 3.3, 3.4, and 4.6, we assumed that we could derive these properties of the periodic source waveform by observing the pressure waveform of a vowel after filtering by the vocal tract and radiation characteristics. The lower waveform in Figure D.1 displays a vowel synthesized from the periodic source in the upper waveform. The negative peaks in the filtered waveform correspond with the instants of glottal closure. Deducing the open and closed phases from a vowel waveform is difficult because of their relative closeness. However, we can assume that samples just prior to the glottal closure instant are present during the open phase of the source waveform.

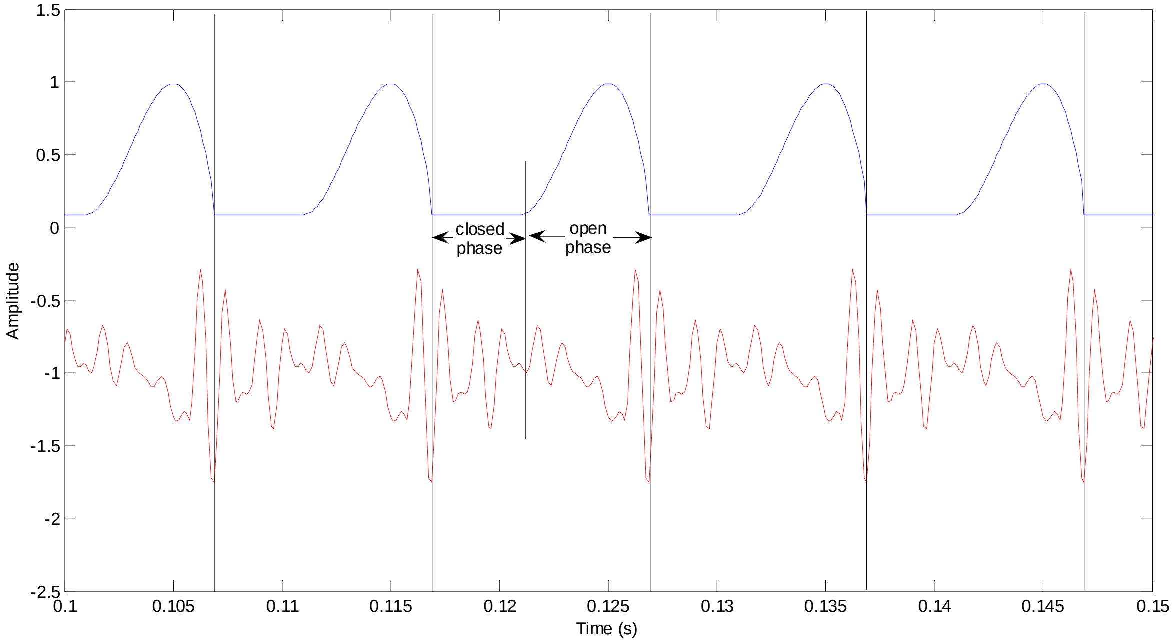

Figure D.1 Defining glottal waveform properties. Synthesized waveforms are of the periodic source (upper) and corresponding vocal tract/radiation-filtered waveform (lower). Vertical lines indicate instants of glottal closure. Synthesis parameters: Vowel = a, f_0 = 100, Gender = m, f_s = 8000, Duration = 1, DC = 0.1, OQ = 0.6.

Appendix E

Linear Prediction of Stochastic Signals

Whitening is accomplished in each short-time segment by estimating the all-pole filter that best fits the vocal tract resonance properties and the radiation characteristic. Since the radiation characteristic has a zero and behaves like a high-pass filter, the estimated poles model the zero as closely as possible depending on the number of poles. The all-pole model of a windowed aspiration noise waveform, $u_w[n]$, where the input is white Gaussian noise, $w[n]$, is displayed in Figure E.1.

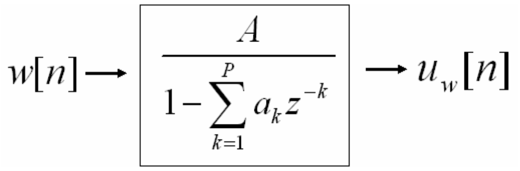

Figure E.1 All-pole model of aspiration noise.

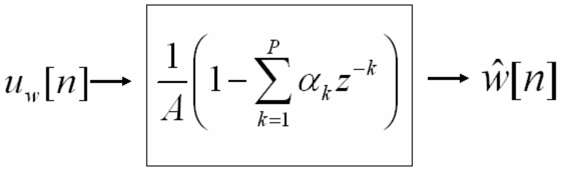

Figure E.2 The inverse approach to solving for the all-pole model in the stochastic case.

Figure E.2 takes the inverse approach to solving for the coefficients of the all-pole filter and rewrites the problem so that the filter coefficients of a corresponding FIR filter are estimated to result in the best estimate, $\hat{w}[n]$, of white noise. Linear prediction of a stochastic signal can be used to find these coefficients by assuming that each noise sample in the segment, $u_w[n,r]$, is predictable by a weighted sum of P prior samples:

$$u_w[n,r] = \sum_{k=1}^{P} \alpha_k[r] u_w[n-k,r], \tag{E.1}$$

where P is also the number of poles and α_k values are the coefficients of the Pth-order filter, in the rth frame. The error function, $\sum_{n=-\infty}^{\infty} e^2[n]$, minimizes the difference between the expected value of $w[n]$ and the expected value of $\hat{w}[n]$.

After minimizing the expected value of the squared error by taking the derivative with respect to each α_k coefficient, a set of P equations in P unknowns is obtained. The complete derivation (see [63] for details) results in a Pth-order FIR filter whose coefficients are equal to the α_k's and the gain is A. We also fold in the inverted radiation characteristic filter to yield the complete short-time inverse filter with impulse response, $h^{-1}[n,r]$, and frequency response, $H^{-1}(z,r)$:

$$H^{-1}(z,r) = \frac{1}{A}\left(1 - \sum_{k=1}^{P} \alpha_k[r] z^{-k}\right). \tag{E.2}$$

Appendix F

Comparison of Envelope Detection Methods with a Broadband Noise Carrier

Asynchronous AM Detection

In the communication systems world, a common method of amplitude modulation (AM) detection is asynchronous envelope detection via a diode rectifier and RC low-pass filter circuit. AM radio receivers further add a DC block circuit so that the resulting envelope, the message of the signal, can be played out over speakers [6]. A block diagram of asynchronous envelope detection is displayed in Figure F.1.

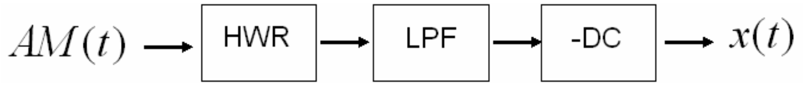

Figure F.1 Classic method of asynchronous detection of AM message. HWR = half-wave rectification, LPF = low-pass filter, -DC indicates that the mean value is subtracted.

The form of AM signals is (from [6])

$$AM(t) = A_c[1 + \mu x(t)]\cos \omega_c t, \tag{F.1}$$

where μ denotes the modulation index or depth, $x(t)$ is the message signal to be transmitted, A_c is the unmodulated carrier signal amplitude, and ω_c is the carrier signal's frequency in rad/sec. The carrier frequency must be much larger than the frequencies in the message signal, so that the low-pass filter can effectively reject energy at the carrier frequency while preserving the signal characteristics of the message.

Figure F.2 shows an example of AM signal construction and the output of the classic AM envelope detector. The message is composed of the sum of two sinusoids at 10 and 17 Hz ($x(t)$ in Figure F.2a), and the carrier signal is a 6000–Hz sinusoid ($\cos(\omega_c t)$ in Figure F.2b). The resulting AM signal is processed through the stages in Figure F.1. Figure F.2d shows that the output of the envelope detector is correct within a gain factor (about 6 in this case). For the application of AM radio reception, this factor is not an issue since the gain can be controlled at the receiver. (The modulation index, μ, in this case was set to 0.5, so its inverse does not make up the entire gain.) The 3-dB cutoff frequency of the low-pass filter was set to 100 Hz and implemented via a 50th-order finite impulse response filter.

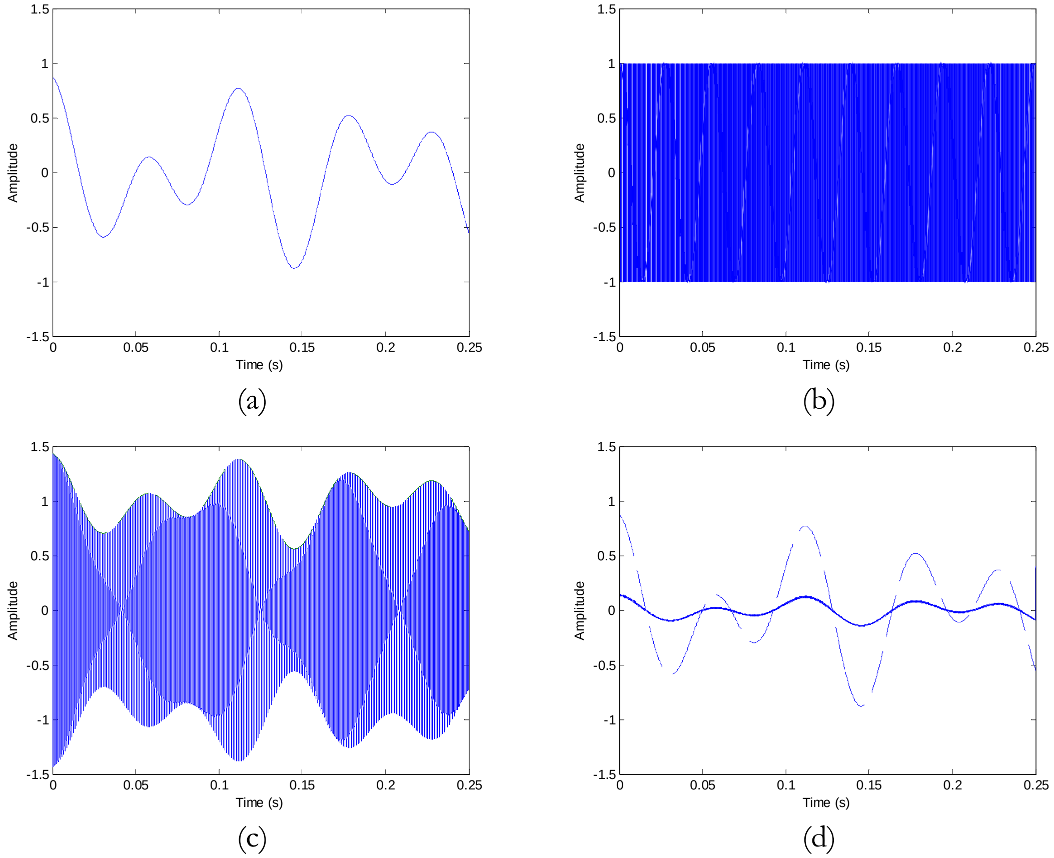

(a)

(b)

(c)

(d)

Figure F.2 Amplitude modulation example. (a) Message, (b) carrier, (c) AM signal, and (d) envelope detected using asynchronous detection (solid line), with desired envelope (dashed line).

As a second example to further test the asynchronous envelope detection method, the same message was used as in the previous case in Figure F.3. The carrier frequency is decreased to 1000.

The resulting message signal does not follow the original message. The method is not robust across different message, carrier, and LPF cutoff frequencies, and this undesirable property prompts us to investigate the Hilbert transform method.

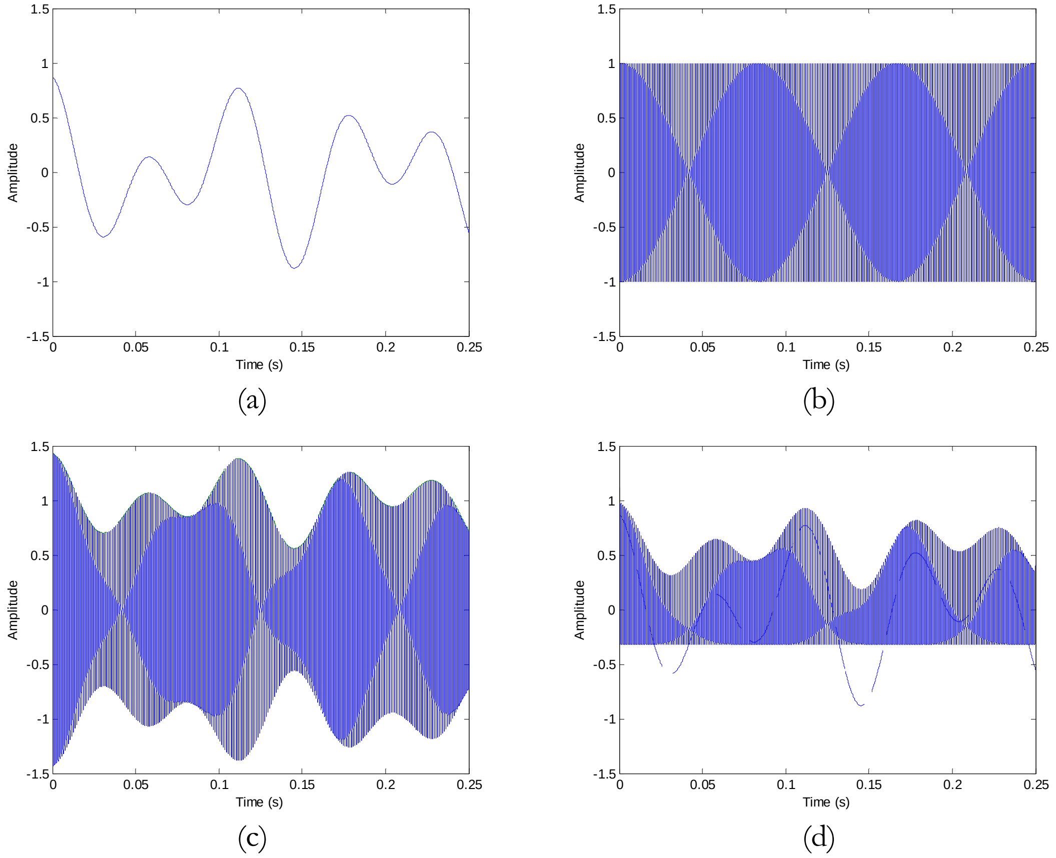

(a)

(b)

(c)

(d)

Figure F.3 Amplitude modulation example with lower carrier frequency. (a) Message, (b) carrier, (c) AM signal, and (d) envelope detected using asynchronous detection (solid line), with desired envelope (dashed line).

Hilbert Transform Method

In the Hilbert transform method, the notion of an analytic signal is introduced. Any real signal can be represented by its one-sided Fourier spectrum due to its Hermitian symmetry, with an even magnitude and odd phase characteristic. As a result, the spectral redundancy may be eliminated, and the right side of the spectrum is termed the analytic representation of a real signal [2]. The envelope of a real signal may be calculated from its analytic representation through a straightforward calculation. A derivation of the analytic signal follows (see [2] for details).

The analytic representation, $z(t)$, is equal to the sum of an original real signal, $x(t)$, plus a term, $y(t)$, derived from the Hilbert transform of the real signal:

$$z(t) = x(t) + jy(t). \tag{F.2}$$

The Hilbert transform, $y(t)$, is calculated by subjecting $x(t)$ to a quadrature filter with impulse response $r_Q(t)$. The impulse response and frequency response, schematized in Figure F.4, are

$$r_Q(t) = \frac{1}{\pi t} \Rightarrow R_Q(f) = -j\,\mathrm{sgn}(f), \tag{F.3}$$

where sgn(f) is the signum function (positive frequencies retain their sign, while the phase of negative frequencies shift by 180°). Thus, the analytic signal is a complex function, its real part equal to the original real signal, $x(t)$, and its imaginary part equal to $x(t) * r_Q(t)$.

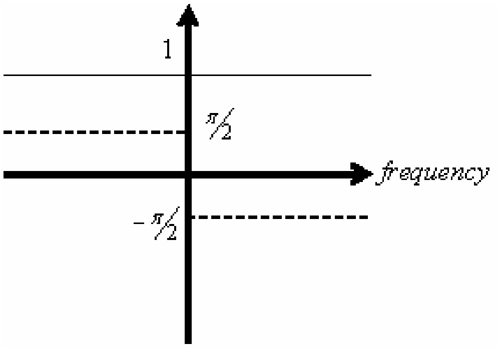

Figure F.4 Schematic of frequency response of the Hilbert quadrature filter. Magnitude (solid line) and phase (dashed line) response.

The spectrum of the analytic signal, $Z(f)$, is simply

$$\begin{aligned} Z(f) &= X(f) + jY(f) \\ &= X(f)[1 + \mathrm{sgn}\, f] \\ &= 2U(f)X(f), \end{aligned} \tag{F.4}$$

where $U(f)$ is the unit step function with $U(0) = 0.5$.

The complex envelope, $e(t)$, of a real signal is derived from its analytic representation:

$$e(t) = z(t)e^{-j2\pi ft} = m(t) + jn(t), \tag{F.5}$$

and the instantaneous amplitude, $a(t)$, of the real signal, $x(t)$, is then defined as

$$\begin{aligned} a(t) &= |e(t)| = \sqrt{m^2(t) + n^2(t)} \\ &= |z(t)| = \sqrt{x^2(t) + y^2(t)}. \end{aligned} \tag{F.6}$$

In the case of AM signal demodulation, $x(t)$ is the AM signal, $AM(t) = A_c[1 + \mu x(t)]\cos\omega_c t,$ from Equation (F.1). Essentially, the Hilbert transform method computes the magnitude of the analytic signal of a real signal. The analytic signal, $z(t)$, is simply

$$z(t) = [1 + \mu x(t)]e^{j2\pi ft}, \tag{F.7}$$

and the instantaneous amplitude, $z(t)$, is

$$z(t) = |1 + \mu x(t)|. \tag{F.8}$$

In the aspiration noise source case, the carrier signal is white noise, $q[n]$, and the message signal is the glottal flow waveform estimate, $u_g[n]$. Since the glottal flow waveform is assumed to always be greater than zero (negative airflow is ignored), notation is transferred from that of AM to that of DSB-SC (double side band-suppressed carrier). The "suppressed-carrier" notation stems from the fact that the modulated signal, $DSB(t)$, eliminates the energy at the carrier frequency:

$$DSB(t) = x(t)\cos(\omega_c t). \tag{F.9}$$

The modulation index, μ, disappears since the depth of modulation is dictated by the AC amplitude of the message, $x(t)$. A demodulation example with the same 1000-Hz carrier and message as before is depicted in Figure F.5. As expected, the demodulated message matches the modulating function.

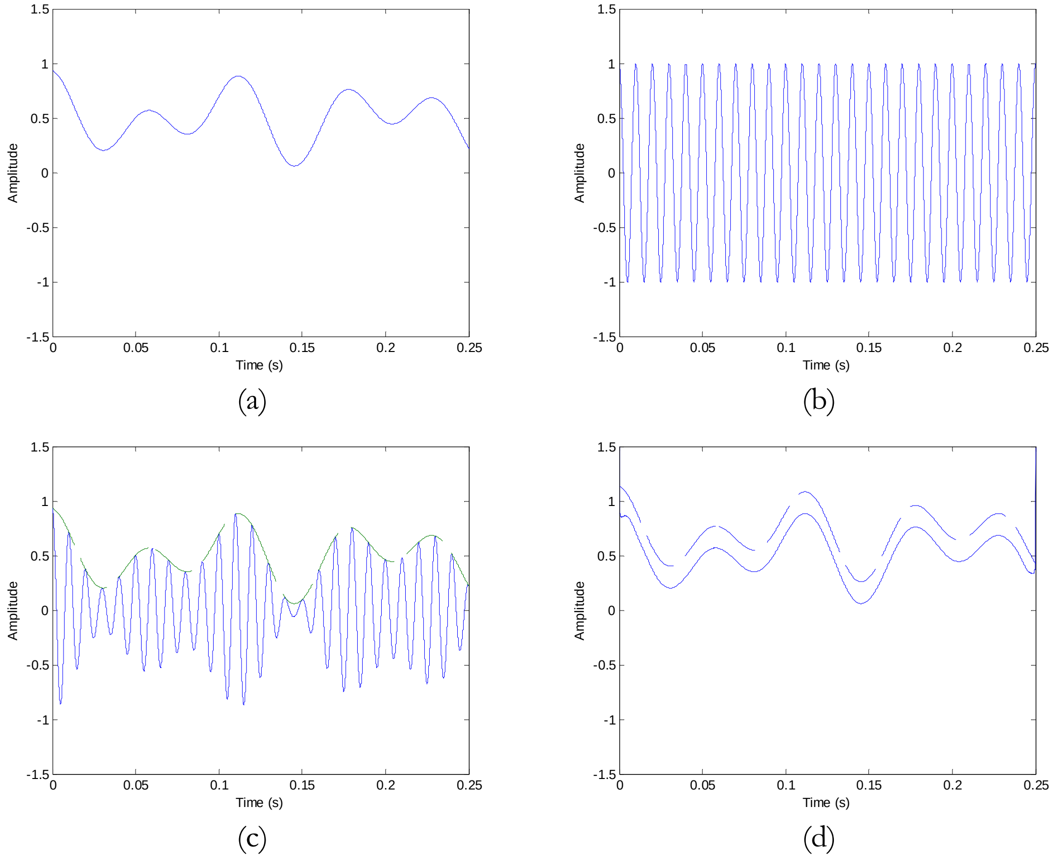

Figure F.5 DSB-SC modulation example. (a) Message, (b) carrier, (c) AM signal (solid line) with message (dashed line), and (d) envelope detected using Hilbert transform method (solid line) with desired envelope (dashed line). Note the lines in (d) are offset vertically by 0.2 for clarity.

Figure F.6 gives an envelope detection example with two sinusoids modulating a white noise carrier. The demodulated signal is shown in Figure F.6d. The magnitude of the analytic signal seems to follow each local peak of the DSB-SC signal instead of tracing the low-frequency message signal. The result is expected since the Hilbert envelope is known to work in the case of narrowband carriers.

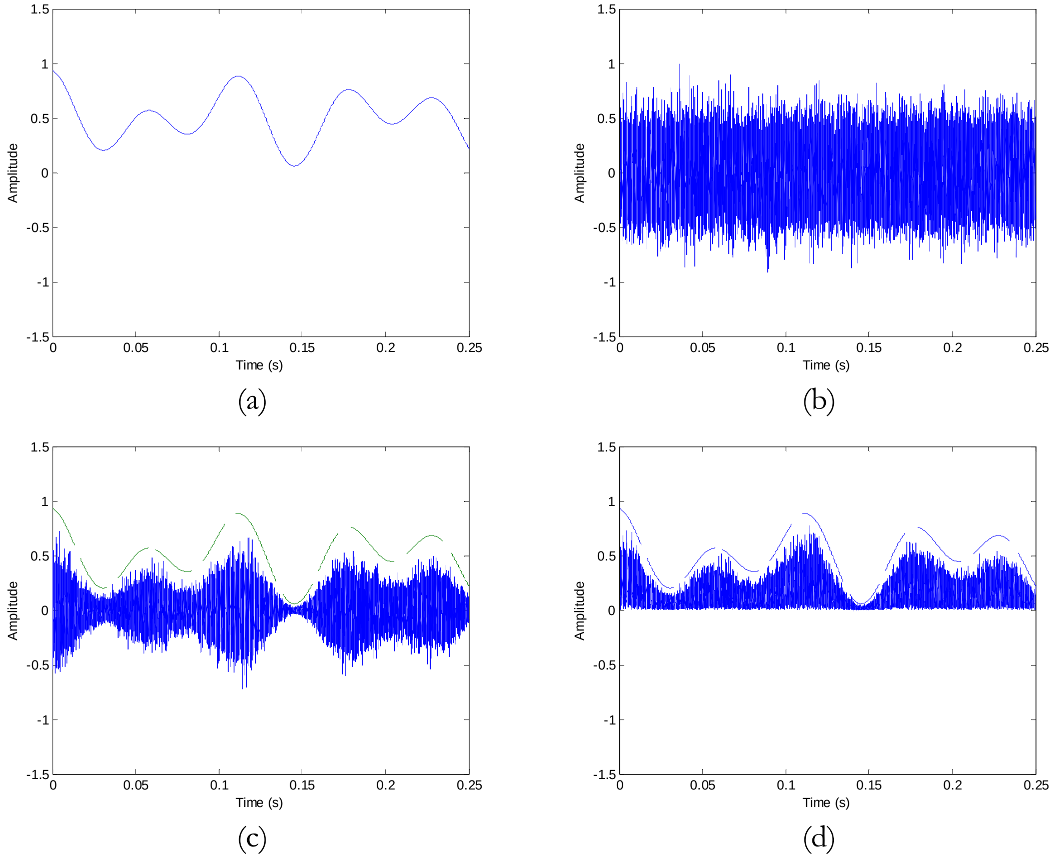

(a)

(b)

(c)

(d)

Figure F.6 DSB-SC modulation example with noise carrier. (a) Message, (b) carrier, (c) AM signal (solid line) with message (dashed line), and (d) envelope detected using Hilbert transform method (solid line) with desired envelope (dashed line).

To recover the low-frequency information, a low-pass filter is appended to the Hilbert transform method in Figure F.7. The cutoff frequency is chosen to be 100 Hz in the example case and waveforms are re-displayed in Figure F.8. The estimated envelope better matches the desired message signal, though the amplitude of the envelope does not match that of the modulation function. The method reveals the modulation function better than the AM envelope detector. In speech applications, we will assume that any relevant modulation information exists below 350 Hz (an upper pitch limit for normal adult pitch ranges). It is known that the envelope cannot be estimated exactly when the carrier is a broadband signal such as white noise. The difficulty of determining the envelope of a noise carrier is evident, but the Hilbert transform method helps approximate time-domain modulations within the context of inherent random ripples in the noise envelope.

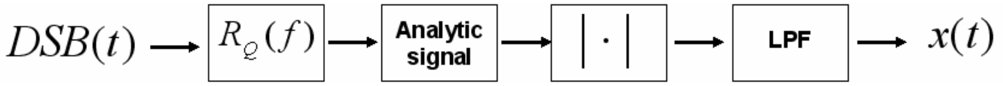

Figure F.7 Hilbert transform/low-pass filter method of envelope detection in a DSB signal. $R_Q(f)$ is the frequency response of the quadrature filter that outputs the Hilbert transform of the input real signal. The complex analytic signal is then formed with its real part equal to $DSB(t)$ and imaginary part equal to the Hilbert transform. Next, the magnitude of the analytic signal is taken. Finally, a low-pass filter acts on the signal.

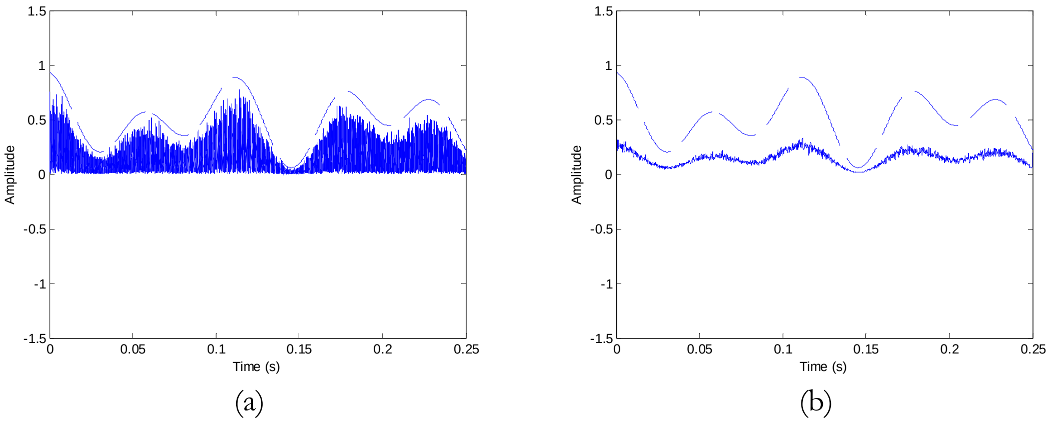

Figure F.8 DSB-SC modulation example with modified Hilbert transform method. Message and carrier as in Figure F.6. (a) Envelope detected using Hilbert transform method (solid line) with desired envelope superimposed (dashed line) and (b) envelope detected (solid line) with desired envelope (dashed line).

In the speech case, the glottal waveform, $u_g[n]$, modulates a white noise signal that is the result of turbulent flow at and around the vocal fold region. Figure F.9 illustrates the effect of overlap between the harmonic and aspiration noise spectra. In particular, the magnitude of the analytic signal derived from the modulated noise waveform, shown in Figure F.9b, is very noisy due to the stochastic nature of its carrier signal. Although difficult to separate the underlying envelope, to smooth out some of the fluctuations, a low-pass filter is applied resulting in the plots in Figure F.9c. Although the original modulation waveform in Figure F.9a is not perfectly reconstructed, the method obtains an envelope with evidence of the general modulation characteristics and temporal patterns, which is of interest in this study.

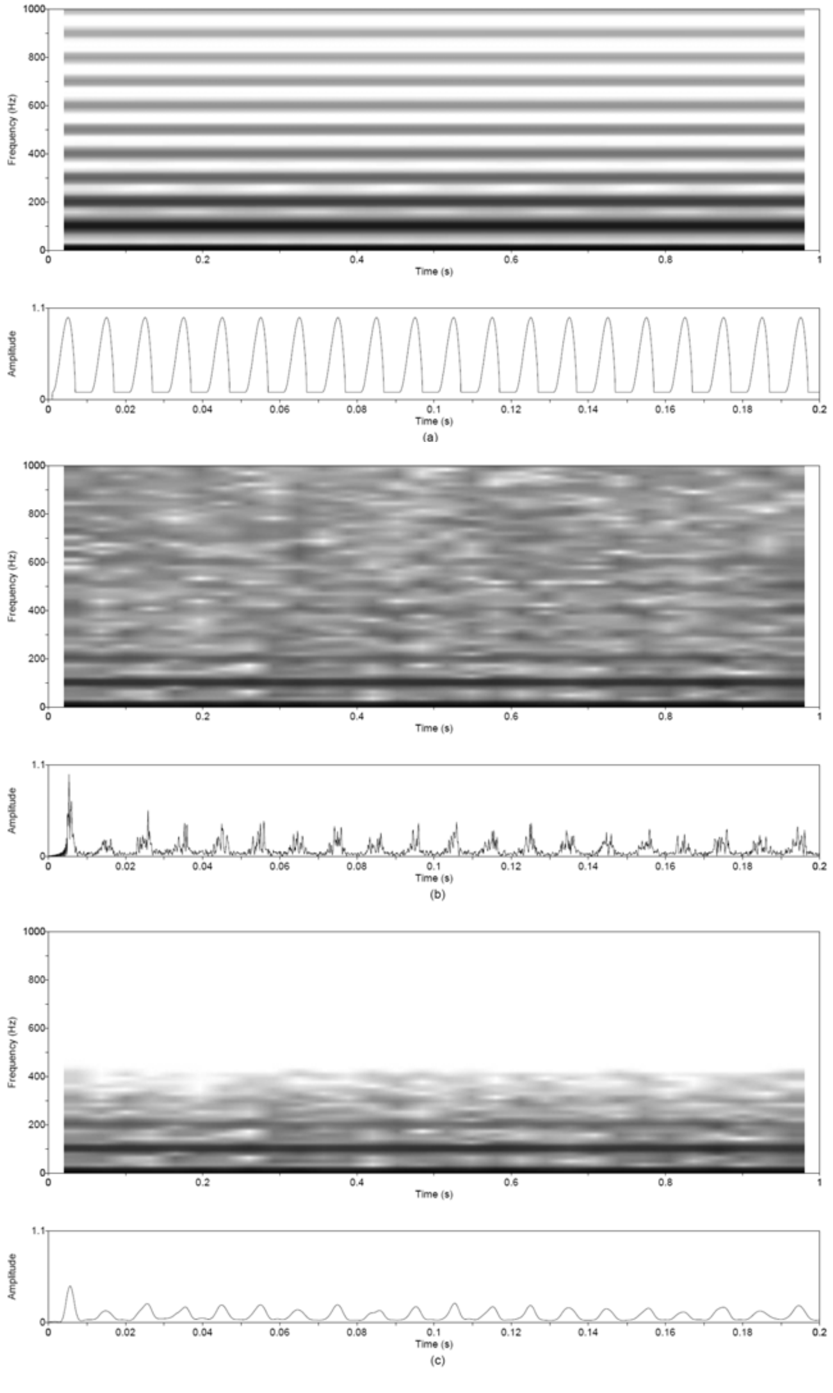

Figure F.9 Estimating the glottal waveform modulation using the Hilbert transform method. (a) Synthesized periodic source, (b) envelope estimated using the Hilbert method of the analytic signal magnitude, and (c) envelope estimated with a low-pass filter appended to the Hilbert transform method. Upper plot is of narrowband spectrogram and lower plot is of waveform over an expanded time scale. Synthesis parameters: Noise type = modulated, f_0 = 100, f_s = 8000, Duration = 1, DC = 0.1, OQ = 0.6.

Bibliography

[1] "Disordered Voice Database," 1.03 ed: Kay Elemetrics Corporation, 1994.

[2] E. E. Azzouz and A. K. Nandi, *Automatic Modulation Recognition of Communication Signals*. Boston: Kluwer Academic Publishers, 1996.

[3] A. Barney, C. H. Shadle and P. O. A. L. Davies, "Fluid flow in a dynamic mechanical model of the vocal folds and tract. I. Measurements and theory," *Journal of the Acoustical Society of America*, 105 (1), pp. 444-455, 1999.

[4] "Praat," version 4.4.04. P. Boersma and D. Weenink.

[5] A. S. Bregman, *Auditory Scene Analysis: The Perceptual Organization of Sound*. Cambridge, MA: MIT Press, 1990.

[6] A. B. Carlson, P. B. Crilly and J. C. Rutledge, *Communication Systems: An Introduction to Signals and Noise in Electrical Communication*. Boston: McGraw-Hill, 2002.

[7] C. d'Alessandro, V. Darsinos and B. Yegnanarayana, "Effectiveness of a periodic and aperiodic decomposition method for analysis of voice sources," *IEEE Transactions on Speech and Audio Processing*, 6 (1), pp. 12-23, 1998.

[8] C. d'Alessandro, B. Yegnanarayana and V. Darsinos, "Decomposition of speech signals into deterministic and stochastic components," Proceedings of IEEE International Conference on Acoustics, Speech, and Signal Processing, 1995.

[9] G. Fant, J. Liljencrants and Q. Lin, "A four-parameter model of glottal flow," *Speech Transmission Lab. Quart. Prog. Status Rep.*, 4, pp. 1-13, 1985.

[10] M. Frohlich, D. Michaelis, H. W. Strube and E. Kruse, "Acoustic voice analysis by means of the hoarseness diagram," *Journal of Speech Language and Hearing Research*, 43 (3), pp. 706-720, 2000.

[11] B. R. Gerratt and J. Kreiman, "Measuring vocal quality with speech synthesis," *Journal of the Acoustical Society of America*, 110 (5), pp. 2560-2566, 2001.

[12] B. R. Gerratt and J. Kreiman, "Toward a taxonomy of nonmodal phonation," *Journal of Phonetics*, 29 (4), pp. 365-381, 2001.

[13] B. R. Gerratt and J. Kreiman, "Perceptual evaluation of voice quality," in *The MIT Encyclopedia of Communication Disorders*, R. D. Kent, Ed. Cambridge, MA: The MIT Press, 2004, pp. 78-80.

[14] C. G. Gordon, "Spoiler-generated flow noise I. The experiment," *Journal of the Acoustical Society of America*, 43, pp. 1041-1048, 1965.

[15] C. G. Gordon, "Spoiler-generated flow noise II. Results," *Journal of the Acoustical Society of America*, 45, pp. 214-223, 1968.

[16] H. M. Hanson, "Glottal characteristics of female speakers," Ph.D. thesis, The Division of Applied Sciences, Harvard University, Cambridge, MA, 1995.

[17] H. M. Hanson, "Glottal characteristics of female speakers: Acoustic correlates," *Journal of the Acoustical Society of America*, 101 (1), pp. 466-481, 1997.

[18] H. M. Hanson and E. S. Chuang, "Glottal characteristics of male speakers: Acoustic correlates and comparison with female data," *Journal of the Acoustical Society of America*, 106 (2), pp. 1064-1077, 1999.

[19] H. M. Hanson, K. N. Stevens, H. K. J. Kuo, M. Y. Chen and J. Slifka, "Towards models of phonation," *Journal of Phonetics*, 29 (4), pp. 451-480, 2001.

[20] D. J. Hermes, "Synthesis of breathy vowels - Some research methods," *Speech Communication*, 10 (5-6), pp. 497-502, 1991.

[21] J. Hillenbrand, "A methodological study of perturbation and additive noise in synthetically generated voice signals," *Journal of Speech and Hearing Research*, 30 (4), pp. 448-61, 1987.

[22] J. Hillenbrand, R. A. Cleveland and R. L. Erickson, "Acoustic correlates of breathy vocal quality," *Journal of Speech and Hearing Research*, 37 (4), pp. 769-778, 1994.

[23] J. Hillenbrand and R. A. Houde, "Acoustic correlates of breathy vocal quality: Dysphonic voices and continuous speech," *Journal of Speech and Hearing Research*, 39 (2), pp. 311-321, 1996.

[24] R. E. Hillman, E. Oesterle and L. L. Feth, "Characteristics of the glottal turbulent noise source," *Journal of the Acoustical Society of America*, 74 (3), pp. 691-694, 1983.

[25] E. B. Holmberg, P. Doyle, J. S. Perkell, B. Hammarberg and R. E. Hillman, "Aerodynamic and acoustic voice measurements of patients with vocal nodules: Variation in baseline and changes across voice therapy," *Journal of Voice*, 17 (3), pp. 269-282, 2003.

[26] E. B. Holmberg, R. E. Hillman, B. Hammarberg, M. Sodersten and P. Doyle, "Efficacy of a behaviorally based voice therapy protocol for vocal nodules," *Journal of Voice*, 15 (3), pp. 395-412, 2001.

[27] E. B. Holmberg, R. E. Hillman and J. S. Perkell, "Glottal airflow and transglottal air pressure measurements for male and female speakers in soft, normal, and loud voice," *Journal of the Acoustical Society of America*, 84 (2), pp. 511-29, 1988.

[28] S. Imaizumi and S. Kiritani, "A preliminary study on the generation of pathological voice qualities," in *Vocal Physiology: Voice Production Mechanisms and Functions*, O. Fujimura, Ed. New York: Raven Press Ltd, 1988, pp. 249-257.

[29] P. J. B. Jackson and C. H. Shadle, "Frication noise modulated by voicing, as revealed by pitch-scaled decomposition," *Journal of the Acoustical Society of America*, 108 (4), pp. 1421-1434, 2000.

[30] P. J. B. Jackson and C. H. Shadle, "Performance of the pitch-scaled harmonic filter and applications in speech analysis," Proceedings of IEEE International Conference on Acoustics, Speech, and Signal Processing, 2000.

[31] P. J. B. Jackson and C. H. Shadle, "Pitch-scaled estimation of simultaneous voiced and turbulence-noise components in speech," *IEEE Transactions on Speech and Audio Processing*, 9 (7), pp. 713-726, 2001.

[32] P. Jinachitra and J. O. Smith, III, "Joint estimation of glottal source and vocal tract for vocal synthesis using Kalman smoothing and EM algorithm," Proceedings of IEEE Workshop on Applications of Signal Processing to Audio and Acoustics, New Paltz, NY, 2005.

[33] J. Kaiser, "Some observations on vocal tract operation from a fluid flow point of view," in *Vocal Fold Physiology: Biomechanics, Acoustics, and Phonatory Control*, I. R. Titze and R. C. Scherer, Eds. Denver Center for the Performing Arts, CO, 1983, pp. 358-386.

[34] R. D. Kent and C. Read, *The Acoustic Analysis of Speech*. San Diego: Singular Publishing Group, Inc., 1992.

[35] N. Kitawaki, "Quality Assessment of Coded Speech," in *Advances in Speech Signal Processing*, S. Furui and M. M. Sondhi, Eds. New York: Marcel Dekker, Inc., 1992.

[36] D. H. Klatt, "Software for a cascade-parallel formant synthesizer," *Journal of the Acoustical Society of America*, 67 (3), pp. 971-995, 1980.

[37] D. H. Klatt, "Chapter 3: Description of the cascade/parallel formant synthesizer," in *KLATTALK: The Conversion of English Text to Speech*, 1990.

[38] D. H. Klatt and L. C. Klatt, "Analysis, synthesis, and perception of voice quality variations among female and male talkers," *Journal of the Acoustical Society of America*, 87 (2), pp. 820-857, 1990.

[39] M. H. Krane, "Aeroacoustic production of low-frequency unvoiced speech sounds," *Journal of the Acoustical Society of America*, 118 (1), pp. 410-427, 2005.

[40] J. Kreiman and B. R. Gerratt, "Perception of aperiodicity in pathological voice," *Journal of the Acoustical Society of America*, 117 (4), pp. 2201-2211, 2005.

[41] J. Kreiman, B. R. Gerratt, G. B. Kempster, A. Erman and G. S. Berke, "Perceptual evaluation of voice quality - Review, tutorial, and a framework for future research," *Journal of Speech and Hearing Research*, 36 (1), pp. 21-40, 1993.

[42] H.-K. J. Kuo, "Voice source modeling and analysis of speakers with vocal-fold nodules," Ph.D. thesis, Harvard-MIT Division of Health Sciences and Technology, Massachusetts Institute of Technology, Cambridge, MA, 1998.

[43] J. Laroche, Y. Stylianou and E. Moulines, "HNS: Speech modification based on a harmonic + noise model," Proceedings of IEEE International Conference on Acoustics, Speech, and Signal Processing, Minneapolis, MN, 1993.

[44] I. Lehiste and G. E. Peterson, "Some basic considerations in the analysis of intonation," *Journal of the Acoustical Society of America*, 33 (4), pp. 419-425, 1961.

[45] M. W. Macon and M. A. Clements, "Speech concatenation and synthesis using an overlap-add sinusoidal model," Proceedings of IEEE International Conference on Acoustics, Speech, and Signal Processing, 1996.

[46] M. W. Macon and M. A. Clements, "Sinusoidal modeling and modification of unvoiced speech," *IEEE Transactions on Speech and Audio Processing*, 5 (6), pp. 557-560, 1997.

[47] "MATLAB," version 7.0.4. MathWorks: Natick, MA.

[48] R. J. McAulay and T. F. Quatieri, "Speech analysis/synthesis based on a sinusoidal representation," *IEEE Transactions on Acoustics Speech and Signal Processing*, 34 (4), pp. 744-754, 1986.

[49] R. S. McGowan, L. L. Koenig and A. Lofqvist, "Vocal-tract aerodynamics in vertical-bar-aca-vertical-bar utterances - Simulations," *Speech Communication*, 16 (1), pp. 67-88, 1995.

[50] D. Mehta and T. F. Quatieri, "Synthesis, analysis, and pitch modification of the breathy vowel," Proceedings of IEEE Workshop on Applications of Signal Processing to Audio and Acoustics, New Paltz, NY, 2005.

[51] D. Michaelis, M. Frohlich and H. W. Strube, "Selection and combination of acoustic features for the description of pathologic voices," *Journal of the Acoustical Society of America*, 103 (3), pp. 1628-1639, 1998.

[52] L. Mongeau, N. Franchek, C. H. Coker and R. A. Kubli, "Characteristics of a pulsating jet through a small modulated orifice, with application to voice production," *Journal of the Acoustical Society of America*, 102 (2), pp. 1121-1133, 1997.

[53] E. Moulines and F. Charpentier, "Pitch-Synchronous Wave-Form Processing Techniques for Text-to-Speech Synthesis Using Diphones," *Speech Communication*, 9 (5-6), pp. 453-467, 1990.

[54] E. Moulines and J. Laroche, "Nonparametric techniques for pitch-scale and time-scale modification of speech," *Speech Communication*, 16 (2), pp. 175-205, 1995.

[55] P. J. Murphy, "Perturbation-free measurement of the harmonics-to-noise ratio in voice signals using pitch synchronous harmonic analysis," *Journal of the Acoustical Society of America*, 105 (5), pp. 2866-2881, 1999.

[56] P. J. Murphy, "Spectral characterization of jitter, shimmer, and additive noise in synthetically generated voice signals," *Journal of the Acoustical Society of America*, 107 (2), pp. 978-988, 2000.

[57] N.C.V.S., "Tutorials -- Equation Exploder, Chapter 8: Control of Fundamental Frequency." Accessed January 23, 2006. http://www.ncvs.org/ncvs/tutorials/voiceprod/equation/chapter8/#/8-7.gif.

[58] N.C.V.S., "Tutorials -- Voice Production -- How humans control pitch." Accessed January 23, 2006. http://www.ncvs.org/ncvs/tutorials/voiceprod/tutorial/cover.html.

[59] D. O'Brien and A. I. C. Monaghan, "Concatenative synthesis based on a harmonic model," *Speech and Audio Processing, IEEE Transactions on*, 9 (1), pp. 11, 2001.

[60] A. V. Oppenheim, R. W. Schafer and J. R. Buck, *Discrete-Time Signal Processing*, Second edition ed. Upper Saddle River, NJ: Prentice-Hall, Inc., 1999.

[61] D. B. Paul, "The spectral envelope estimation vocoder," *IEEE Transactions on Acoustics Speech and Signal Processing*, 29 (4), pp. 786-794, 1981.

[62] G. E. Peterson and H. L. Barney, "Control methods used in a study of the vowels," *Journal of the Acoustical Society of America*, 24 (2), pp. 175-184, 1952.

[63] T. F. Quatieri, *Discrete-Time Speech Signal Processing: Principles and Practice*. Upper Saddle River, NJ: Prentice Hall PTR, 2002.

[64] T. F. Quatieri and R. J. McAulay, "Speech transformations based on a sinusoidal representation," *IEEE Transactions on Acoustics Speech and Signal Processing*, 34 (6), pp. 1449-1464, 1986.

[65] T. F. Quatieri and R. J. McAulay, "Shape invariant time-scale and pitch modification of speech," *IEEE Transactions on Signal Processing*, 40 (3), pp. 497-510, 1992.

[66] E. Rank and G. Kubin, "Towards an oscillator-plus-noise model for speech synthesis," Proceedings of ISCA Tutorial and Research Workshop on Non-linear Speech Processing, Le Croisic, France, 2003.

[67] A. E. Rosenberg, "Effect of glottal pulse shape on the quality of natural vowels," *Journal of the Acoustical Society of America*, 49 (2), pp. Suppl 2:583+, 1971.

[68] M. Rothenberg, "New inverse filtering technique for deriving glottal air-flow waveform during voicing," *Journal of the Acoustical Society of America*, 53 (6), pp. 1632-1645, 1973.

[69] M. Rothenberg, "Acoustic reinforcement of vocal fold fold vibratory behavior in singing," in *Vocal Physiology: Voice Production, Mechanisms and Functions*, O. Fujimura, Ed. New York: Raven Press, 1988, pp. 379-389.

[70] X. Serra and J. Smith, "Spectral modeling synthesis: A sound analysis/synthesis system based on deterministic plus stochastic decomposition," *Computer Music Journal*, 14 (4), pp. 12-24, 1990.

[71] C. H. Shadle, A. Barney and P. O. A. L. Davies, "Fluid flow in a dynamic mechanical model of the vocal folds and tract. II. Implications for speech production studies," *Journal of the Acoustical Society of America*, 105 (1), pp. 456-466, 1999.

[72] K. N. Stevens, "Airflow and turbulence noise for fricative and stop consonants: Static considerations," *Journal of the Acoustical Society of America*, 50 (4 Pt 2), pp. 1180-1192, 1971.

[73] K. N. Stevens, *Acoustic Phonetics*. Cambridge, MA: MIT Press, 1998.

[74] Y. Stylianou, "Applying the harmonic plus noise model in concatenative speech synthesis," *IEEE Trans. Speech and Audio Processing*, 9 (1), pp. 21-29, 2001.

[75] Y. Stylianou, J. Laroche and E. Moulines, "High-quality speech modification based on a harmonic + noise model," Proceedings of EUROSPEECH, 1995.

[76] J. E. F. Sundberg, "Formant technique in a professional soprano singer," *Acustica*, 32, pp. 89-96, 1975.

[77] H. M. Teager, "Some observations on oral air-flow during phonation," *IEEE Transactions on Acoustics Speech and Signal Processing*, 28 (5), pp. 599-601, 1980.

[78] H. Valbret, E. Moulines and J. P. Tubach, "Voice transformation using PSOLA technique," *Speech Communication*, 11 (2-3), pp. 175-187, 1992.

[79] D. H. Whalen and A. G. Levitt, "The universality of intrinsic F0 of vowels," *Journal of Phonetics*, 23 (3), pp. 349-366, 1995.

[80] B. Yegnanarayana, C. d'Alessandro and V. Darsinos, "An iterative algorithm for decomposition of speech signals into periodic and aperiodic components," *IEEE Transactions on Speech and Audio Processing*, 6 (1), pp. 1-11, 1998.

[81] Z. Y. Zhang, L. Mongeau, S. H. Frankel, S. Thomson and J. B. Park, "Sound generation by steady flow through glottis-shaped orifices," *Journal of the Acoustical Society of America*, 116 (3), pp. 1720-1728, 2004.